Structure/function correlates and protein/lipid interaction of the viral potassium channel Kcv_{NTS}

TECHNISCHE UNIVERSITÄT DARMSTADT

Vom Fachbereich Biologie der Technischen Universität Darmstadt

zur Erlangung des akademischen Grades

eines Doctor rerum naturalium

genehmigte Dissertation von

Dipl.-Biol. Christian J. Braun

aus Weingarten

Berichterstatter: Prof. Dr. Gerhard Thiel

Mitberichterstatter: Prof. Dr. Adam Bertl

Eingereicht am: 25.04.2014

Mündliche Prüfung am: 27.06.2014

Darmstadt 2014

D17

Wahrheit kann man, wenn überhaupt, nur in der Einfachheit finden.

Sir Isaac Newton (1643 – 1727)

1. Table of contents

2. Summary

Ion channels are present in every domain of life. They catalyze the rapid and selective flux of ions across membranes. It is well established that mutations or dysfunctions of ion channels often cause severe diseases. To understand the molecular mechanisms behind these so-called channelopathies it is necessary to understand the structure/function correlates and protein/lipid interaction of channels at the single-protein level. Planar lipid bilayer techniques, the oldest and most reduced systems for a functional characterization of ion channels, are well suited to examine basic structure/function relations in a defined lipid environment. Here we improved the performance of the conventional planar lipid bilayer technique. An air-bubble functions as a tool for the rapid creation and stabilization of bilayers and even more important for reducing the number of active channels in the bilayer for real single-channel recordings. A further technical improvement is the establishment of an *in vitro* (cell-free) expression system for ion channels, which supports a rapid protein production and a contamination free reconstitution. With these systems we performed a detailed single-channel analysis of the viral K^+ channel Kcv_{NTS}, one of the smallest potassium channels known so far. The data show that the protein has a very high selectivity for K^+ over Na^+; it is permeable for Rb^+ although the unitary conductance is lower than that of K^+. When Cs^+ is the only cation present in the buffer the channel conducts it, albeit with a low conductance. If Cs^+ is present together with K^+ even at a low concentration it will block the K^+ inward current in a side specific and voltage dependent manner. The Cs^+ block increases in strength over several minutes suggesting a slow conformational change in the protein. A further characteristic feature of the Kcv_{NTS} is a distinct pH dependency of the open probability. The latter decreases from a value close to 90% with acidification of the buffer down to ca. 10%. This pH dependent open probability is correlated with an increase in the voltage dependency of the channel suggesting a titratable amino acid in the protein, which acquires the function of a voltage sensor and presumably of a gate.

Because of its small size with only 82 aa per monomer the Kcv_{NTS} protein is quasi fully embedded in the membrane. A functional test in planar lipid bilayers of different thickness, which are made from lipids with different acyl chain length (C14 - C16/18) or by adding solvents or cholesterol, shows that the channel is functional under all conditions. While the unitary conductance is not affected by the thickness the open probability is sensitive to it. With increasing bilayer thickness the channel exhibits more frequently a second gating mode, which is characterized by a voltage dependency. In the latter mode positive voltages cause a decrease in the channel open probability. The question of the molecular mechanism, which is responsible for this unusual gating in a channel without a notable charge in the electrical field, remains unanswered. Also the question why the membrane thickness affects this gating mode remains unsolved. The data however show for the first time that the lipid environment can have a dramatic effect on the voltage dependency of a protein.

Since the bilayer technique bears the hazard of artifacts from impure protein isolations and from lipid pores Kcv_{NTS} is as a control also produced and purified from *Pichia pastoris* and expressed heterologously in HEK293 cells. Comparing the aforementioned data of the *in vitro* expressed protein reconstituted in conventional planar lipid bilayers with those recorded with other methods and in particular with those measured by the conventional patch clamp technique in HEK293 cells show no large difference between the different systems. The results of these experiments stress that the obtained data with the *in vitro* expressed Kcv_{NTS} channel in conventional bilayers is indeed representative for the function of this channel protein.

Collectively the present results show that a protein as small as the Kcv_{NTS} is able to function in a robust manner as a selective K^+ channel in different membrane environments. The protein, which is equivalent to the pore module of more complex K^+ channels, has inherent gating properties, which are sensitive to the pH, Cs^+ and the membrane thickness. This underscores the view of multiple gates in the pore module of K^+ channels.

3. Zusammenfassung

Ionenkanäle, welche einen schnellen und selektiven Ionenfluss über Membranen katalysieren, werden in allen Domänen des Lebens gefunden. Mutationen oder Fehlfunktionen dieser Kanäle können oft schwerwiegende Folgen haben. Um die molekularen Mechanismen hinter diesen sogenannten „Channelopathien“ zu verstehen, sind Struktur-Funktionsbeziehungen sowie Protein-Lipidinteraktionen auf Einzelkanalebene erforderlich. Zu den ältesten und reduziertesten elektrophysiologischen Messsystemen, um Proteine auf Einzelkanalniveau in einer definierten Lipidumgebung zu untersuchen, gehören die konventionellen planaren lipid bilayer Syteme. In dieser Studie verbesserten wir die konventionelle bilayer Technik mit Hilfe einer Luftblase, welche als ein Werkzeug dient, mit der ein lipid bilayer schnell aufgespannt und gleichzeitig ein unstabiler lipid bilayer stabilisiert werden kann. Des Weiteren kann mit der Luftblase die Anzahl der Ionenkanäle innerhalb der Membran aktiv reduziert werden, sodass echte Einzelkanalmessungen möglich sind.

Eine weitere technische Verbesserung ist die Etablierung eines *in vitro* (künstliches/zellfreies) Expressionssystems, mit dem Proteine zeitsparend exprimiert und kontaminationsfrei in den lipid bilayer rekonstituiert werden können. In dieser Arbeit wird, mit den obengenannten Verbesserungen, der virale Kaliumkanal Kcv_{NTS}, einer der kleinsten bekannten Kaliumkanäle, auf Einzelkanalebene untersucht. Das Kanalprotein zeigt eine hohe Selektivität für K^+ gegenüber Na^+. Trotz einer geringeren Leitfähigkeit ist der Kanal auch für Rb^+ permeabel. Ist Cs^+ das einzige verfügbare Kation wird dieses ebenfalls geleitet. In Experimenten aus einer Mischung mit K^+ und Cs^+ wirkt bereits eine geringe Konzentration an Cs^+ einseitig blockierend auf den Kanal; der Einwärtsstrom wird spannungsabhängig blockiert. Die Stärke des Blocks und damit die Sensitivität gegenüber Cs^+ ist zeitabhängig was auf eine langsame Konformationsänderung innerhalb des Proteins zurück zu führen ist. Ein weiteres Charakteristikum des Kcv_{NTS} ist eine pH abhängige Offenwahrscheinlichkeit, welche sich in einer Verringerung von ca. 90% zu etwa 10% mit zunehmender Ansäuerung des Milieus widerspiegelt. Die pH abhängige Offenwahrscheinlichkeit korreliert mit einer zunehmenden Spannungsabhängigkeit welche zu der Annahme führt, dass im Kanal eine titrierbare Aminosäure vorliegt, die als Spannungssensor und auch als Gate fungieren kann.

Mit einer geringen Größe von nur 82 Aminosäuren pro Monomer ist Kcv_{NTS} quasi vollständig in der Lipidmembran eingebettet. Veränderungen der Membrandicke durch Variationen der Fettsäurelängen der Lipide (C14 - C16/18), durch Lösungsmittel oder durch Zugabe von Cholesterol zeigen, dass der Kanal in jeder Umgebung funktionsfähig ist. Die Leitfähigkeit des Kanalproteins wird nicht durch die Membrandicke beeinflusst, jedoch die Offenwahrscheinlichkeit. Dies zeigt sich in einem alternativen, spannungsabhängigen Gating des Kanals. Mit zunehmend positiven Spannungen nimmt die Offenwahrscheinlichkeit ab. Der molekulare Mechanismus hinter einem spannungsabhängigen Gating, in einem Kanal ohne nennenswerte Ladung im elektrischen Feld, bleibt unbeantwortet. Des Weiteren ist nicht geklärt in wieweit unterschiedliche Membrandicken Einfluss auf diesen Gating-Mechanismus

haben. Dennoch zeigen diese Daten zum Ersten mal, dass die Lipidumgebung einen drastischen Effekt auf die Spannungsabhängigkeit eines Proteins hat.

In Einzelkanalmessungen besteht die Gefahr von Artefakten darin, dass Proteine unsauber aufgereinigt sind oder Lipidporen die Messungen erschweren. Aus diesem Grund haben wir, neben des *in vitro* exprimierten Kcv_{NTS}, denselben Kanal in *Pichia pastoris* sowie heterolog in HEK293 Zellen exprimiert und diese Daten miteinander verglichen. Die Ergebnisse zeigen, dass das Kanalschalten des *in vitro* exprimierten Kcv_{NTS} in der Tat auf die Funktion des Kanals zurück zu führen ist.

Zusammenfassend zeigen die Daten, dass ein kleines Protein, wie der Kcv_{NTS}, in einer robusten Weise als selektiver K^+ Kanal funktionieren kann. Dieses Kanalprotein alleine, welches bei komplexeren K^+ Kanäle lediglich als Porenmodul fungiert, zeigt Gating-Eigenschaften die sensitiv gegenüber pH, Cs^+ und der Membrandicke sind. Diese Eigenschaften heben den Standpunkt mehrerer Gates im Porenmodul von K^+ Kanälen hervor.

4. Single-channel characterization of the minimal viral potassium channel Kcv_{NTS}

4.1. Abstract

Potassium channels from *chlorella* viruses are the smallest potassium channels known so far. In spite of their small size of less than 100 aa per monomer they still show the structural and functional hallmarks of more complex potassium channels. Here we present a detailed single-channel characterization of Kcv_{NTS} (K^+ channel *chlorella* virus Next-to-Smith) as a model system to study structure/function correlates. When the channel protein is reconstituted in planar lipid bilayers, single-channel recordings revealed that the small channel is selective for potassium against sodium; it is permeable to rubidium. With no other cation present the channel also conducts cesium. In the presence of K^+, Cs^+ acts already at low concentrations as volatge dependent blocker of the K^+ conductance. The channel block by Cs^+ is side specific and effective only when Cs^+ is present in the external solution. The degree of Cs^+ induced inhibition of Kcv_{NTS} increases with time (τ = 27 min) suggesting that the sensitivity of the channel to Cs^+ increases via a slow conformational change in the protein. In addition to Cs^+ also H^+ affect gating of Kcv_{NTS}. Even though the channel is fully submerged in the lipid bilayer it exhibits a pH dependency with the effect that the open probability decreases from a value of 90% in alkaline pH to 10% in acidic pH. The pH dependency comes along with an increase in voltage dependency of the channel suggesting that a titratable amino acid becomes protonated by acidification and that this amino acid acquires the role of a voltage sensitive gate in the selectivity filter.

4.2. Introduction

Membrane proteins, and in particular ion channels, catalyze the flux of ions across membranes in a very defined manner (Ashcroft, 2000). This is important to maintain the function of many cellular processes which include among others nervous functions, signaling or the rate of the heartbeat (Doyle, 1998; Hille, 2001; Koert, 2005). Mutations or dysfunctions of these proteins can cause severe diseases like the long and short QT-syndromes, cystic fibrosis or epilepsy with febrile seizures (Barrett et al., 2012; Morita et al., 2008; Spampanato et al., 2003). These diseases, which originate from an aberrant function of ion channels are commonly known as channelopathies (Ashcroft, 2000). To understand the structural features of channel functionality and non-functionality it is necessary to understand these membrane proteins at the molecular level. For instance, it is obvious that a clinical search for drugs that restore channel function or drugs that control unregulated channels, requires information on structure and function correlates of channel proteins.

Potassium channels are a very important group of ion channels and can be found in every domain of life (Hille, 2001). Every functional potassium channel is build either as a dimer, a homo- or heterotetramer. Tetramers are assembled by four monomers (Miller, 2000). One monomer consists of a cytosolic N- and a C-terminal region, different numbers of transmembrane domains (TMD) and a pore region (Gazzarrini et al., 2009). The variable numbers of transmembrane domains determine different classes of potassium channels. The

main classes consist of two to eight transmembrane domains (Thiel et al., 2011). Each potassium channel has in common the same architecture of the core complex. This complex is assembled of four monomers; each of them comprises two transmembrane domains with the pore region in between (Thiel et al., 2011). The aforementioned pore can already create a functional channel by itself (Gazzarrini et al., 2009) bearing a selectivity filter, a cavity and a gate (Sansom et al., 2002). The selectivity filter serves as a bottleneck for the transport of ions through K^+ channels and the particular architecture of this filter makes a potassium channel selective. A hydrated potassium ion, which arrives at the "mouth"/entrance of the channel, has to strip of its water shell in order to permeate through the channel. This process costs energy (Koert, 2005). To avoid an energy loss, the selectivity filter of the channel is composed of an amino acid sequence, which is the same for each potassium channel. This canonical sequence, the so called signature sequence, contains 8 amino acids with the sequence TxxTxGF/YG; x denotes here a random amino acid (Heginbotham et al., 1999). The negatively charged oxygen atoms of the carbonyl groups of the signature sequence are arranged in such a manner that they extend into the filter with the oxygen atoms pointing into the channel pore. In this arrangement these oxygen atoms have the same distance to the K^+ ion as its surrounding hydrogen atoms from the water shell (MacKinnon, 2004). The filter effectively mimics in this way the water shell of the potassium ion with the result that the ion can pass through the filter without a loss of energy. Even though sodium ions are smaller than potassium ions, they are not efficiently transported through the selectivity filter. The reason for this is that the oxygen atoms of the filter perfectly mimic the water shell of the permeant potassium ion but not of the smaller sodium ion. The latter is only stabilized from two oxygen atoms rather than four like in the case of K^+; this prevents the loss of the hydration shell and makes a transport of Na^+ less favorable (Doyle, 2004). At the end of the selectivity filter the cavity begins. This is a water filled space in which an ion, which has been transported through the channel, can receive a new hydration shell (Yellen, 2002). In addition to providing a permeation pathway for potassium ions, a channel protein is also capable of opening and closing. This gating mechanism, which allows a control over ion permeation, describes the stochastic fluctuation of the protein between open and close states (Doyle, 2004). The location of the gate or of the gates in K^+ channels is currently controversially debated in the literature. There are two potential regions for the localization of the gates. One is on the cytoplasmic site of the protein where the inner transmembrane domains of the pore can form a hydrophobic gate. This gate results from the so-called bundle crossing mechanism e.g. the clustering of the C-terminal ends of the inner transmembrane domains (Perozo et al., 1999). The second position of the gate is in the selectivity filter where the structure of the selectivity filter can undergo conformational changes with the consequence that ions can or cannot pass the filter (Zheng & Sigworth, 1997). The current view is that both gates are relevant in most K^+ channels and that different types of channel activation or inactivation are controlled by either of the two gates (Blunck et al., 2006; Cuello et al., 2010)

In this study we focus on a potassium channel, which lacks the aforementioned cytoplasmic C- and N-terminal regions. This channel is fully submerged into the lipid bilayer (Braun et al.,

2013); it belongs to the viral Kcv ($\underline{K}^+$ channel *chlorella* virus) type channels, a family of potassium channels, which includes the smallest potassium channels known so far. Kcv channels are encoded by viruses, which infect certain unicellular green algae (Thiel et al., 2011). These viral potassium channels are necessary in the early stage of host cell infection. It is assumed that the Kcv channel is part of the virion and is inserted in the viral membrane. In the early stage of infection, the viral membrane presumably fuses with the host membrane. As a result the Kcv channels cause a depolarization of the host membrane. This in turn generates with other channels a driving force for potassium and subsequently water efflux from the host. The net result of these fluxes is a loss of turgor pressure in the host, which in turn enables the virus to inject its DNA into the host cell (Frohns et al., 2006; Mehmel, 2003; Neupärtl et al., 2008).

In spite of the small size with less than 100 aa per monomer these viral potassium channels show the main hallmarks of more complex potassium channels. They have a K^+ channel typical selectivity filter (with the signature sequence), which provides them a cation selectivity. They reveal gating and they are sensitive to common K^+ channel blockers (Thiel et al., 2011). The channel of this study, Kcv Next-to-Smith (Kcv_{NTS}), has a monomer size of 82 aa and is with its homolog Kcv *acanthocystis turfacea chlorella* virus-1 (Kcv_{ATCV-1}) (Gazzarrini et al., 2009) one of the smallest potassium channels known. The Kcv_{NTS} channel was found in a lake next to the Smith lake in western Nebraska (USA) (Greiner, 2011). In previous studies it was already shown, with patch clamp recordings in the whole-cell configuration, that Kcv_{NTS} has the functional features of a K^+ channel. It occurred that cations like sodium or lithium are weakly or not permeable. Furthermore the Kcv_{NTS} channel was sensitive against the well-known channel blockers barium and cesium (Greiner, 2011). For studying structure/function correlates in more detail it is necessary however to examine the channel function at the single-channel level. In this report we present a detailed characterization of this small Kcv type channel at the single-channel level. The data show that the channel has a unitary conductance of 80 pS in 100 mM KCl. The conductance saturates with increasing K^+ and shows a maximal conductance of 144 pS; half maximal conductance is obtained with 73 mM KCl. Experiments on the selectivity of the channel show that Kcv_{NTS} does not conduct sodium; Rb^+ is conducted but the unitary channel conductance is lower than in K^+. When Cs^+ is the only cation available Kcv_{NTS} is able to conduct Cs^+; in mixed solutions with K^+, Cs^+ turned out to block the K^+ conductance only from the external side in a voltage dependent manner. The voltage dependency increased slowly over several minutes suggesting that the channel acquired an increasing sensitivity to Cs^+ as a result of a very slow conformational change in the protein. Further experiments show that the open probability of the channel is sensitive to the pH in the medium. The open probability decreases with acidic pH and has a half maximal value at around pH 6. A detailed scrutiny of the open probability as a function of voltage shows an increasing voltage dependency of the channel with acidification. This suggests the presence of a titratable amino acid in the channel, which becomes charged via titration and which then serves a voltage sensor.

4.3. Methods

4.3.1. Protein expression in *Pichia pastoris*, *in vitro* and purification

The production and purification of Kcv_{NTS} in *Pichia pastoris* and *in vitro* (cell-free system) is described in 5.3.1 and 5.3.2.

4.3.2. Planar lipid bilayer experiments

Planar lipid bilayer experiments are described in 5.3.3 and 7.3. The formation of stable membranes was done by the monolayer technique (Montal & Mueller, 1972) and by a pseudo painting/air bubble technique, which is described in detail in 7.3. All membranes tested contained pure lipids of 1,2-diphytanoyl-*sn*-glycero-3-phosphocholine (DPhPC) (Avanti Polar Lipids, Alabaster, AL, USA). These lipids were dissolved in n-pentane (MERCK KGaA, Darmstadt, Germany) with a final concentration of 15 mg/ml. Symmetrical experiments were done with either KCl (100 mM, 250 mM, 500 mM, 750 mM, 1 M or 1.5 M) or CsCl (100 mM) solution buffered with HEPES (10 mM) and adjusted to a pH of 7. Asymmetrical experiments were done with either KCl (100 mM and 500 mM), NaCl (100 mM), RbCl (100 mM) or CsCl (100 mM) solution buffered with HEPES (10 mM) and adjusted to pH 7. For block experiments 2 mM CsCl (final concentration) was added to the experimental solution (100 mM KCl, 10 mM HEPES, adjusted to a pH of 7). Experiments with variation of the pH conditions were done with symmetrical KCl solution (100 mM), buffered with 10 mM of different Good buffers (TAPS (SIGMA CHEMICAL CO., St. Louis, MO, USA), HEPES (AppliChem GmbH, Darmstadt, Germany), MES (AppliChem GmbH, Darmstadt, Germany)) or potassium acetate (CH_3COOK).

4.3.3. Data analysis

Data analysis was done as indicated in chapter 5.3.6.

4.4. Results

4.4.1. Characterization of Kcv_{NTS}

Kcv_{NTS} is known to be a functional potassium channel (Greiner, 2011). Since the characteristics of this potassium channel were so far only examined in HEK293 cells, we focus here on the single-channel characteristics within artificial planar lipid bilayers. First measurements were done in neutral salt solutions (100 mM KCl, 10 mM HEPES) with a pH of 7. Fig 1A shows current responses of the Kcv_{NTS} channel in a DPhPC membrane with symmetrical KCl solutions. At positive voltages the channel shows clear single-channel currents whereas at negative voltages the open states seem very noisy. The latter effect starts to appear at holding potentials more negative than -80 mV.

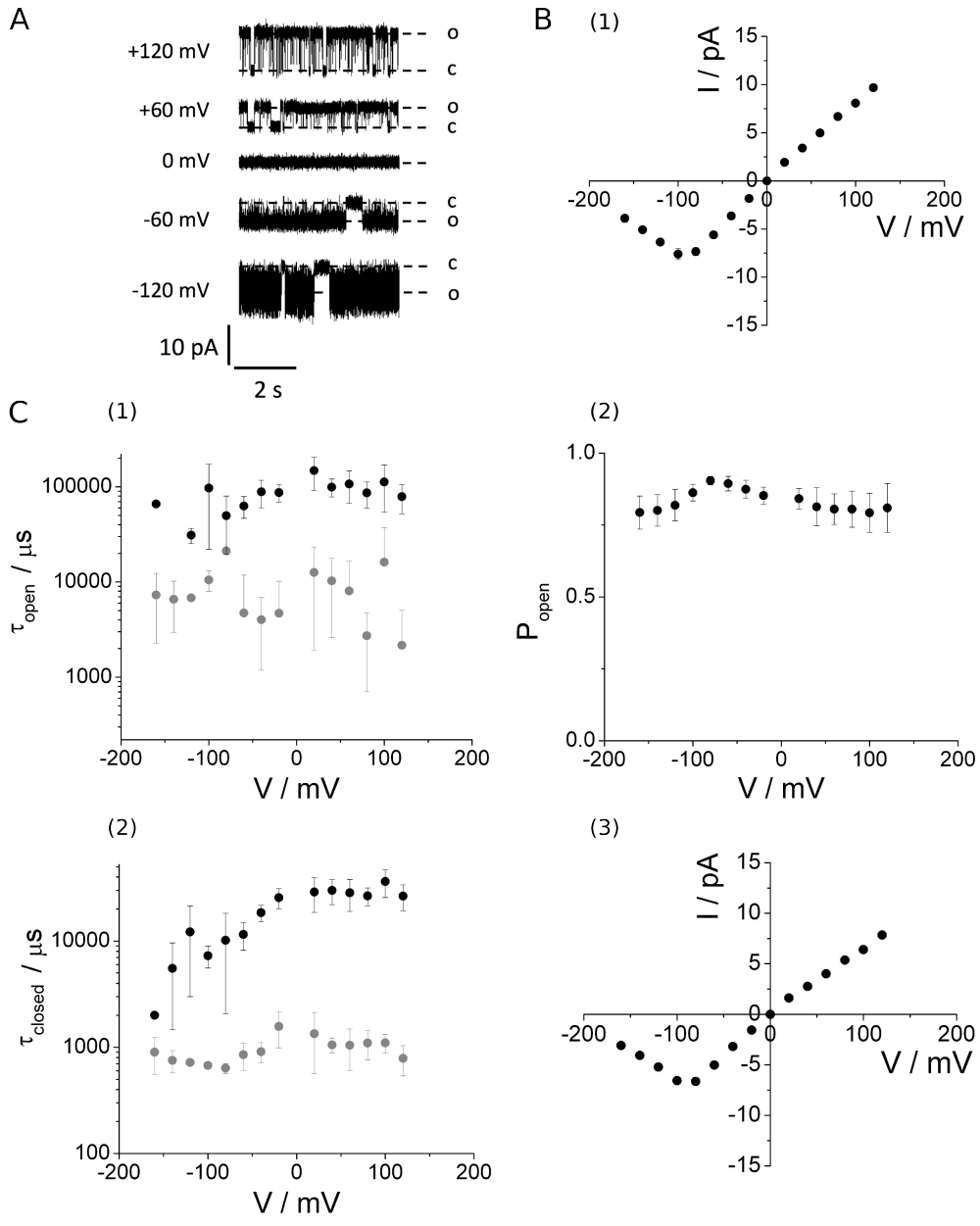

Fig 1 Characteristic properties of Kcv_{NTS} in DPhPC membranes.

(A) Representative single-channel currents responses at different holding potentials. Open and closed states are denoted with o and c respectively. (B) Single-channel I/V-curve (1), open probability (2) and time averaged single-channel I/V-curve (3). (C) Open and closed dwell times of the time constants from the data of (A). (B) and (C) values are means +- SD of n = 3-6 experiments.

At voltages positive of -80 mV the open and closed states are well defined and the unitary conductance of the channel reveals an ohmic behavior in a voltage window from -80 mV to +120 mV. In this voltage range the channel has a conductance of about 80 pS. Worth noting is that Kcv_{NTS} and its well characterized homologe Kcv_{ATCV-1} differ in only four aa in the first transmembrane domain (Braun et al., 2013) and that their unitary conductance is very similar. Also Kcv_{ATCV-1} has a unitary conductance of 80 pS (Gazzarrini et al., 2009). While the conductance is ohmic for positive voltages it exhibits a negative slope conductance at extreme negative potentials (discussed below). The Fig 1B(2) shows the open probability of the channel over the entire voltage window tested. The data show that the channel reveals a very robust and high voltage independent open probability of about 85%. Only at high negative holding potentials it seems that the open probability is slightly reduced. In order to extrapolate from the single channel data the macroscopic I/V relation of the Kcv channel we calculated the time averaged I/V-curve as a product of the single channel current (i) and the open probability (P_o) (with $i * P_o$). The resulting data in Fig 1 A(3) show the expected behavior that the I/V relation has a negative slope conductance at extreme negative potentials and an outward rectification at positive potentials. It has been mentioned above that Kcv_{NTS} is voltage independent. This voltage independency is analyzed in more detail by the dwell-time analysis (Fig 1C). The channel reveals two main open (1) and closed (2) states respectively. The average short and long open states are 10 ms and 100 ms long; both are voltage independent. The average short and long closed states are 1 ms and 10 ms long; the short closed states are voltage independent. The long closed states seem to exhibit a slight voltage dependency at negative potentials. This slight dependency is related to a fast gating of the channel at voltage ≥ -80mV, a phenomenon, which will be described in more detail below.

It has been mentioned that the channel resides in the voltage window tested mainly in the open states. The aforementioned negative slope conductance at extreme negative holding potentials originates from the well-known effect of potassium channels, the so-called fast gating or flickering effect (Abenavoli et al., 2009; Bertl et al., 1993; Huth et al., 2006; Schroeder & Hansen, 2007). This effect occurs at extreme holding potentials where the channel opens and closes too fast for the sampling frequency (bandwidth) of the amplifier, which is not able to record the whole process of opening and closing. As a consequence the currents seem to be cut off, resulting in smaller apparent current amplitudes. Fig 2A shows two representative current responses of Kcv_{NTS} at a holding potential of +120 mV and -120 mV respectively. A more detailed view at higher magnification of the channel openings is given for both holding potentials above (1) and below (2) the traces. For +120 mV transitions from the closed to open state are fully resolved and represent the true current amplitude. A closer view at the corresponding channel fluctuations at -120 mV reveals the phenomenon of

fast gating of Kcv_{NTS}. When the channel switches from the closed to the open state it is no longer possible to resolve a clear-cut level of the open state. The currents become very noisy because the channel gates too fast for the recording system, resulting in the apparent reduced single-channel amplitude. To obtain a measure for the true current amplitude we employed the beta-fit method (Fig 2B). In this process we took a truncated Markov-Model with one open and two closed states ($O - C_{flicker} - C_{slow}$). The C_{slow} can be neglected because it has no big influence on the rate constants of $OC_{flicker}$ (k_1) to $C_{flicker}O$ (k_{-1}). It is only used to determine the ratio of the rate constants of the c_{slow} peak in B, which results in an improved fit. The process of fitting is described elsewhere (Abenavoli et al., 2009).

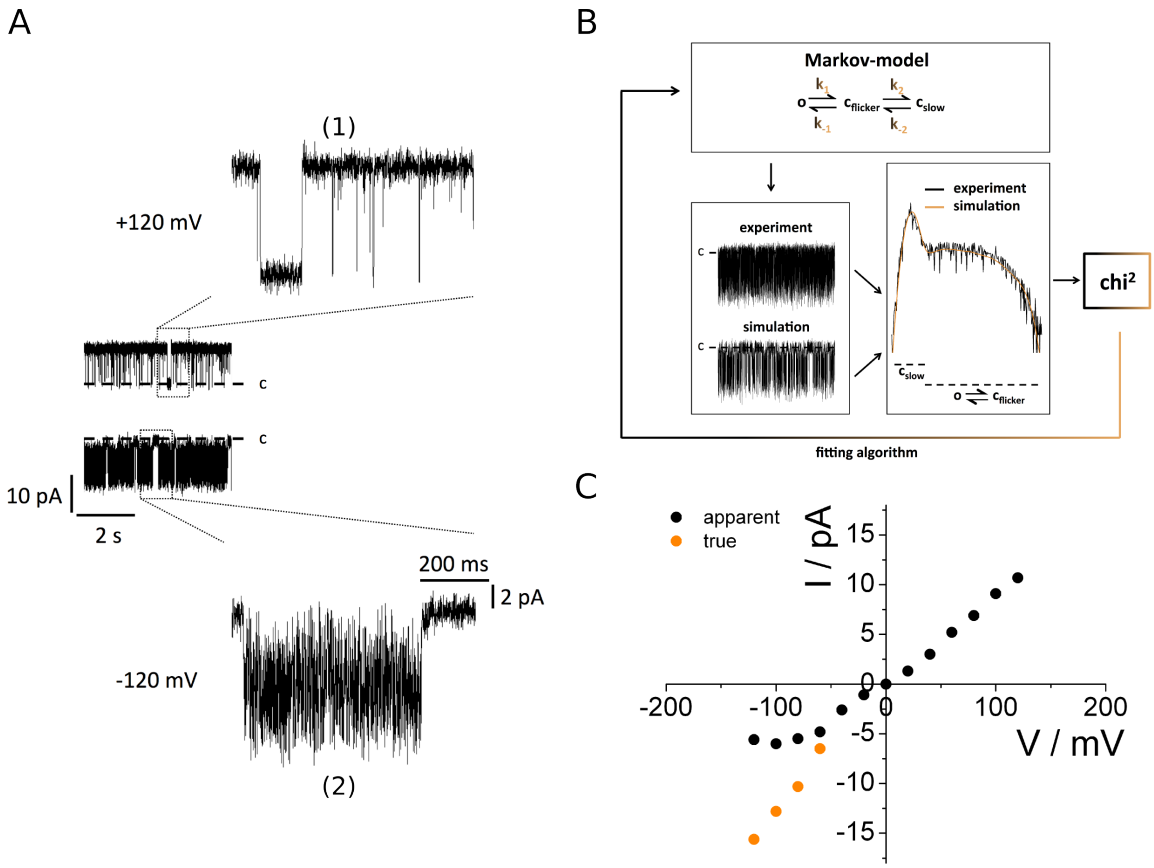

Fig 2 Fast gating of Kcv_{NTS}.

(A) Representative current responses at holding potentials of +120 mV and -120 mV. The effect of fast gating appears at extreme negative holding potentials. The closed states are denoted with c. (B) Sketch of the beta-fit simulation; from apparent single-channel amplitudes to the true single-channel amplitudes. (C) Representative single-channel I/V-curve of the apparent currents, with a negative slope conductance at high negative holding potentials (black) and the reconstructed true currents, which have an ohmic behavior at all given potentials (orange).

Fig 2C shows the measured apparent (black) and calculated true (orange) current amplitudes of the channel at negative holding potentials > -60 mV; for completeness also the measured true currents at positive (black) potentials are shown. After analyzing the fast gating of the Kcv channel with the beta-fit method it turns out that the true currents are quasi linear; they are a good approximate linear extrapolation of the unitary conductance measured at positive

voltages. The resulting reconstructed I/V relation shows an ohmic behavior with no saturation in the voltage window tested. A detailed view of the currents at positive and negative voltages shows that the inward currents are apparently bigger than the outward ones. This may indicate a slight rectification of the unitary conductance but it could also be due to a not perfect beta fit.

In the next step we examined the conductance of the channel as a function of the K^+ concentration as well as the selectivity of Kcv_{NTS} for different cations. Fig 3A shows the conductance of Kcv_{NTS} within the ohmic range as a function of different symmetrical K^+ concentration on both sides of the membrane.

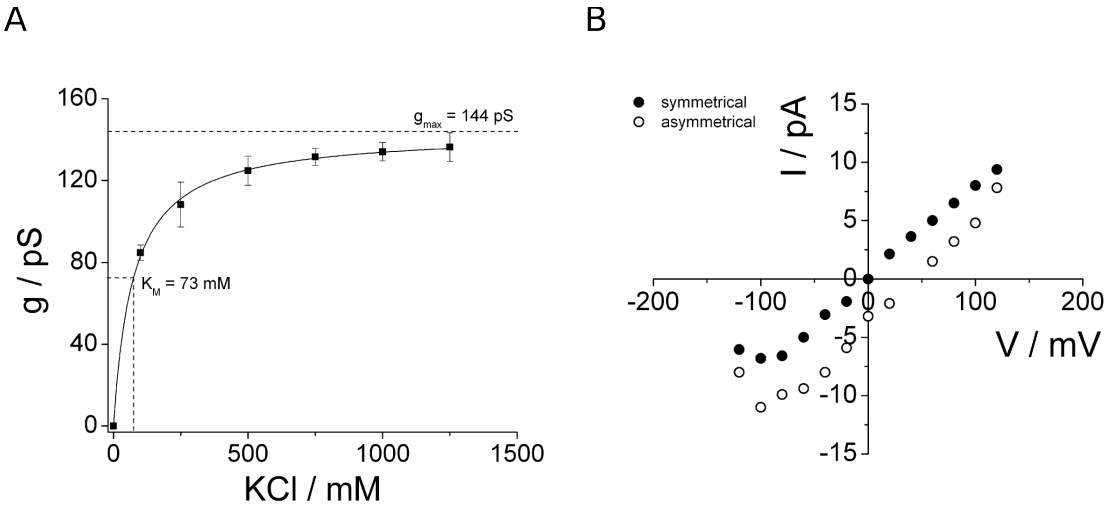

Fig 3 Conductance- and shift- experiments of Kcv_{NTS}

(A) Conductance measurements with different symmetrical KCl concentration. Values are means +- SD of n = 4 experiments (B) Representative K^+ selective experiment with a shift of the reversal potential from 0 mV (black dots; symmetrical 100 mM KCl solution) to ca. + 40 mV (white circles; asymmetrical KCl solution (trans: 500 mM/cis: 100 mM).

The single-channel conductances from these experiments are fitted with a modified Michaelis-Menten function (Eq 1), with g_{max} as the maximum conductance, K_M as the half maximum conductance and [x] as the K^+ concentration. This provides a maximum conductance of (g_{max}) = 144 pS and a half maximum conductance of (K_M) = 73 mM.

$$y = g_{max}\frac{[x]}{K_M * [x]}$$

Eq 1 Michaelis-Menten function

The conductance of Kcv_{NTS} exhibits a strong increase in the low concentration window; a 2.5 fold increase in K^+ from 100 mM to 250 mM results in a 1.4 fold increase in conductance. A further increase in K^+ causes only a small increase in conductance; at concentrations > 1M the conductance approaches saturation. The maximum conductance, which can be achieved, is a unitary conductance of 144 pS. The fit yields a half maximal conductance at 73 mM K^+.

The results of this analysis fit well with another Kcv-channel, the Kcv_{PBCV-1} (Kcv *Paramecium bursaria chlorella* virus – 1), which reveals a similar saturation of the conductance at a potassium concentration > 500 mM (Pagliuca et al., 2007). The maximum conductance of the latter channel however is larger; it approaches a maximal conductance of 362 pS.

To test whether Kcv_{NTS} is a K^+ selective channel, we measured the single channel conductance not only in symmetrical but also under non-symmetrical conditions.

$$E_{rev} = \frac{R * T}{z * F} * ln \frac{c_{trans}}{c_{cis}}$$

$$E_{rev} = \frac{-60\ mV}{z} * log \frac{c_{cis}}{c_{trans}}$$

Eq 2 Nernst equations

The regular (upper equation) and simplified (lower equation) form of the Nernst equation.

From the Nernst equation (Eq 2), with the ideal gas constant R = 8.31447 $J*Mol^{-}1*K^{-1}$, the temperature T = 298.15 K, the valence z of the ion, the Faraday constant F = $9.64853*10^4$ $C*Mol^{-1}$ and the concentration c of the solutes in the trans/cis compartment, we expect that the equilibrium voltage should shift from a value of 0 mV under symmetrical conditions to +42 mV when the channel is measured in asymmetrical solutions with 500 mM KCl in trans and 100 mM KCl in cis. The result of such an experiment is shown in Fig 3B. The open channel I/V relation reverses at 0 mV in symmetrical conditions and shifts positive under the asymmetrical condition by +40 mV. This value is in good agreement with the calculated reversal potential of + 42 mV for a K^+ conducting channel.

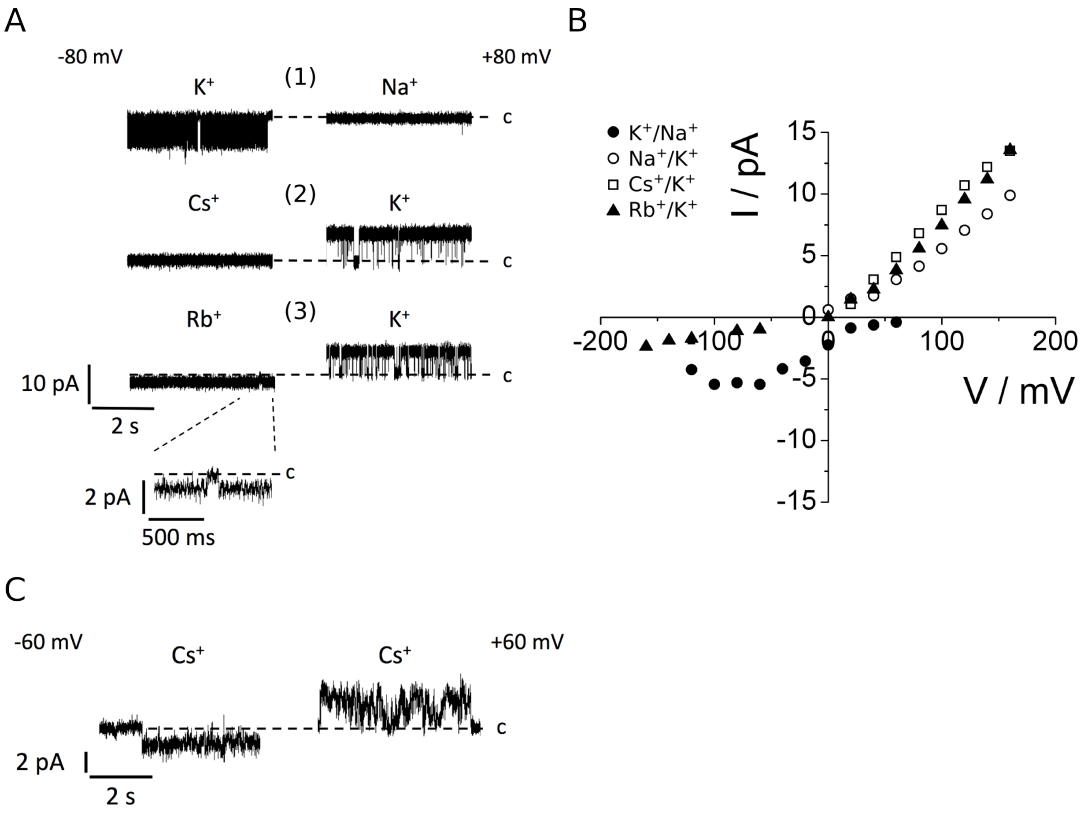

Fig 4 Selectivity experiments of Kcv_{NTS}

(A) Representative current traces in response to different cations. The magnification in (3) is offline filtered with 200 Hz. (B) Selectivity experiments in trans/cis configuration with Na^+ (black dots and open circles), Cs^+ (open squares) or Rb^+ (black triangles) (concentration 100 mM). (C) Representative current responses with symmetrical CsCl (concentration 100 mM).

In further experiments we examined the cation selectivity of the channel. Fig 4 summarizes these experiments. Representative channel current responses are given in A at holding potentials of -80 mV and +80 mV respectively. When K^+ is replaced on one side of the membrane by either sodium or cesium there are no more channel openings detectable. This means that the Kcv_{NTS} channel is not permeant to either of these ions. The plot in Fig. 4B shows the respective I/V curves of experiments with K^+ on the one side and different cations on the other side of the membrane. Experiments with sodium (black and white circles) show that the channel is highly selective for K^+ over Na^+. The I/V curve is not crossing the voltage axis meaning that Na^+ is not conducted. The black circles show an experiment in which sodium is on the cis side and potassium on the trans side (and Fig 4 (1)). The inward current, which is carried by K^+, shows the normal behavior of the K^+ conducting channel with a negative slope conductance at negative potentials; there is no measurable outward current consistent with the view that the channel does not conduct Na^+. The asymptotic trend of each curve is due to the chemical gradient for potassium ions. Experiments with rubidium show a different behavior of Kcv_{NTS}. Rb^+ is presumably a permeant ion; this is expected from structural and functional work with other potassium channels (Doyle, 1998). However in the case of Kcv_{NTS} the conductance is very low. The data in Fig 4 show that the current is

systematically below the zero current level indicating that the channel is constantly open with a low unitary amplitude. It was challenging to determine open/closed transitions, because the currents were so small, that they often disappeared in the background noise (Fig 4A (3)); the single to noise ratio was very low. Still individual channel fluctuations could be detected meaning that the small current is indeed due to channel activity (Fig 4A (3) magnification).

The experiments with cesium reveal another unexpected property. When Cs^+ is on the trans side of the membrane the channel does not generate an inward current meaning that it does not carry this cation (Fig 4A (2)). But the I/V curve shows in this situation no the asymptotic trend; the I/V curve is linear and extrapolates to 0 mV. This behavior is unusual and cannot be explained by common theories of channel selectivity. It seems as if the channel is not conducting Cs^+ and that Cs^+ may even enter the pore and block it. Experiments with symmetrical cesium chloride solution instead reveal that the channel is able to conduct cesium Fig 4C. The current amplitudes are different from the canonical fluctuations of potassium currents. This finding is in agreement with other findings of e.g. $K_v2.1$ (K^+ voltage-gated channel 2.1), which is also able to conduct Cs^+ when K^+ is not present (Kiss et al., 1998). The channel is able to conduct an ion, which is in mixed solutions non permeant, when this sort of ion is the only one available. This interpretation is in good agreement with the data from recordings in asymmetrical potassium and cesium solutions. In this case Kcv_{NTS} conducts potassium ions only, because this cation competes out Cs^+. The data are also in good agreement with findings, which show that Cs^+ is, unlike Na^+, able to enter the pore of Kcv channels and that it can stabilize the channel tetramer (Pagliuca et al., 2007). In the next section we examined the blocking effect of cesium on Kcv_{NTS}.

4.4.2. Cesiumblock of Kcv_{NTS}

Cesium ions are known to block potassium channels (Hille, 2001); previous experiments have shown that also the macroscopic Kcv_{NTS} current is blocked by extracellular Cs^+ when the channel is expressed in HEK293 cells (Greiner, 2011). Here we examined the blocking effect of cesium on Kcv_{NTS} on the single-channel level from the extracellular, the intracellular as well from both sides. As planar lipid bilayer setups have no extra- and intracellular compartments, we defined the trans side as the extracellular and the cis side as the intracellular compartment following to the orientation of the channel in whole-cell. In both measuring conditions Kcv_{NTS} revealed a negative slope conductance at negative holding potentials, which is in according to the whole cell data the extracellular side (Gazzarrini et al., 2009).

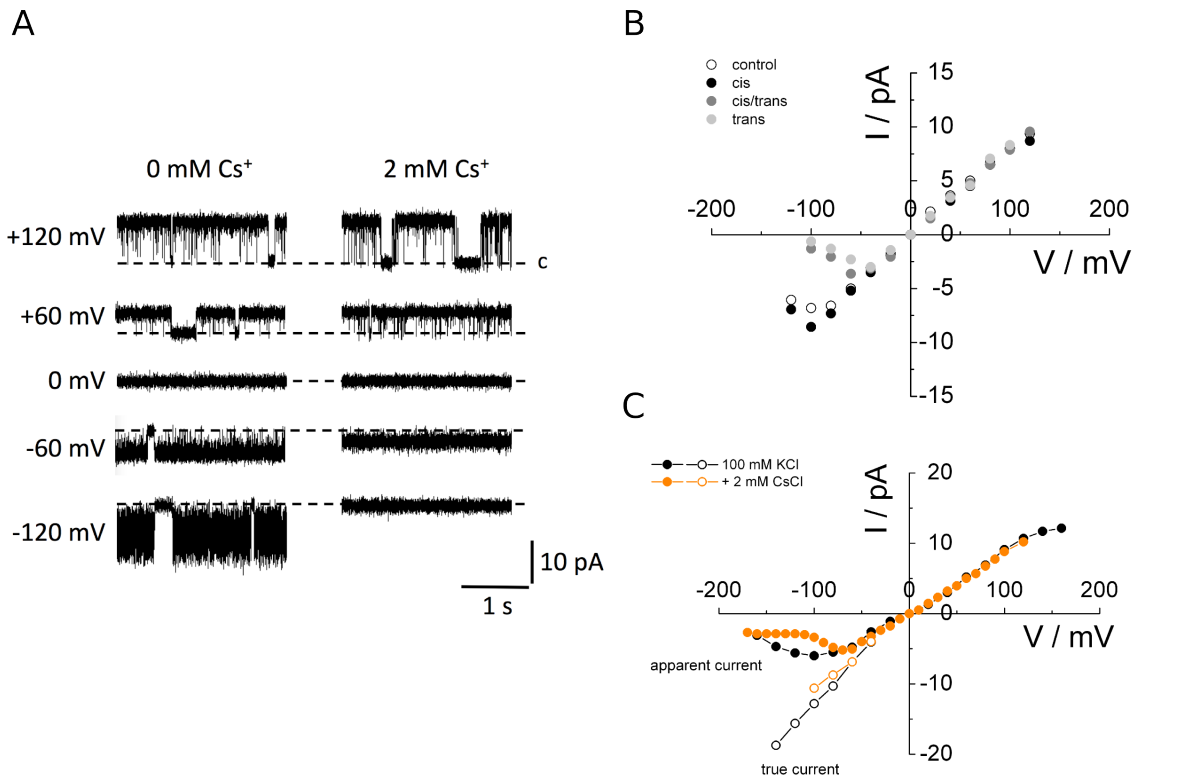

Fig 5 Kcv_{NTS} is blocked by cesium from the trans side.

(A) Representative single-channel current responses of Kcv_{NTS} with 0 mM CsCl and 2 mM CsCl (trans/cis) (in 100 mM KCl symmetric). The closed states are denoted with c and dashed lines. (B) Single-channel I/V curve with 0 mM CsCl (control) and 2mM CsCl either in the cis, cis/trans or trans compartment. (C) The apparent and true single-channel I/V curve of two representative measurements with 0 mM CsCl and 2 mM CsCl

The current responses indicate that cesium has a strong blocking effect on the inward currents of Kcv_{NTS}, if cesium is in the trans compartment. The outward currents seem not to be affected in this condition. The single-channel I/V curve in B confirms these findings. Experiments were done in 100 mM KCl solution with 2 mM CsCl in the cis, the trans and in the cis/trans compartment. The control (0mM CsCl) and 2mM CsCl in the cis compartment show the same behavior of the I/V relations. Both reveal the flickering phenotype at negative potentials and a normal outward current at positive potentials indicating that CsCl has no effect when it is added to the cis compartment. An experiment with CsCl in both compartments (cis/trans) shows a block of the inward currents, indicating that CsCl has an effect when it is added to the trans compartment. The single-channel amplitudes > -60 mV seem to be reduced. The flickering behavior (negative slope conductance) of Kcv_{NTS} is still found but right shifted. The last experiment with cesium in the trans compartment shows that the channel is blocked just from one side. The aforementioned blocking effect of cesium in the cis/trans compartment is the same of the blocking effect, which occurs in the trans compartment only. This is in agreement with an effective Cs^+ block of the inward current of inward rectifier channels (Hille, 2001).

In order to evaluate the mechanistic basis of the block we again analyzed the reduced single-channel amplitudes in the presence of Cs^+ with a beta-fit. This provides information on whether the reduced amplitudes are caused by a very fast block (Hille, 2001). Fig 5C shows that the block (orange circles) can be reconstructed by this analysis to the true current values (orange circles). The true current amplitudes from the two experiments with the control (no Cs^+) and 2 mM Cs^+ overlap perfectly. This indicates that cesium is able to block Kcv_{NTS} by amplifying a mechanism, namely the one, which is responsible for the fast gating at negative voltages. This effect of Cs^+ leads to the increase in negative slope conductance, which arises from a fast unresolved gating of the channel; as a result it appears as if the channel is blocked.

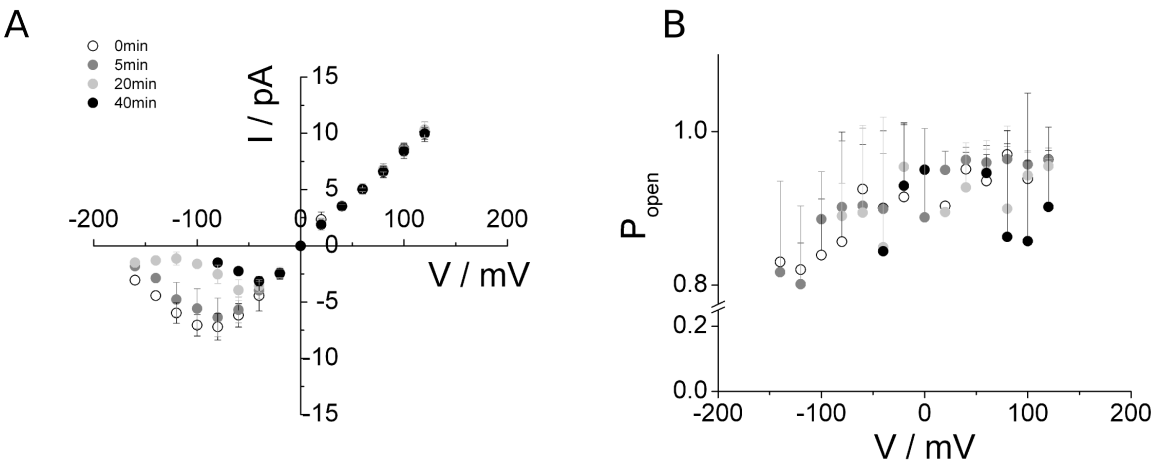

Fig 6 The cesium effect on Kcv_{NTS} is time dependent.

(A) Single-channel I/V curves. (B) Single-channel open probabilities. Experiments were done in symmetrical 100 mM KCl solution and 2 mM CsCl in the trans/cis compartment. The legend in A indicates the time after CsCl addition for A and B. Values are means +- SD of n = 4 experiments.

The data in Fig 6A show a surprising time dependent increase in the Cs^+ generated block. Single-channel I/V curves are obtained at different time points after adding 2 mM CsCl to the cis and trans compartment (3 of 4 measurements were done with CsCl in the cis/trans compartment; one experiment was done with CsCl in the trans compartment. Since Cs^+ blocks the channel only from the trans side all measurements were pooled). The obtained data just before addition of CsCl (0 min) can be seen as control; at this point of time cesium has no effect on the I/V relation. Already 5 min after cesium addition the channel shows slight reduced amplitudes at holding potentials more negative than -60 mV. The full effect of the Cs^+ block as in Fig 5A occurs only more than 20 min after cesium was added to the bath medium. Even 40 min after the application of the blocker there is still an increase in the Cs^+ block. At this time point channel fluctuations were collected in the presence of Cs^+ only up to -80 mV; at more negative voltages channel fluctuations could no longer be distinguished from the noise.

To address the question whether Cs^+ blocks the unitary conductance or the open probability of the channel we estimated the latter parameter in the presence of Cs^+. The plot in Fig 6B

shows that cesium has no appreciable effect on the open probabilities of Kcv_{NTS}. The channel has a very high voltage independent open probability > 80% at each time point, with a slight decrease at extreme negative holding potentials; the latter is due to the fast gating effect. The insensitivity of the open probability to Cs^+ means that the entire block of Kcv_{NTS} by Cs^+ is exerted on the single-channel amplitudes. It has been mentioned before that the Cs^+ block develops over time. Such a low process for the block of an ion channel is very unusual. To further examine the dynamics of this process we analyzed the block in more detail (Fig 7).

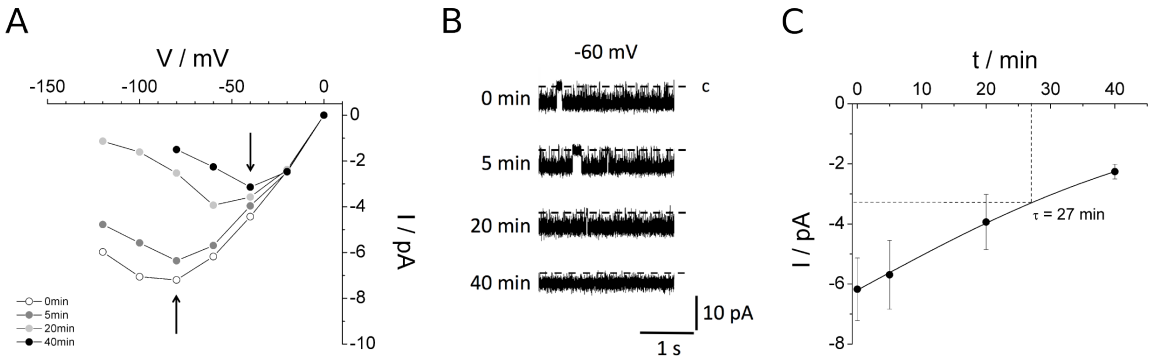

Fig 7 Time dependent effect of cesium at negative holding potentials

(A) Negative slope conductances at different time points. The inflection points shift with increasing time of cesium treatment (arrows) (B) Representative single-channel responses at different time points and at a holding potential of -60 mV. (C) Time dependent effect of cesium on the current amplitude at a holding potential of -60 mV.

The I/V curves in A show the negative slope conductance of Kcv_{NTS} as a function of time with Cs^+ in the medium. The error bars are omitted here for clarity. To estimate the dynamics of the block, the point of inflection of the I/V curve i.e. from -80 mV to -40 mV is determined (arrows). This value shifts with time of cesium treatment to more positive values. Fig 7B shows representative current responses of Kcv_{NTS} from one continuous recording at a holding potential of -60 mV at different time points after adding cesium to the medium. From 0 min to 5 min there are only slight differences in the single-channel amplitudes (Fig 7A). A stronger reduction in channel amplitudes occur 20 min after start of the treatment. At a time point of 40 min it was challenging to determine clear openings because the amplitudes of the open channel states disappeared often into the background noise of the closed state (most lower panel; dashed line). The single to noise ratio was very low. Fig 7C shows a plot of the open channel amplitudes as a function of time in Cs^+ at a holding potential of -60 mV. The data imply an exponential decay in the unitary current, which can be fitted with a single exponential Eq 3 were f is the amplitude, t the time and τ the time constant.

$$y = \frac{f}{1 + e^{\frac{t}{\tau}}}$$

Eq 3 Current-time function

The fit yields a time constant (τ) of 27 min for the Cs^+ induced decay in single-channel amplitudes. As a result it can be concluded that a cesium block, with such a low dynamic is rather unusual. In other channels Cs^+ blocks the channel immediately. A relatively low concentration of cesium is sufficient to achieve over time the same phenotypically voltage dependent block of a K^+ current, which is in other channels obtained by increasing concentrations of Cs^+ (Draber & Hansen, 1994; Pagliuca et al., 2007).

4.4.3. pH dependent behavior of Kcv_{NTS}

The activity of membrane proteins is influenced by many environmental factors. In addition to the direct environment like lipids, sterols or other proteins, signal molecules are very important to determine channel function. Protons e.g. are known to alter channel function (Thompson et al., 2008). KcsA the most extensively studied potassium channel (Roux, 2005), is very sensitive to the proton concentration i.e. to the pH. KcsA has a very high open probability in an acidic pH range and closes drastically at a pH > 5 (Thompson et al., 2008). To test whether Kcv_{NTS} is sensitive to the proton concentration, we performed experiments in buffers with different pH values, ranging from a pH of 9 to a pH of 4. The potassium chloride concentration was kept constant at 100 mM KCl. Furthermore we took buffers out of the Good buffer family in order to keep the buffer properties similar (except at a pH of 4 were we took potassium acetate (CH_3COOK), because no Good buffer has a pks around 4). Fig 8 shows typical single-channel current responses in buffers with different pH values.

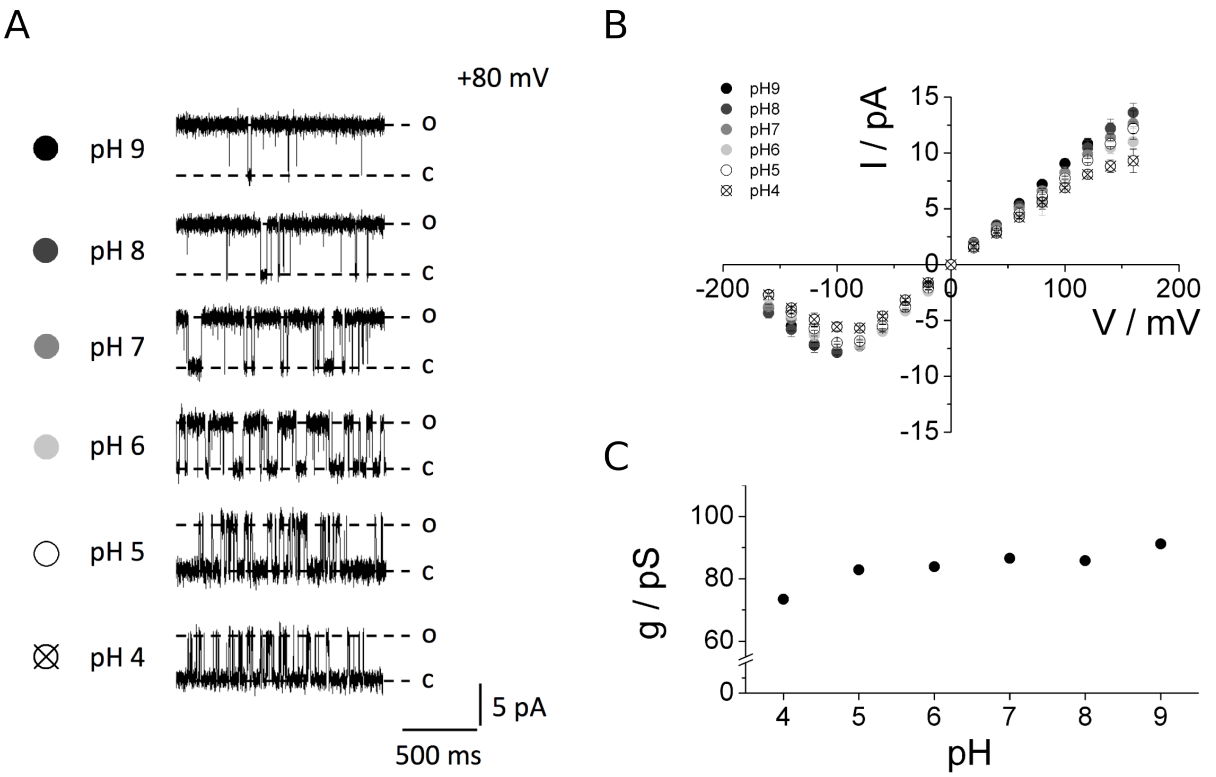

Fig 8 Gating behavior of Kcv_{NTS} at different pH conditions.

(A) Representative current responses at a holding potential of +80 mV. Open and closed states are denoted with o and c respectively. (B) Single-channel I/V curves at all tested pH conditions. Values are means +- SD of n = 5 experiments. (C) Conductance of Kcv_{NTS} within the ohmic ranges of (B).

Fig 8A shows representative single channel currents of Kcv_{NTS} at a holding potential of + 80 mV at all tested pH conditions. The channel has at each pH mainly the same single-channel amplitude; the unitary single channel I/V relation is plotted in Fig 8B. Notable neither the negative slope conductance nor the outward currents are much affected. At a pH of 4 the channel has slightly reduced current amplitudes over the whole voltage window tested. To test whether this effect is related to the potassium acetate (CH_3COOK) buffer we performed experiments at a neutral pH of 7 and compared them with the normal conditions with HEPES (pH 7) as a representative buffer of the Good buffer family (Fig 9). The results of these experiments show no distinct difference in single-channel amplitudes (A) and in the open probabilities (B). This suggests that the buffer has no effect on channel function. Since CH_3COOK is titratable from a pH of 7 to 4 we decided to take this buffer for the aforementioned experiments at pH 4.

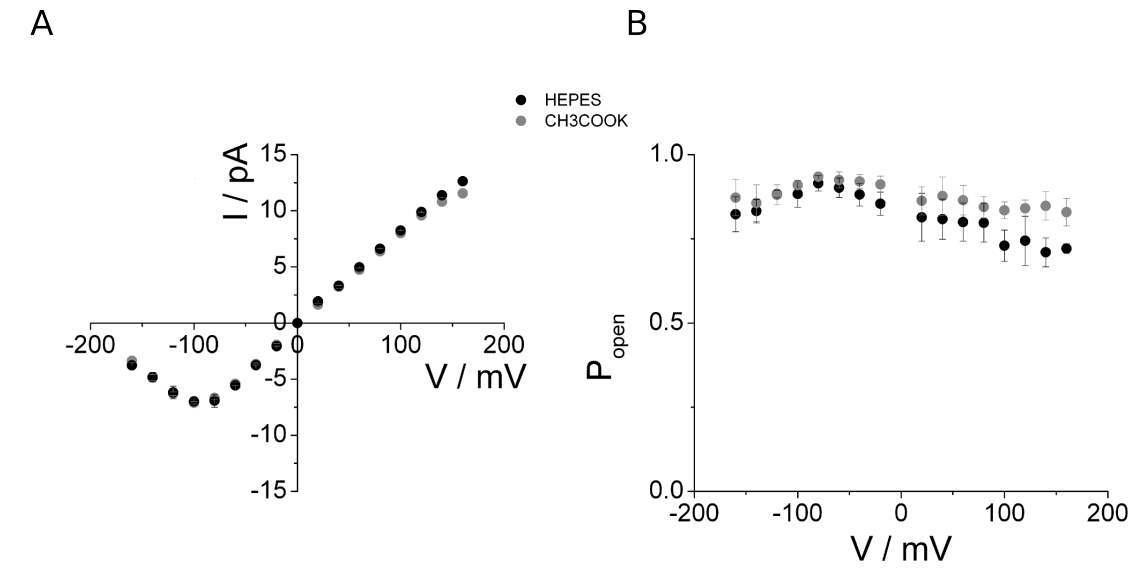

Fig 9 Properties of Kcv_{NTS} in potassium chloride solutions (100 mM) buffered with either HEPES or CH_3COOK at pH 7. (A) Single-channel I/V curves and (B) open probabilities of Kcv_{NTS}. Values are means +- SD of n = 5 experiments.

After excluding effects of the buffer on channel function we estimate the unitary conductance of the channel as a function of the pH; the data are plotted in Fig 8C. The data show a very slight increase from ca. 70 pS at a pH of 4 to 85 pS at a pH of 7 to ca. 90 pS at a pH of 9. Collectively the data show that the pH has no drastic impact on the unitary conductance of Kcv_{NTS}. In contrast the pH has a strong effect on channel gating (Fig 8A).

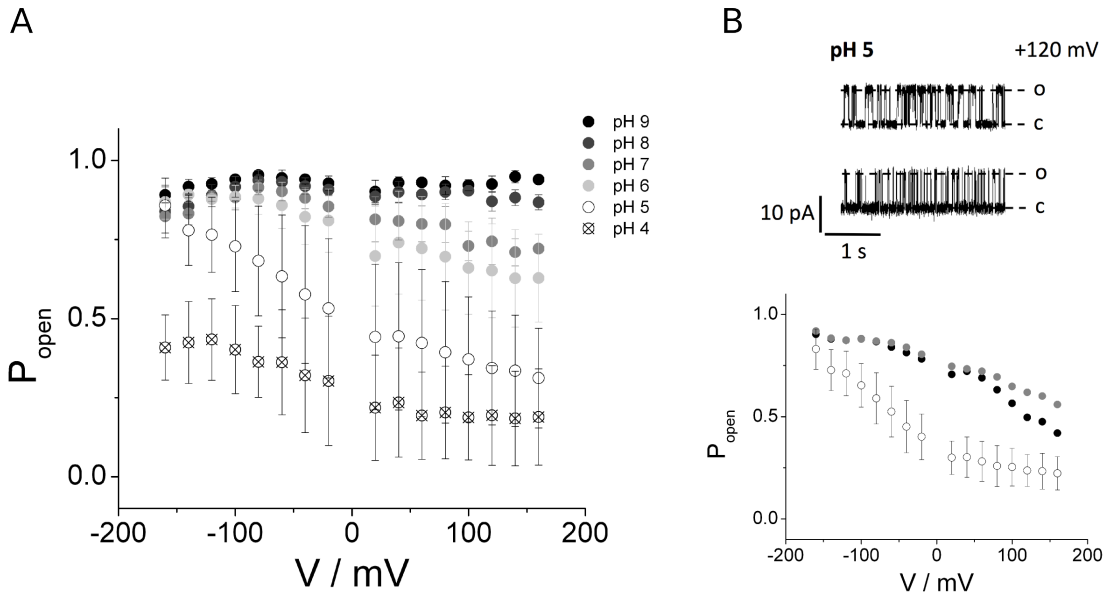

Fig 10 pH and voltage dependent open probabilities of Kcv_{NTS}

(A) Open probabilities with different pH conditions within the whole voltage window tested. All experiments were done in symmetrical 100 mM KCl solution and 10 mM Good buffer (pH 9-5) or CH_3COOK (pH 4). Values are means +- SD of n experiments; pH 9-7 n = 5; pH 6 and 5 n = 6; pH 4 n = 4 (B) Gating behaviors (upper panel) and open probabilities (lower panel) of the channel within the same pH condition of 5. Because of the large standard deviations, the open probabilities at this pH were divided into two groups with a higher and lower open probability.

Fig 10A shows the open probabilities of Kcv_{NTS} over the whole voltage window tested. The channel exhibits a very high P_o with > 90% at an alkaline pH of 9. At neutral pH values of 8 and 7 the P_o is around 80% with a slightly higher P_o at pH of 8 than at pH 7. With decreasing pH values in the range of 6 to 4 the open probability is drastically reduced. At a pH of 4 the P_o decreases to ca. 10% at +160 mV.

Important to note is that the decrease in P_o with acidic pH values correlates with an increase in voltage dependency of the channel. While P_o is essentially voltage independent it shows an increasing voltage dependency with acidification. Another observation is that the standard deviations of the P_o values increase for acidic pH values. A reason for this large variability is due to different gating modes, which could be seen in measurements in pH 5 (buffer MES). Under this condition we saw two different gating behaviors (Fig 10B; upper panel) with two different open probabilities (Fig 10B), which are both voltage dependent. Out of 6 experiments we saw twice a channel with a high, voltage dependent P_o (90% at -160 mV to 50% at +160 mV). Four times we saw a steeper decrease of the P_o from a P_o value of ca. 80% down to ca. 10%. The channel shows in both gating modes a high frequency of openings but they vary in the open times. The open times in the voltage dependent gating mode with a higher P_o are longer than the open times of the lower P_o. The same two gating modes were also observed at a pH of 6 and 4 (data not shown).

The results of these experiments suggest that an alkaline pH stabilizes the activity of Kcv_{NTS}; the channel has only one gating mode and the open probability is high. Acidic pH introduces more variability with two distinct gating modes and a higher sensitivity to the voltage.

To titrate the pH sensitive site in Kcv_{NTS} we plotted the strong voltage dependent open probability (mean values without standard deviations) of the channel at positive holding potentials as a function of the pH values (Fig 11).

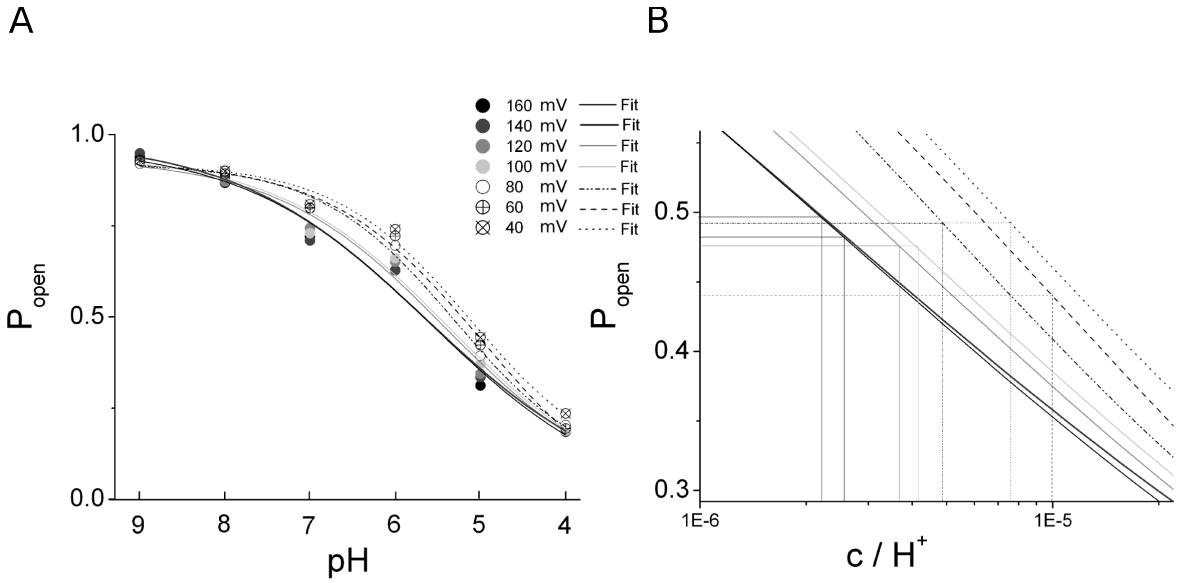

Fig 11 Strong voltage dependency of Kcv_{NTS} at positive holding potentials

(A) The open probabilites of the positive holding potentials are plotted against the pH values. The standard deviations are ommited for clarity. The fit analysis was done with a Hill equation (see below). (B) A detailed view of the half maximum open probability at the given proton concentration. The colors of the lines refer to the voltages given in the legend.

The data were fitted with an alternative Hill-equation (Eq 4), with start- and endpoints of the open probability, n as the Hill-factor and k the Michaelis-Menten constant.

$$y = Start + (End - Start)\frac{x^n}{k^n + x^n}$$

Eq 4 Alternative Hill equation

The plot in Fig 11 shows that the open probabilities of each positive holding potential can be fitted well with the Hill-equation. The channel is half maximal open at pH values ranging from 5 to 6 (Fig 11A). There is only a slight shift of the fitted curves from alkaline to acidic pH values with decreasing holding potentials. The Hill-Factor (k) of Eq 4 determines a cooperativity of the H^+ effect on the channel. A reaction shows cooperativity with k values > 1, no cooperativity with k = 1 and an negative-cooperativity with k < 1 (Saboouri & Moosavimovahedi, 1994). The fits in A reveal k values between 0.4 and 0.5 suggesting a negative-cooperativity for the effect of H^+ on Kcv_{NTS} gating.

The plot in B shows the half maximum open probability in more detail. We plotted the open probability of the channel as a function of the proton concentration between pH 5 and pH 6. The colors/symbols of the curves refer to the positive holding potentials given in the legend of Fig 11A. Even though the range of proton concentrations is small the value for the half maximum open probability shows a systematic dependency on the membrane voltage. At extreme potentials of +140 mV and +160 mV the fits yield the same curves meaning that the value for the H^+ concentration is saturated. For lower voltages the results of the fit shift to lower H^+ concentrations. This means that the channel tolerates at lower voltages a higher H^+ concentration at half maximal open probability. Collectively the data imply that a pH value of around 6 corresponds to the value of the H^+ concentration, which generates a half maximal voltage dependent open probability of the channel.

4.5. Discussion

The sequence of Kcv_{NTS} contains many of the structural hallmarks of functional K^+ channels (5.4). From this and from a comparison of the amino acid sequence of Kcv_{NTS} with that of the well-studied potassium channel $Kcv_{ATCV\text{-}1}$, it was already anticipated that Kcv_{NTS} is a functional potassium channel (5.4). Furthermore previous work by Greiner (Greiner, 2011) had already demonstrated that Kcv_{NTS} generates a conductance in HEK293 cells. The present data, in which Kcv_{NTS} was functionally reconstituted in planar lipid bilayers, finally proves that the

small Kcv_{NTS} protein is indeed a functional channel; the protein generates canonical K^+ selective single-channel fluctuations. This excludes the possibility that the data in HEK293 cells, which express this protein, are due to an unspecific up-regulation of endogenous K^+ channels.

A detailed analysis of Kcv_{NTS} shows that the channel has a very high cation selectivity. Kcv_{NTS} does not conduct sodium ions. The degree of selectivity in the bilayer experiments is even higher than that, which was determined from expressing the channel in HEK293 cells (Greiner, 2011). Here we find that the channel does not pass at all Na^+; in the latter study it was found that the channel has a selectivity for K^+ over Na^+ in the range of 10:1. This discrepancy may be explained by the fact that the determination of selectivity is more precise on the basis of single-channel data than on the basis of the reversal voltage of macroscopic current measurements; the latter approach was used by Greiner (Greiner, 2011). Alternatively the artificial bilayer may also affect the channel fold in such a way that the selectivity is higher than in the membrane of cells.

The present data further show that Kcv_{NTS} conducts rubidium. This observation fits well with the results of single-channel experiments with the closely related channel Kcv_{ATCV-1} (Gazzarrini et al., 2009). In the latter study the channel was expressed in Xenopus oocytes and recorded in the cell-attached configuration. This only allows a control of the external cation concentration. Like in the case of Kcv_{NTS} also Kcv_{ATCV-1} conducts Rb^+ and also in the latter the unitary channel currents are very small with Rb^+ as a substrate. The consequence is a low inward conductivity in these channels compared to experiments with K^+ as charge carrier. Also in this case the data from whole-cell measurements in HEK293 cells, which express Kcv_{NTS} (Greiner, 2011) show different results. These data conclude from the relative position of the reversal voltages of the macroscopic currents in an external solution with either K^+ or Rb^+ that Kcv_{NTS} conducts rubidium better than potassium. Also in this case the data from single-channel experiments are more precise than those obtained from whole cell recordings so that the present data and those with Kcv_{ATCV-1} (Gazzarrini et al., 2009) suggest that the channels in question conduct K^+ better than Rb^+. With Rb^+ as a charge carrier the unitary conductance is only about half of that in K^+.

At the single-channel level, the open probability of the channel with Rb^+ is very high but the amplitudes are so small that the analysis becomes very difficult. Under the assumption that the channel shows in whole-cell experiments with Rb^+ a similar high P_o we must expect that the reduced single-channel currents are compensated by a higher activity. In the whole-cell recordings, which measure the product of the single-channel current and the open probability this could indeed result in a higher whole-cell current.

Very interesting are the data on Cs^+ permeation through Kcv_{NTS}. It occurs that the channel conducts cesium but only if the experiments are performed in a pure CsCl solution; in this case the cesium currents are different from those of potassium currents. The amplitudes are smaller and not as discrete as the ones of potassium. If however Cs^+ is present in a buffer with

K^+ the former becomes a blocker of K^+ currents. This means that if the channel can choose between potassium and cesium ions, cesium will not be conducted. The findings of the selectivity experiments fit well with the aforementioned findings in the potassium channel $K_v2.1$ (Kiss et al., 1998). A selective ion channel can under certain circumstances conduct non-permeant ions when this sort of ions is the only one available.

When Cs^+ is added to a buffer with K^+ the Cs^+ blocks the K^+ current in a voltage dependent manner. One interesting aspect of this block is the fact that the block is strictly side-specific: Cs^+ only blocks from the trans side. This together with the voltage dependency suggests that Cs^+ is reaching a binding side in the selectivity filter from the trans side and that this entry is supported by voltage; the data are consistent with a model according to which Cs^+ competes with K^+ for this site. With increasing time of Cs^+ treatment the probability of occupying the binding site with Cs^+ increases, which in turn leads to a stronger block. This holds true if the binding constant of Cs^+ to this binding site progressively increases over that for K^+. Remarkable is the slow dynamics with which this process develops. The phenotype of the time dependent block correlates with a concentration dependent block (Draber & Hansen, 1994; Pagliuca et al., 2007). This type of block leads to a negative slope conductance, which shift with time to more positive voltages. The time dependent increase in the block mimics the increase in the Cs^+ block of other K^+ channels, which is achieved by increasing concentrations of the blocking ion Cs^+. Collectively the data suggest that the sensitivity of the channel to Cs^+ increases over a time window of tens of minutes presumably driven by a Cs^+ selective very slow conformational change of the channel protein. This interpretation is further supported by data from patch-clamp recordings at single-channel level in HEK293 cells expressing Kcv_{NTS}. These recordings show a slow reduction of the unitary conductance after adding 1 mM Cs^+ to the bath solution in inside-out configuration (P. Becker unpublished data).

The question on the mechanism by which Cs^+ affects the fold of the channel remains unanswered. Cs^+ could bind to a yet unidentified binding side in the channel. An additional explanation of the Cs^+ block could be a time dependent increase of Cs^+ ions at the outer leaflets of the membrane. This may also result in the aforementioned block. Anionic phospholipids (e.g. DPhPS) can be used to test this hypothesis. In this case a faster block would be achieved due to a higher attractivity of the cationic cesium ions to the anionic headgroups than cesium ions to the zwitterionic headgroup of DPhPC.

Further interesting inside into structure function correlates in Kcv_{NTS} derived from experiments in different pH buffers. It is probably not too surprising to find a pH dependency of the channel since most enzymes show some sort of pH sensitivity. Also many channels are pH sensitive. KcsA for example is highly active at acidic pH and becomes inactive very steeply with pH > 5.5 (Cuello et al., 1998; Thompson et al., 2008). The present data show that Kcv_{NTS} has the inverse dependency on the pH; the channel becomes more active with increasing pH values.

The interesting observation here is that an acidification of the buffer causes a decrease in open probability of the channel without any effect on the unitary conductance. The peculiar feature of this pH effect is that it introduces a voltage dependency. While the channel is at alkaline pH virtually voltage independent, it acquires a titratable voltage dependency at more acidic pH values. It occurs as if the slope of the P_o value as a function of voltage becomes steeper with acidic pH (Fig 10).

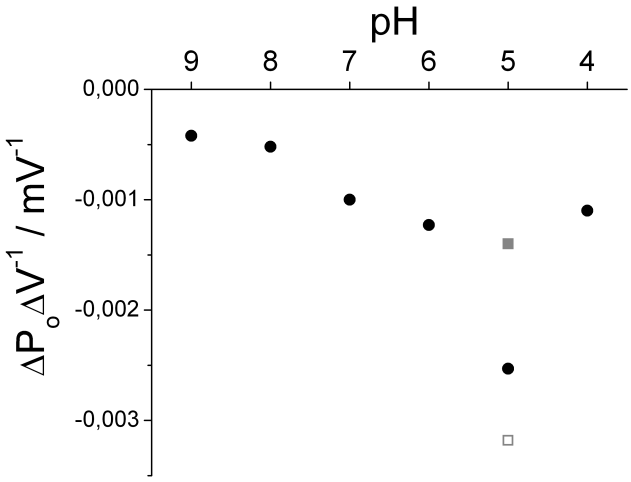

Fig 12 Voltage dependency of the open probability as a function of pH.

The data show the maximal slope of the P_o/V dependency in Fig 10A in a voltage window between -80 mV and -20 mV. Black dots indicate the slopes at different pH values. Gray and white squares indicate the slope values for the two different gating modes at pH 5 (Fig 10A). The standard deviations are omitted for clarity.

A plot of the steepest slope as a function of the pH shows that the voltage dependency can be titrated with pH. The data point at pH 5 seems not to fit the trend of this curve (black circles). Since we observed two gating modes at pH 5 the slope values were determined individually from both data sets. The plot in Fig 12 shows that the data from one gating mode e.g. the one with a higher open probability are in the trend of the general titration curve. If we assume that the alternative gating mode in pH 5 follows a different pH dependency the open probability of the channel is nicely titratable and the half maximal pH value for this effect is at about pH 6-7.

Since the channel protein is quasi fully embedded in the membrane (Braun et al., 2013) it is interesting to speculate on the mechanism, which is responsible for the pH dependency. The fact that an acidic pH introduces a voltage dependency is best explained by a model in which the channel contains a titrable amino acid. This amino acid becomes protonated and acquires a charge with protonation. Only when the amino acid is charged the channel has a sensor for the membrane voltage and this sensor is then directly or indirectly connected to a gate of the channel. The aa sequence of the channel shows nine charged aa in the protein plus the C- and N-terminus, which all are probable sites for a pH sensor. With the Hill-function we calculated at which pH the channel shows the half maximal open probability. For each positive holding

potential we calculated pH values around 5 to 6. At extreme holding potentials the fits match nicely with a half maximal open probability around pH 6. With decreasing positive potential, the half maximum open probability shifts more to a pH of 5. This implies that the channel needs to sense less protons at extreme positive potentials to achieve the half maximum open probability. When the voltage decreases the channel has to sense more protons in order to achieve the half maximal open probability. The higher the electric field the more protons are probably pulled into the channel pore. This may lower the need for protons to achieve a half maximal open probability. In the context of this scenario the question about the nature of the amino acid arises, which one is able to sense protons? The only aa with a pka value close to the calculated pH around 5 to 6 is histidine (His, H) with a pka of 6 for the side chain. Kcv_{NTS} bears three His (H7, H44 and H66); one in the first TMD (H7), one in the second TMD (H66) and the third adjacent to the selectivity filter (H44). If we assume that the first and the second TMD are fully submerged into the lipid bilayer, than the His (H44) adjacent to the filter could probably be the amino acid candidate, which senses the protons. This hypothesis is even more likely since the His is presumably in the ion pathway and can hence also serves as a voltage sensor and a gate. To determine the significance of the histidine as the pH sensor and the gate, mutations are required in which the histidine is exchanged for a phenylalanine; the latter has a similar size and is not titratable. If such a mutation does not impede channel function the Kcv_{NTS} channels should show a voltage independency over the whole pH range.

4.6. Conclusion

The analyses of the minimal viral potassium channel Kcv_{NTS} at the single-channel level show that the viral channel shares many functional hallmarks with more complex potassium channels. The channel is selective for K^+ against Na^+. In addition it is permeable to Rb^+ and Cs^+. The latter cation is only conducted when no other permeable cation is present. In mixed solutions with K^+, Cs^+ becomes already at low mM concentrations a voltage dependent blocker of K^+ currents. The slow increase in sensitivity of the channel to Cs^+ block over minutes indicates a slow Cs^+ induced conformational change in the protein, which increases the susceptibility of the protein to Cs^+ block. This must occur in a side specific manner since Cs^+ blocks Kcv_{NTS} only from the extracellular (trans) side. In addition Kcv_{NTS} is also able to sense different pH conditions, which suggests a pH sensor presumably in the selectivity filter. Altogether the data show that the small Kcv channels in particular the Kcv_{NTS} are a very good model system to study structure/function correlates and protein/lipid interaction. In spite of their small size they have many functional properties of complex channels with respect to selectivity and gating. This means that these properties are already inherent in the miniature pore structure of K^+ channels and must hence be understood on the basis of these small structures.

4.7. References

Abenavoli, A., DiFrancesco, M. L., Schroeder, I., Epimashko, S., Gazzarrini, S., Hansen, U. P., Thiel, G., & Moroni, A. (2009). Fast and slow gating are inherent properties of the pore module of the K+ channel Kcv. *The Journal of General Physiology*, *134*, 219–29. doi:10.1085/jgp.200910266

Ashcroft, F. M. (2000). *Ion Channels and Disease*. Academic Press.

Barrett, P. M., Alagely, a, & Topol, E. J. (2012). Cystic fibrosis in an era of genomically guided therapy. *Human Molecular Genetics*, *21*, R66–71. doi:10.1093/hmg/dds345

Bertl, A., Slayman, C. L., & Gradmann, D. (1993). Membrane Biolo Membrane of Saccharomyces cerevisiae. *The Journal of Membrane Biology*, *199*, 183–199.

Blunck, R., Cordero-Morales, J. F., Cuello, L. G., Perozo, E., & Bezanilla, F. (2006). Detection of the opening of the bundle crossing in KcsA with fluorescence lifetime spectroscopy reveals the existence of two gates for ion conduction. *The Journal of General Physiology*, *128*, 569–581. doi:10.1085/jgp.200609638

Braun, C. J., Lachnit, C., Becker, P., Henkes, L. M., Arrigoni, C., Kast, S. M., Moroni, A., Thiel, G., Schroeder, I. (2013) Viral potassium channels as a robust model system for studies of membrane-protein interaction. *Biochimica et Biophysica Acta - Biomembranes*, *1838, 1096-1103.* doi:10.1016/j.bbamem.2013.06.010

Cuello, L. G., Jogini, V., Cortes, D. M., Pan, A. C., Gagnon, D. G., Dalmas, O., Cordero-Morales, J. F., Chakrapani, S., Roux, B., & Perozo, E. (2010). Structural basis for the coupling between activation and inactivation gates in K(+) channels. *Nature*, *466*, 272–275. doi:10.1038/nature09136

Cuello, L. G., Romero, J. G., Cortes, D. M., & Perozo, E. (1998). pH-Dependent Gating in the Streptomyces lividans K+ Channel. *Biochemistry*, *37*, 3229–3236.

Doyle, D. A. (1998). The Structure of the Potassium Channel: Molecular Basis of K+ Conduction and Selectivity. *Science*, *280*, 69–77. doi:10.1126/science.280.5360.69

Doyle, D. A. (2004). Structural changes during ion channel gating. *Trends in Neurosciences*, *27*, 298–302. doi:10.1016/j.tins.2004.04.004

Draber, S., & Hansen, U. P. (1994). Fast single-channel measurements resolve the blocking effect of Cs+ on the K+ channel. *Biophysical Journal*, *67*, 120–129. doi:10.1016/S0006-3495(94)80461-8

Frohns, F., Käsmann, A., Kramer, D., Mehmel, M., Kang, M., Etten, J. L. Van, Gazzarrini, S., Moroni, A., Thiel, G., Ka, A., & Scha, B. (2006). Potassium Ion Channels of Chlorella Viruses Cause Rapid Depolarization of Host Cells during Infection Potassium Ion Channels of Chlorella Viruses Cause Rapid Depolarization of Host Cells during Infection. doi:10.1128/JVI.80.5.2437

Gazzarrini, S., Kang, M., Abenavoli, A., Romani, G., Olivari, C., Gaslini, D., Ferrara, G., van Etten, J. L., Kreim, M. Kast, S. Thiel, G. & Moroni, A. (2009). Chlorella virus ATCV-1 encodes a functional potassium channel of 82 amino acids. *The Biochemical Journal*, *420*, 295–303. doi:10.1042/BJ20090095

Greiner, T. (2011). Characterization of novel potassium transport proteins from Chlorella viruses. Dissertation at TU Darmstadt

Heginbotham, L., LeMasurier, M., Kolmakova-Partensky, L., & Miller, C. (1999). Single streptomyces lividans K(+) channels: functional asymmetries and sidedness of proton activation. *The Journal of General Physiology*, *114*, 551–559.

Hille, B. (2001). *Ionic Channels of Excitable Membranes*. Sinauer Associates Inc.

Huth, T., Schroeder, I., & Hansen, U.-P. (2006). The power of two-dimensional dwell-time analysis for model discrimination, temporal resolution, multichannel analysis and level detection. *The Journal of Membrane Biology*, *214*, 19–32. doi:10.1007/s00232-006-0074-6

Kiss, L., Immke, D., LoTurco, J., & Korn, S. J. (1998). The Interaction of Na+ and K+ in Voltage-gated Potassium Channels Evidence for Cation Binding Sites of Different Affinity. *Journal of General Physiology*, *111*, 195–206.

Koert, U. (2005). Synthetic ion channels: functional analysis and structural studies. *Physical Chemistry Chemical Physics : PCCP*, *7*, 1501–1506.

MacKinnon, R. (2004). Potassium channels and the atomic basis of selective ion conduction (Nobel Lecture). *Angewandte Chemie (International Ed. in English)*, *43*, 4265–4277. doi:10.1002/anie.200400662

Mehmel, M. (2003). Possible function for virus encoded K+ channel Kcv in the replication of chlorella virus PBCV-1. *FEBS Letters*, *552*, 7–11. doi:10.1016/S0014-5793(03)00776-2

Miller, C. (2000). An overview of the potassium channel family. *Genome Biology*, *1*, REVIEWS0004. doi:10.1186/gb-2000-1-4-reviews0004

Montal, M., & Mueller, P. (1972). Formation of bimolecular membranes from lipid monolayers and a study of their electrical properties. *Proceedings of the National Academy of Sciences of the United States of America*, *69*, 3561–3566.

Morita, H., Wu, J., & Zipes, D. P. (2008). The QT syndromes: long and short. *Lancet*, *372*, 750–763. doi:10.1016/S0140-6736(08)61307-0

Neupärtl, M., Meyer, C., Woll, I., Frohns, F., Kang, M., Van Etten, J. L., Kramer, D., Hertel, B., Moroni, A., & Thiel, G. (2008). Chlorella viruses evoke a rapid release of K+ from host cells during the early phase of infection. *Virology*, *372*, 340–348. doi:10.1016/j.virol.2007.10.024

Pagliuca, C., Goetze, T. A., Wagner, R., Thiel, G., Moroni, A., & Parcej, D. (2007). Molecular properties of Kcv, a virus encoded K+ channel. *Biochemistry*, *46*, 1079–1090. doi:10.1021/bi061530w

Perozo, E., Cortes, D. M., & Cuello, L. G. (1999). Structural Rearrangements Underlying K+-Channel Activation Gating. *Science*, *285*, 73–78. doi:10.1126/science.285.5424.73

Roux, B. (2005). Ion conduction and selectivity in K(+) channels. *Annual Review of Biophysics and Biomolecular Structure*, *34*, 153–171. doi:10.1146/annurev.biophys.34.040204.144655

Saboouri, A. A., & Moosavimovahedi, A. A. (1994). Evaluation of the Hill Coefficient from Scatchard and Klotz Plots. Biochemical Education, *22*, 48–49.

Sansom, M. S. P., Shrivastava, I. H., Bright, J. N., Tate, J., Capener, C. E., & Biggin, P. C. (2002). Potassium channels: structures, models, simulations. *Biochimica et Biophysica Acta*, *1565*, 294–307.

Schroeder, I., & Hansen, U.-P. (2007). Saturation and microsecond gating of current indicate depletion-induced instability of the MaxiK selectivity filter. *The Journal of General Physiology*, *130*, 83–97. doi:10.1085/jgp.200709802

Spampanato, J., Escayg, a, Meisler, M. H., & Goldin, a L. (2003). Generalized epilepsy with febrile seizures plus type 2 mutation W1204R alters voltage-dependent gating of Na(v)1.1 sodium channels. *Neuroscience*, *116*, 37–48.

Thiel, G., Baumeister, D., Schroeder, I., Kast, S. M., Van Etten, J. L., & Moroni, A. (2011). Minimal art: or why small viral K(+) channels are good tools for understanding basic structure and function relations. *Biochimica et Biophysica Acta*, *1808*, 580–588. doi:10.1016/j.bbamem.2010.04.008

Thompson, A. N., Posson, D. J., Parsa, P. V, & Nimigean, C. M. (2008). Molecular mechanism of pH sensing in KcsA potassium channels. *Proceedings of the National Academy of Sciences of the United States of America*, *105*, 6900–6905. doi:10.1073/pnas.0800873105

Yellen, G. (2002). channels and their relatives. *Nature*, *419*.

Zheng, J., & Sigworth, F. J. (1997). Selectivity Changes during Activation of Mutant Shaker Potassium Channels. *Journal of General Physiology*, *110*.

5. Viral potassium channels as a robust model system for studies of membrane-protein interaction

5.1. Abstract

The viral channel Kcv_{NTS} belongs to the smallest K^+ channels known so far. A monomer of a functional homotetramer contains only 82 amino acids. As a consequence of the small size the protein is almost fully submerged into the membrane. This suggests that the channel is presumably sensitive to its lipid environment. Here we perform a comparative analysis for the function of the channel protein embedded in three different membrane environments. 1. Single-channel currents of Kcv_{NTS} were recorded with the patch clamp method on the plasma membrane of HEK293 cells. 2. They were also measured after reconstitution of recombinant channel protein into classical planar lipid bilayers and 3. into horizontal bilayers derived from giant unilamellar vesicles (GUVs). The recombinant channel protein was either expressed and purified from *Pichia pastoris* or from a cell-free expression system; for the latter a new approach with nanolipoprotein particles was used. The data show that single-channel activity can be recorded under all experimental conditions. The main functional features of the channel like a large single-channel conductance (80 pS), high open-probability (>50%) and the approximate duration of open and closed dwell times are maintained in all experimental systems. An apparent difference between the approaches was only observed with respect to the unitary conductance, which was ca. 35% lower in HEK293 cells than in the other systems. The reason for this might be explained by the fact that the channel is tagged by GFP when expressed in HEK293 cells. Collectively the data demonstrate that the small viral channel exhibits a robust function in different experimental systems. This justifies an extrapolation of functional data from these systems to the potential performance of the channel in the virus/host interaction.

Keywords

black lipid membrane, cell-free protein expression, membrane-protein interaction, patch clamp, planar patch clamp, single-channel measurement, viral potassium channel

Abbreviations

BLM: black lipid membrane; DPhPC: 1,2-diphytanoyl-*sn*-glycero-3-phosphocholine; GUV: giant unilamellar vesicle

5.2. Introduction

Potassium channels are membrane proteins, which catalyze the flux of K^+ ions in a selective and regulated (gated) manner across membranes. Because of their high transport capacity, the activity of single K^+ channels can be measured at high temporal resolution with various

electrophysiological methods. This detailed functional information is paralleled by explicit knowledge on the molecular architecture of K^+ channels, which is available from crystal structures (Doyle, 1998, 2004; Santos et al., 2012) and MD simulations (Tayefeh et al., 2007; Treptow & Klein, 2012). The combination of these high-resolution data is now frequently used to correlate structural properties with functional features (Kast et al., 2011; Roux, 2005).

In this context, however, it occurs that for a full understanding of ion channel function also the membrane, in which the protein is embedded, has to be considered. Crystal structures for example reveal the binding of anionic phospholipids to specific pockets in the KcsA protein (Valiyaveetil et al., 2002). Complementary functional studies underscore the role of these interactions for channel function (Dopico et al., 2012; Rodriguez-Menchaca et al., 2012; Seeger et al., 2010). Structural data furthermore suggest that the architecture and orientation of transmembrane domains of membrane proteins are designed in such a way that they avoid a thermodynamically unfavorable hydrophobic mismatch between protein and lipid bilayer (Hertel et al., 2006; Killian, 2003; Kim et al., 2012). This predicts that the thickness of the membrane, which can vary in the plasma membrane within microscopic domains (Simons & Sampaio, 2011), may affect the structure of a channel and as a consequence also its activity. Functional studies in this context have indeed shown that the conductance of the BK channel (big conductance K^+ channel) is depending on the thickness of the lipid bilayer in which it is inserted (Yuan et al., 2004). But not only the membrane-spanning domains of the proteins seem to be involved in lipid-channel interaction. A recent study suggests that the M0 helix of KcsA, which is lying on the cytosolic membrane interface, performs a “barrel roll” movement upon channel opening; this event seems to be dependent on the presence of anionic lipids in the inner membrane leaflet (Iwamoto & Oiki, 2012).

The activity of ion channels is generally recorded with the patch clamp method (Neher & Sakman, 1976) in membranes from living cells, which express a channel of interest in a homologous or heterologous manner. In this case, the composition of the membrane in which the channel functions, is largely unknown and not under the control of the experimenter. In such a system, there is also little control over the arrangement of the channel proteins in clusters, their interaction with endogenous proteins or their insertion into micro-domains like lipid rafts. A reduced system, which offers more control over the environment of a channel protein, is provided by the planar lipid bilayer technique (Montal & Mueller, 1972; Williams, 1994). With this method, the lipid bilayer can be chosen and modified by the experimenter on demand. This offers the opportunity to reconstitute a purified protein into a pure and defined bilayer. The problem with this approach is that bilayers may under certain circumstances also generate lipid pores (Laub et al., 2012) so that bilayer recordings with reconstituted proteins are sometimes challenged as artifacts (Becucci et al., 2012). Another source of artifacts in bilayer recordings is related to the isolation procedure of the channel proteins. Protein produced recombinantly or isolated from cells may be contaminated with endogenous channel proteins from the expression system (Accardi et al., 2004; Labarca & Latorre, 1992). A further

disadvantage of the bilayer technique is that some protocols require a solvent like decane for building the bilayer (Williams, 1994). In the procedure some solvent may stay in the bilayer and modify the membrane in an unpredictable fashion. Another technique generates planar lipid bilayers from giant unilamellar vesicles (GUVs) (Kreir et al., 2008). This approach does not require any solvents; but in this protocol, usually 10% cholesterol is used for the fabrication of stable membranes.

In this work, we compare the basic single-channel properties of a model K^+ channel in a variety of different recording systems. The small viral K^+ channel Kcv_{NTS} is encoded by a *Chlorella* virus isolated from an alkaline lake in Nebraska (Greiner, 2011). Kcv_{NTS} is structurally very similar to Kcv_{ATCV-1} from *Acanthocystis turfacea Chlorella* virus-1. The latter is the prototype of the most recently isolated *Chlorella* virus group, which infects SAG type *chlorella* cells (Bubeck & Pfitzner, 2005) (Fig. 1). Previous studies have already shown that the both viral proteins are functional K^+ channels (Gazzarrini et al., 2009; Greiner, 2011). The interesting aspect in the context of the present work is that Kcv_{ATCV-1} and its orthologs are miniature indeed (Thiel et al., 2011). The four monomers, which form the functional tetramer, each contain only 82 amino acids. As we will demonstrate below by molecular dynamics (MD) simulations this small channel is quasi fully immersed in the lipid bilayer. We consider this an ideal model system for studying the relevance of protein/bilayer interactions. The environment of the protein is dominated by the lipid bilayer; extracellular or cytosolic domains can, if any, only play a minor role for channel function.

The systematic examination of viral K^+ channel function in different experimental conditions is important for a proper understanding of their role in the virus/host system. The current knowledge is that the great majority of *chlorella* viruses (39 over 41), which were sequenced so far, contain genes for small K^+ channels (Jeanniard et al., 2013). Expression studies show that the channel protein is produced as a late gene in the infected host cell (Kang et al., 2004). Recent experiments confirm with the help of a monoclonal antibody that the prototype channel Kcv from virus PBCV-1 is indeed present in the mature virion; it is presumably located in the inner membrane of the virus particle (Romani et al., n.d.). A bulk of circumstantial data suggests that the viral channel has a crucial role during early infection. Measurements of the membrane potential in the host *chlorella* NC64A, a unicellular green alga, have shown that the cells depolarize within the first few minutes of virus infection (Frohns et al., 2006). This depolarization is most likely caused by an insertion of few individual viral K^+ channels into the plasma membrane of the host during fusion of virus and host cell membrane (Thiel et al., 2010). Experimental support for this hypothesis comes from the observation that the same blockers, which inhibit the viral channel in heterologous systems or after reconstitution in planar lipid bilayers, also block the host depolarization (Frohns et al., 2006; Thiel et al., 2010). The crucial role of the viral channel in host infection is further underscored by experiments, which show that the sensitivity of host depolarization to channel blockers reflects the distinct inhibitor sensitivity of K^+ channel orthologs from

different viruses (Frohns et al., 2006). It was further found that a block of viral K^+ channel activity and the consequent inhibition of the host depolarization prevent infection. The latter could be attributed to a block of DNA ejection from the virus particle into the host (Thiel et al., 2010). A plausible explanation for this scenario is that the depolarization of the host cell, which is initiated by the viral channel, causes an efflux of K^+ salts and consequently water from the host cells (Neupärtl et al., 2008). This lowers the high internal pressure of the host cell and makes it easier for the virus to transfer its large dsDNA genome into the host. This interpretation of viral channel function during infection is based on extrapolations of functional data from heterologous expression systems and from reconstituting the viral channel protein in planar lipid bilayers. Because of the small size of the channels and the aforementioned potential dependency of channel function on the lipid bilayer it was so far not known whether these extrapolations are indeed valid.

The present data now show that conductance and gating properties of the channel are robust and observable in conventional patch clamp recordings and in different planar lipid bilayer experiments. With the exception of a smaller conductance and a slightly lower open-probability in the mammalian cell system, the basic functional features of the channel are maintained in all experimental approaches. There is little difference on whether the protein is synthesized by a mammalian cell, expressed and purified from yeast or produced in a cell-free system. The results of these experiments stress that functional data from different approaches can be used to draw conclusions on structure/function correlates in this miniature channel; the experimental data are also sufficiently general and allow an extrapolation of channel function in the virus/host system.

5.3. Methods

5.3.1. Protein expression in *Pichia pastoris*

The ORF encoding the Kcv_{NTS} gene was subcloned into a modified *P. pastoris* expression vector pPICZ A (Invitrogen) containing a Kozak consensus sequence, a His7 tag, a proteolytic site for the H3C protease and a LIC (ligation independent cloning) site on the N-terminus of the protein sequence. *P. pastoris* cells (SMD 1163 strain) were transformed with 3 μg of the PmeI linearized construct by using the *Pichia* Easy CompTM kit as described by the manufacturer (Invitrogen, Carlsbad, CA, USA). Positive colonies were selected from YPDS (10 g/l bacto yeast, 20 g/l bacto peptone and 20 g/l dextrose) agar plates containing 50 μg/ml zeocin. Single-colony starting cultures were grown in BMGYH medium [see the *Pichia* expression kit manual (Invitrogen)] at 30°C, 300 rpm for 36 hours. After centrifugation at 3,000 g for 10 min at 4°C, the pellet was resuspended to a D600 of 4 in BMMH medium [see the *Pichia* expression kit manual (Invitrogen)] and grown at 30°C, 300 rpm for 24 h. Each gram of cells was suspended in 1:20 ratio of breaking buffer as in Gazzarrini et al. (Gazzarrini et al., 2009). The presence of the overexpressed protein at the correct molecular weight was

verified on SDS-PAGE and Western blot. Cells were broken with a Cell Disruptor (TS Series Benchtop, Constant System Inc.) set on a 40 kPa pressure. The cell homogenate was centrifuged at 3,000 g for 10 min at 4°C. The supernatant was centrifuged at 30,000 g for 45 min at 4°C in presence of PEG 8000 10% (w/v) and NaCl 200 mM. The pellet, consisting of the microsomial fraction of the membrane, was solubilized with 200 mM octyl-glucopyranoside (Anatrace) for 4 hours at 4°C. Elution of the protein was performed as in Pagliuca et al. (Pagliuca et al., 2007), in presence of 40 mM octyl-glucopyranoside. The integrity and purity of the protein was checked on SDS-PAGE.

5.3.2. Cell-free protein production and purification

Cell-free production of the Kcv_{NTS} protein was done with the MembraneMax™ *HN* Protein Expression Kit (Invitrogen) following the manufacturer's instructions. The gene of Kcv_{NTS} was cloned into a pEXP5-CT/TOPO®-vector. To express the protein in its native form, a STOP-Codon was inserted right before the gene of a 6xHis-tag. Briefly, the DNA template was incubated with the synthesis reaction mix (MembraneMax™ *HN* reagent carrying a polyHis-tag, ribosomes, T7 RNA polymerase and energy renewal system) for 35 min at 37°C (1,000 rpm). The feeding buffer was added and the reaction was incubated for 1 h 45 min at 37°C (1,000 rpm). After the expression the protein sample was centrifuged (12 min, 16060 x g, RT) to remove insoluble material. The supernatant was loaded for 30 min onto a Ni-NTA column, which was equilibrated with an equilibration buffer [500 mM NaCl, 30 mM HEPES, 10% glycerin (all from AppliChem GmbH, Darmstadt, Germany), pH 7.5]. Unspecific binding was removed by washing the column with 20 mM imidazole (Sigma Chemical, Deisendorf, Germany) twice. The protein was then eluted with 250 mM imidazole in 7 fractions à 100 μL. After elution the protein was used directly in the planar bilayer system.

5.3.3. Vertical black lipid membrane (BLM) experiments

Planar lipid bilayers were formed in a vertical bilayer set up (IonoVation, Osnabrück Germany) by the monolayer folding technique (Montal & Mueller, 1972) over a hole (ca. 100 μm in diameter) in a Teflon foil. The hole was pretreated with a 1% hexadecane solution (MERCK KGaA, Darmstadt, Germany) in n-hexane (Carl ROTH, Karlsruhe, Germany). In the next step a lipid solution of 1,2-diphytanoyl-*sn*-glycero-3-phosphocholine (DPhPC, 15 mg/ml, from Avanti Polar Lipids, Alabaster, AL, USA) in n-pentane (MERCK) was pipetted onto the experimental solution (100 mM KCl, 10 mM HEPES, adjusted with KOH to a pH of 7.0). After evaporation of the solvent, the solutions in both chambers were raised to form a lipid bilayer. After formation of the bilayer a voltage protocol was applied for at least 5-10 min to exclude contaminations or unspecific channel activity of e.g. lipid pores (Laub et al., 2012). For incorporation of ion channels either in detergent (octyl-glucopyranoside) or imidazole (250 mM) a small amount (1-3 μl) was added into the trans compartment directly. After fusion of ion channels with the lipid bilayer different voltage protocols were applied to record the resulting currents.

All planar lipid bilayer measurements were done at room temperature (20-25°C). Ag/AgCl electrodes were connected to the head-stage of a patch clamp amplifier (L/M-EPC 7, List–Medical, Darmstadt). Membrane potentials are referred to the cis compartment. Single-channel currents were filtered at 1 kHz and digitized with a sampling interval of 280 μs (3.57 kHz) by an A/D-converter (LIH 1600, HEKA Electronik, Lambrecht, Germany).

5.3.4. Preparation of liposomes and formation of horizontal lipid bilayers

Giant unilamellar vesicles (GUVs) were formed by electroformation (Walde et al., 2010) with the Vesicle Prep Pro station (Nanion Technologies GmbH, München, Germany). The lipid solution contained 10 mM DPhPC and 1 mM synthetic cholesterol (AppliChem), dissolved in chloroform (AppliChem). The preparation of GUVs is reported elsewhere (Kreir et al., 2008). After formation of GUVs they were used (3 μl) in the Port-a-Patch system (Nanion) directly. GUVs touching the surface of the glass chip burst immediately to form stable lipid bilayers with high ohmic resistance (Kreir et al., 2008). In case of instable bilayers a 0.1 M HCl solution was used to stabilize the membrane. After stabilization the HCl solution was washed out with the experimental solution (100 mM KCl, 10 mM HEPES, adjusted with KOH to a pH of 7.0).

To avoid artifacts in the measurements the bilayer were tested prior to the addition of protein for at least 5-10 min; only bilayers, which revealed during the test no current fluctuations were used for further experiments. Afterwards, 0.5 – 2 μl of the protein (solubilized in octyl-glucopyranoside) was added directly onto the chip. After fusion of ion channels with the lipid bilayer different voltage protocols were applied to record the resulting currents. Single-channel currents were filtered at 3 kHz and with a sampling interval of 100 μs (10 kHz) with an EPC9 (HEKA) amplifier.

5.3.5. HEK cell experiments

Kcv_{NTS} was cloned between the *BglII* and *EcoRI* restriction sites of the multiple cloning site of the pEGPF-N2 vector (BD Biosciences, Heidelberg, Germany). No stop codon was inserted, so EGPF was fused in frame directly to the C-terminus of the channel protein. HEK293 cells were transiently transfected with GeneJuice (MERCK) following the manufacturer's instructions. The experiments were done 24-36 hours after transfection; the GFP fluorescence served to identify successfully transfected cells.

Patch clamp recordings were performed in cell-attached and inside-out mode. Pipette and bath solution were identical and contained 100 mM KCl, 1 mM $MgCl_2$, 1.8 mM $CaCl_2$, 10 mM HEPES, 100 mM Mannitol. pH was adjusted to 7.4 with KOH. Pipettes were pulled from borosilicate glass (Science Products, Hofheim, Germany) on a two-step puller (L/M-3P-A, List-Medical) and typically had a resistance of 15-20 MOhm. Currents were measured by a Dagan 3900 amplifier (Dagan corporation, Minneapolis, MN, USA) and digitized by a LIH8+8

(Instrutech/HEKA) at a rate of 200 kHz. The low-pass filter on the amplifier was set to 10 kHz or 5 kHz.

5.3.6. Data analysis

Current traces at different membrane voltages were recorded via Patchmaster (HEKA) and analyzed with Fitmaster (HEKA) and lab-built software (KielPatch, www.zbm.uni-kiel.de/aghansen/software.html). Current amplitudes were determined visually, an automated jump detector (Schultze & Draber, 1993) was used to construct the open-probability and dwell time histograms. The dwell time histograms were fitted with sums of 1-3 exponential functions.

5.4. Results and Discussion

5.4.1. Structural properties of Kcv_{NTS}

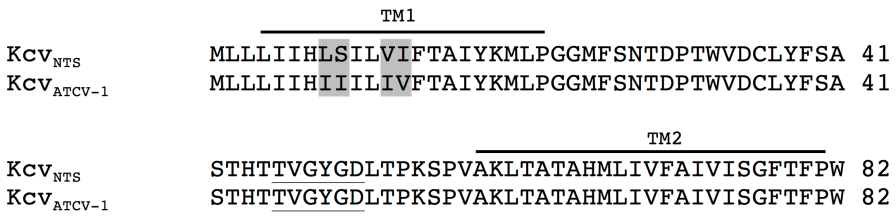

Fig 13 Amino acid sequence alignment of Kcv_{NTS} and Kcv_{ATCV-1}.

Exchanges are marked in gray, the signature potassium filter sequence is underlined. The predicted location of the two transmembrane helices TM1 and TM2 of Kcv_{ATCV-1} was taken from (Gazzarrini et al., 2009).

The Kcv_{NTS} channel is a very close relative of the previously characterized viral channel Kcv_{ATCV-1} (Gazzarrini et al., 2009); with only 82 amino acids they are the so far smallest known K^+ channels. The alignment shows that both channels differ in only 4 out of 82 amino acids (Figure 1). When transfected into HEK293 cells Kcv_{NTS} generates macroscopic currents (Greiner, 2011), which are similar to those obtained with Kcv_{ATCV-1} (Gazzarrini et al., 2009).

5.4.2. Comparison of channel activity in different systems

The influence of different systems for channel expression and reconstitution was studied by recording single-channel currents from Kcv_{NTS} under four different experimental conditions:

1.) The channel was produced in *Pichia pastoris* and the isolated protein reconstituted in a classical planar lipid bilayer (black lipid membranes, BLM).
2.) The channel was produced in a cell-free system and examined in the BLM.
3.) Giant unilamellar vesicles (GUVs) were used to form a horizontal membrane in an integrated planar patch clamp system. Protein from *Pichia pastoris* was reconstituted into this membrane.

4.) HEK293 cells were transfected with a plasmid containing the gene for a Kcv_{NTS}-GFP fusion protein and examined in a classical patch clamp setup.

Under all experimental conditions, it was possible to measure the single-channel characteristics of Kcv_{NTS}. After achieving in each system the appropriate conditions for single-channel recordings a transmembrane potential was applied. Because of the high open-probability of Kcv_{NTS} (see Fig 16B, below), the number of active channels could be easily estimated from a simple visual inspection of the current records. Bilayers or patches with no or too many (5 or more) channels were discarded. If current fluctuations of one to four channels were visible, a voltage protocol ranging from -120 to +120 mV with steps of 20 mV was applied. If the membrane stability allowed it, the protocol was repeated multiple times. For the determination of single-channel I/V curves (current voltage relationships) and for the estimation of the open-probability, single- and multi-channel data were used. Dwell-time histograms were obtained from recordings with one channel only.

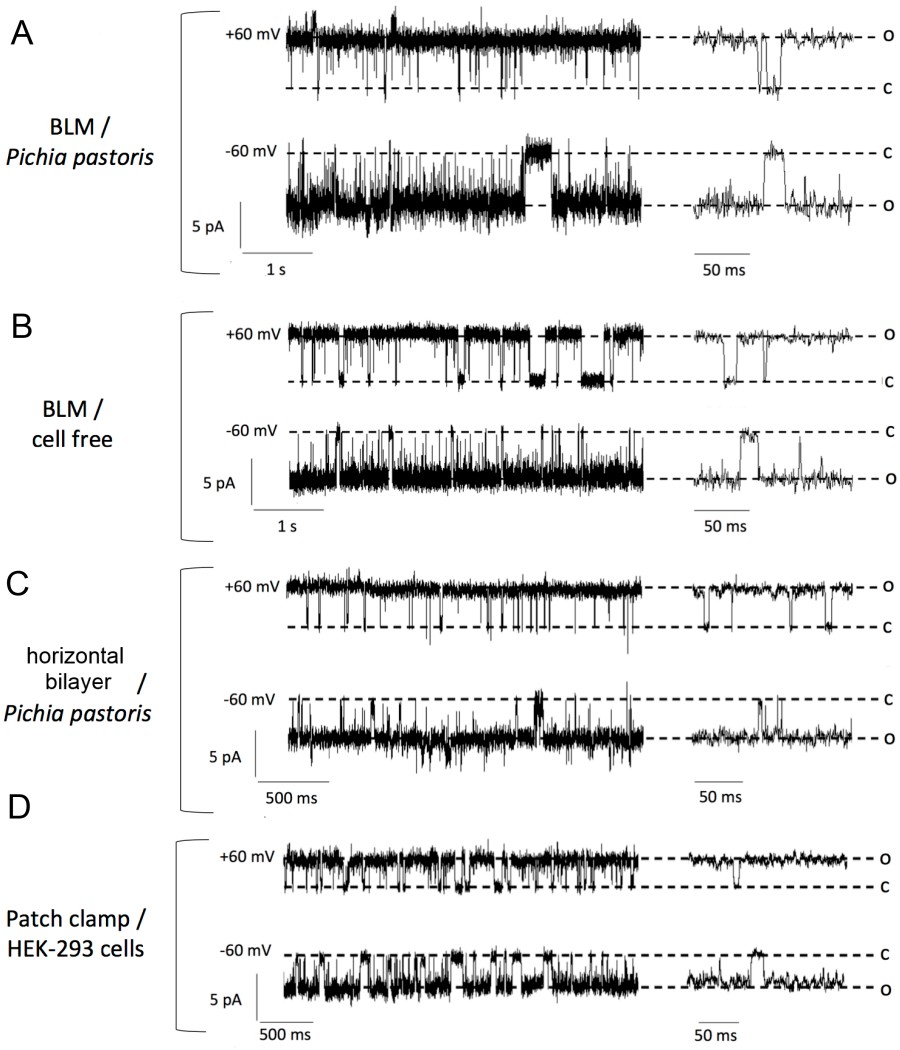

Fig 14 Representative current traces of single Kcv_{NTS} channels in different expression systems.

Currents were recorded in steady state at membrane potentials of +60 mV and -60 mV, respectively. C and O denote the closed and open channel, respectively. (A) Protein produced in *Pichia pastoris* and reconstituted in symmetric planar lipid bilayer. (B) Protein produced in a cell-free system in the same type of bilayer. (C) Protein from *Pichia pastoris* reconstituted into horizontal membranes formed from GUVs with planar patch clamp. (D) Inside-out patch clamp on HEK293 cells transiently transfected with a Kcv_{NTS}-GFP fusion protein. Data was offline filtered at 500 Hz (A,B) or 1 kHz (C,D)

Fig 14 shows representative current traces of single Kcv_{NTS} channels at +60 and -60 mV for all four experimental approaches. The characteristics of the channels are consistent under all conditions: the unitary conductance is similar and the channel exhibits very high open-probability throughout. The temporal behavior shows bursts of activity interrupted by short sojourns in a closed state. During bursts of activity, the channel approaches an open-probability of virtually 100% even though it is interrupted by very short closing events. They are visible as incomplete transitions towards the baseline because of the limited temporal resolution. The results of these experiments show that the large unitary conductance and the gating with a high open-probability, which is recorded by patch clamp measurements in living cells, is also maintained in the reduced bilayer systems. This overall similarity confirms that

the channel fluctuations, measured in the bilayer systems are not caused by lipid pores or solvent-induced membrane defects (Laub et al., 2012). Also a contamination from the expression system can be excluded as the source of channel activity.

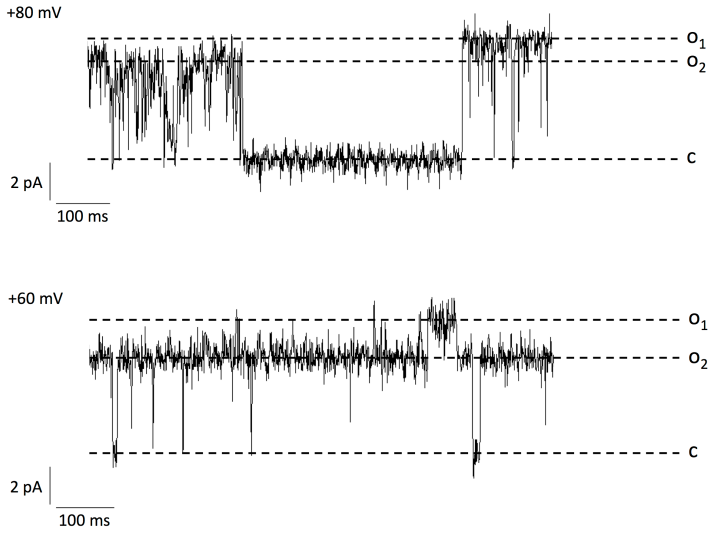

Fig 15 Subconductance states of a single Kcv_{NTS} channel purified from *Pichia pastoris* and reconstituted in BLM.

The dominant current level is O_2. Jumps into a higher level O_1 occur either via a closed state (upper panel) or directly (lower panel).

In addition to the prevailing conductance (marked by dashed lines in Fig 14), the channel occasionally displays other conductance states. This behavior is most obvious in the BLM system, where the channel could fluctuate between the dominant conductance and a level, which exceeded the latter by approximately 30 %. The channel is able to switch between the two conductance levels either via a closed state (Fig 15, upper panel) or directly (lower panel). This indicates that both conductances are indeed a property of Kcv_{NTS} and not introduced by a contamination. Because these types of fluctuations between a sub-state and a fully open state were not observed in all measurements it is possible that the unitary conductance of the channel is underestimated in the data of the I/V relation.

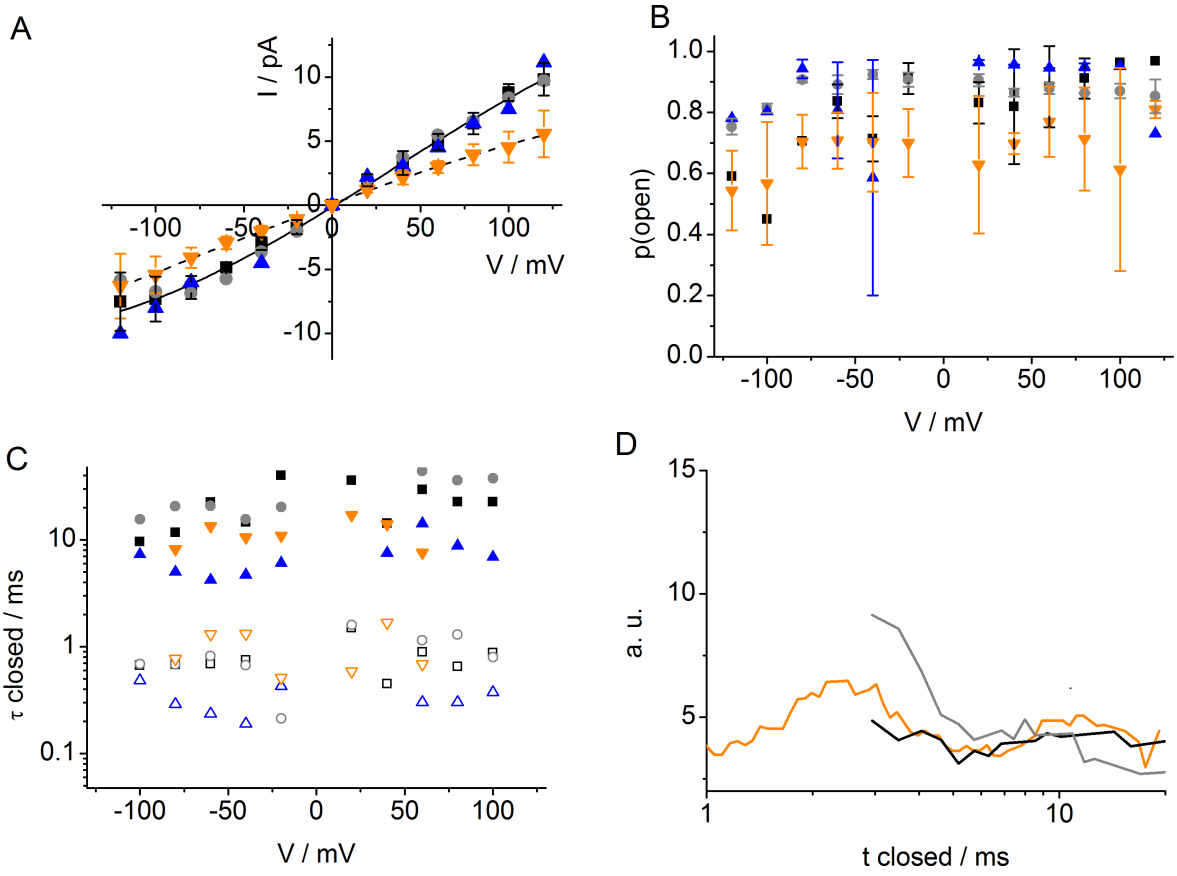

Fig 16 Electrophysiological properties of Kcv_{NTS} under different experimental conditions.

All panels use the same colors and symbols. Black (squares) and gray (circles): reconstitution in BLM with protein from *Pichia pastoris* and from cell-free synthesis, respectively. Blue (upright triangles): horizontal bilayers formed from GUVs by planar patch clamp. Orange (inverted triangles): patch clamp recordings on HEK cells. (A) Single-channel I/V curves of the dominant conductivity. Number of experiments: *Pichia pastoris* (n = 5) and cell-free production in BLM (n = 4), *Pichia* protein in horizontal bilayers (n = 2) and transfected HEK cells (n = 9, cell-attached and inside-out data were pooled). For clarity, the standard deviation is only shown for the HEK cell experiments and the *Pichia* protein in BLM. The lines are polynomial fits (without theoretical meaning) to the HEK cell data (dashed) and the other three conditions (solid line). (B) Single-channel open-probability. (C) Time constants of closed dwell times from one representative experiment for each condition. Open and closed symbols denote the two different time constants. (D) Representative closed dwell time histograms obtained at -60 mV from BLM and HEK cells.

Tab 1 Single-channel conductivity of Kcv_{NTS} in 100 mM KCl in different systems as determined by a linear fit from -60 to +60 mV to the I/V curves from several experiments. The number of experiments is given in brackets. From the channel protein expressed in *P. pastoris* and reconstituted in the planar patch clamp set up, only two data sets are available. The individual conductance values, which are appreciably different, are given instead of the average.

Pichia / BLM	81 ± 7 pS (5)
In vitro / BLM	87 ± 6 pS (4)
Pichia / planar patch clamp	68 / 80 pS
HEK	50 ± 6 pS (9)

The single-channel I/V curve of the dominant conductance level is essentially linear over the voltage range tested (Fig 16A). The slope conductance between +60 mV and -60 mV lies between 50 and 90 pS for the different recording conditions. The results are summarized in Table 1. There was no apparent difference between the unitary conductance measured in cell-attached and inside-out experiments on HEK293 cells; the data were therefore pooled for the I/V relation. A comparison of the unitary conductance values from different methods shows that the conductivity of the channel in HEK293 cells was significantly lower (50 pS) than in the all artificial systems (~80 pS). The present data cannot answer the question of why the unitary conductance is lower in cells than in the bilayers systems. The similarity in channel conductance from records in cell-attached mode and excised patches excludes cytosolic factors as an explanation for the low conductance in cells. One reason could be that the channel, which is expressed in HEK293 cells is C-terminally tagged with GFP. This explanation is plausible because the single-channel conductance of the similar Kcv_{ATCV-1} channel (Fig 13) is also 80 pS when measured without a GFP tag in the plasma membrane of *Xenopus* oocytes (Gazzarrini et al., 2009). This value corresponds to the conductance of Kcv_{NTS} in artificial bilayers (Tab 1). In patch clamp experiments in HEK cells, GFP-tagged Kcv_{ATCV-1} also shows a lower conductance (data not shown). The results of these experiments suggest that the unitary conductance of the channel is not per se smaller in a native plasma membrane.

We quantified the gating of the channel by calculating the open-probabilities and, where possible, time constants from dwell-time histograms. Fig 16B shows that the open- probability is practically voltage-independent and similar under all experimental conditions tested. The open-probability has an average of about 80%. Such a high open-probability has already been found for the close relative of Kcv_{NTS}: Kcv_{ATCV-1} also has a single-channel open-probability of about 80% in *Xenopus* oocytes (Gazzarrini et al., 2009) as well as in HEK293 cells (data not shown).

Dwell-time histograms were constructed and exponential fits of the closed-state histograms revealed two different time constants (Fig 16C) in all four systems. A third, faster, time constant could be observed only in HEK cells (not shown), most likely because of the faster

filtering and sampling in the patch clamp setup compared to the artificial bilayers. As expected from the overall open-probability, the time constants do not depend appreciably on the membrane potential; they are also within the scatter independent on the expression and recording system.

5.4.3. The small Kcv_{NTS} like channels are fully embedded in the lipid bilayer

The data show that the small Kcv_{NTS} channel maintains its overall activity in a variety of experimental systems. It will be a future goal to understand the correlations between structure of a channel in its membrane environment and function in more detail. To tackle this problem we illustrate the membrane location of such a short channel by performing preliminary MD simulations of the Kcv_{ATCV-1} variant. Omitting details of the model building process, which follows closely our earlier simulation studies of truncated KirBac1.1 (Tayefeh et al., 2007) and Kcv_{PBCV-1} (Tayefeh et al., 2009) in a solvated DMPC membrane and which will be described elsewhere, a homology model was derived from the X-ray crystallographic KirBac1.1 structure (Kuo et al., 2003), embedded in two different membrane environments, DMPC (fully saturated) and POPC (unsaturated), built-up using VMD 1.9 (Humphrey et al., 1996) by cutting overlapping lipid molecules from an initial 256 lipid bilayer, and simulated with NAMD 2.9 (Phillips et al., 2008) in 0.1 M aqueous KCl solution at 310 K and 1 bar with a time step of 2 fs on the basis of the CHARMM22 force field (Schlenkrich, Brickmann, MacKerell, 1996; Mackerell et al., 1998).

The key result is that this very short channel is practically fully immersed in the relatively thin lipid bilayers. This is illustrated in Fig. 17, which shows snapshot structures in DMPC and POPC after 40 ns simulation time. The protein remains very stable over several tens of nanoseconds although the different membrane environments induce structural modulations, which will be further analyzed in future work. As a signature, we show the diverging trends of the solvent-accessible surface of the two simulation setups, which indicate slightly differing overall shapes of the protein (Fig 17C).

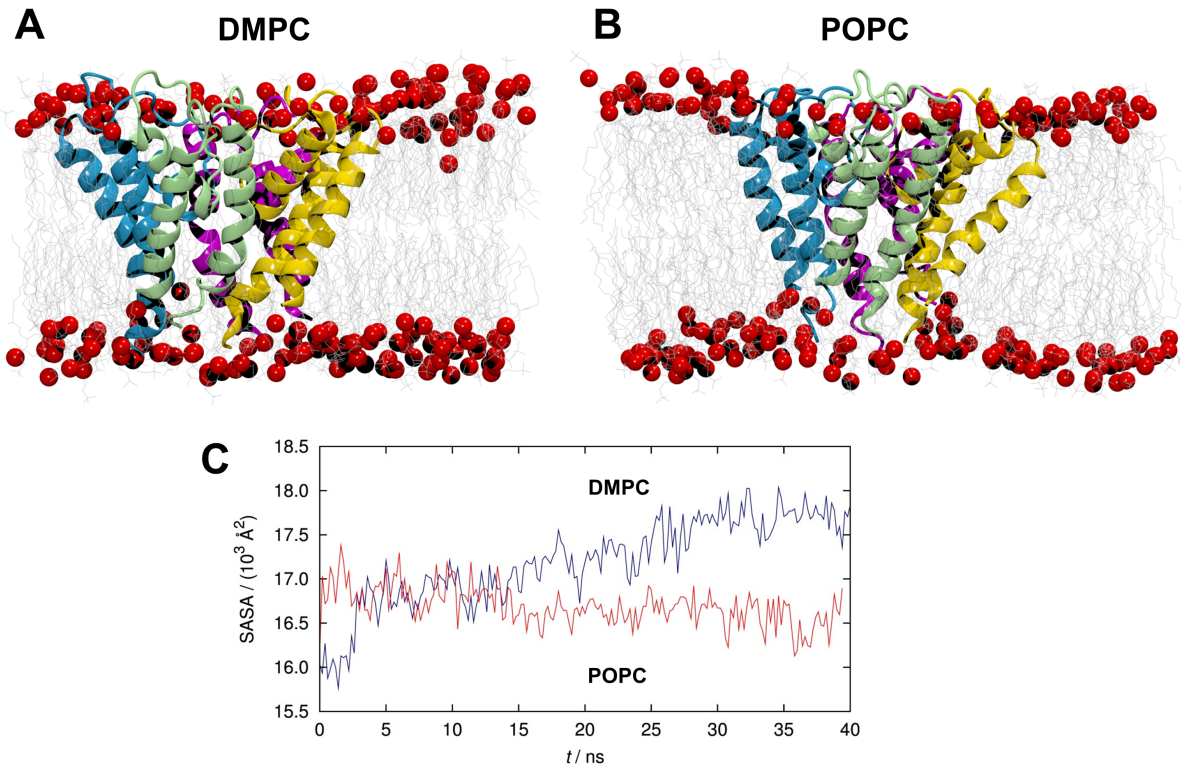

Fig 17 Results of MD simulations of Kcv_{ATCV-1} in DMPC and POPC membranes.

Two snapshot structures after a total simulation time of 40 ns are shown for DMPC (A) and POPC (B) embedding. The channel monomers are depicted in cartoon representation and are colored individually. Lipid headgroups are shown as red balls, hydrocarbon tails as wire. Solvent components have been omitted for clarity. (C) The solvent-accessible surface area (SASA) is shown as a function of simulation time (blue: DMPC, red: POPC), indicating different overall shape in response to varying membrane environments. All calculations and visualizations have been done using VMD (Humphrey et al., 1996).

5.5. Conclusion

The comparative analysis of Kcv_{NTS} activity shows that the channel maintains its basic functional features under all four experimental conditions. There is no appreciable difference between recordings in a classical bilayer system, which still contains some solvent, and the solvent free bilayer. The absence of a solvent effect is consistent with previous data, which also found no difference on channel function between bilayers with or without solvent (Williams, 1994). The present data also show no systematic difference between the function of channel proteins obtained from a cell-free expression system or from expression in *Pichia pastoris*. The results of these experiments suggest that the protein is properly folded after the different purification procedures. It also occurs that the scaffold protein, which surrounds the channel in the cell-free expression system (Katzen et al., 2008), is not affecting channel fold or function. The technique of inserting membrane proteins into nanoscale membrane discs held together by scaffold proteins has been already successfully used for pharmacological (Yang et al., 2011) and NMR studies (Tzitzilonis et al., 2013). To our knowledge, we present here the first case of an electrophysiological application of this system.

The robust function of the channel in different membrane environments and the prevailing high single-channel open-probability of $P > 0.5$ in all experimental conditions support the notion that gating is not dramatically affected by the experimental conditions tested here. The results of these experiments are important for a further understanding of the role of the viral channel in infection of the host cell. It appears that data on channel conductance and activity obtained from heterologous expression in cells or from reconstitution of the channel in bilayers can be directly extrapolated into the situation in the host cell.

The present data from the functional assays are also interesting in the context of the computational data. The MD simulations of the small Kcv_{ATCV-1} channel in different membranes imply that the microscopic structure of the channel can be influenced by the thickness of the bilayer. If these structural changes, which are imposed by the membrane, turn out to be functionally relevant we can assume that a DPhPC membrane, which is used in the bilayer methods, is sufficiently mimicking the plasma membrane of a mammalian cell.

5.6. Acknowledgments

We thank J. Van Etten (Lincoln, USA) and T. Greiner (Darmstadt) for initial characterization of the Kcv_{NTS} channel and also U.P. Hansen (Kiel) for suggestions to the manuscript.

5.7. References

Accardi, A., Kolmakova-Partensky, L., Williams, C., & Miller, C. (2004). Ionic currents mediated by a prokaryotic homologue of CLC Cl- channels. *J. Gen. Physiol.*, *123*, 109–119. doi:10.1085/jgp.200308935

Becucci, L., Papina, M., Verardi, R., Veglia, G., & Guidelli, R. (2012). Phospholamban and its phosphorylated form require non-physiological transmembrane potentials to translate ions. *Soft Matter*, *8*, 3881–3888.

Bubeck, J. A., & Pfitzner, A. J. P. (2005). Isolation and characterization of a new type of chlorovirus that infects an endosymbiotic Chlorella strain of the heliozoon Acanthocystis turfacea. *J. Gen. Virol.*, *86*, 2871–2877. doi:10.1099/vir.0.81068-0

Dopico, A. M., Bukiya, A. N., & Singh, A. K. (2012). Large conductance, calcium- and voltage-gated potassium (BK) channels: Regulation by cholesterol. *Pharmacology & Therapeutics*, *135*, 133–50. doi:10.1016/j.pharmthera.2012.05.002

Doyle, D. A. (1998). The Structure of the Potassium Channel: Molecular Basis of K+ Conduction and Selectivity. *Science*, *280*, 69–77. doi:10.1126/science.280.5360.69

Doyle, D. A. (2004). Structural changes during ion channel gating. *Trends in Neurosciences*, *27*, 298–302. doi:10.1016/j.tins.2004.04.004

Frohns, F., Käsmann, A., Kramer, D., Schäfer, B., Mehmel, M., Kang, M., Van Etten, J. L., Gazzarrini, S., Moroni, A., & Thiel, G. (2006). Potassium ion channels of chlorella viruses cause rapid depolarization of host cells during infection. *J. Virol.*, *80*(5), 2437. doi:10.1128/JVI.80.5.2437

Gazzarrini, S., Kang, M., Abenavoli, A., Romani, G., Olivari, C., Gaslini, D., Ferrara, G., van Etten, J. L., Kreim, M. Kast, S. Thiel, G. & Moroni, A. (2009). Chlorella virus ATCV-1 encodes a functional potassium channel of 82 amino acids. *The Biochemical Journal*, *420*, 295–303. doi:10.1042/BJ20090095

Greiner, T. (2011). Characterization of novel potassium transport proteins from Chlorella viruses. Dissertation at TU Darmstadt

Hertel, B., Tayefeh, S., Mehmel, M., Kast, S. M., Van Etten, J., Moroni, A., & Thiel, G. (2006). Elongation of outer transmembrane domain alters function of miniature K+ channel Kcv. *The Journal of Membrane Biology*, *210*, 21–29. doi:10.1007/s00232-005-7026-4

Humphrey, W., Dahlke, A., & Schulten, K. (1996). VMD - visual molecular dynamics. *J. Molec. Graphics*, *14*, 33–38.

Iwamoto, M., & Oiki, S. (2012). Amphipathic antenna of an inward rectifier K+ channel responds to changes in the inner membrane leaflet. *Proceedings of the National Academy of Sciences*, *110*. doi:10.1073/pnas.1217323110

Jeanniard, A., Dunigan, D. D., Gurnon, J. R., Agarkova, I. V, Kang, M., Vitek, J., Duncan, G., McClung, O. W., Larsen, M. Claverie, J-M. Van Etten, J-L. Blanc, G. (2013). Towards defining the chloroviruses: a genomic journey through a genus of large DNA viruses. *BMC Genomics*, *14*, 158. doi:10.1186/1471-2164-14-158

Kang, M., Graves, M., Mehmel, M., Moroni, A., Gazzarrini, S., Thiel, G., Gurnon, J. R., & Van Etten, J. L. (2004). Genetic diversity in chlorella viruses flanking kcv, a gene that

encodes a potassium ion channel protein. *Virology*, *326*, 150–159. doi:10.1016/j.virol.2004.05.023

Kast, S. M., Kloss, T., Tayefeh, S., & Thiel, G. (2011). A minimalist model for ion partitioning and competition in a K+ channel selectivity filter. *The Journal of General Physiology*, *138*, 371–373. doi:10.1085/jgp.201110694

Katzen, F., Fletcher, J. E., Yang, J., Kang, D., Peterson, T. C., Cappuccio, J. A., Blanchette, C. D., Sulchek, T., Chromy, B.A., Hoeprich, P.D. Coleman, M.A. & Kudlicki, W. (2008). Insertion of Membrane Proteins into Discoidal Membranes Using a Cell-Free Protein Expression Approach research articles. *Journal of Proteom Research*, *7*, 3535–3542

Killian, J. A. (2003). Synthetic peptides as models for intrinsic membrane proteins. *FEBS Letters*, *555*, 134–138. doi:10.1016/S0014-5793(03)01154-2

Kim, T., Lee, K. Il, Morris, P., Pastor, R. W., Andersen, O. S., & Im, W. (2012). Influence of hydrophobic mismatch on structures and dynamics of gramicidin a and lipid bilayers. *Biophysical Journal*, *102*, 1551–60. doi:10.1016/j.bpj.2012.03.014

Kreir, M., Farre, C., Beckler, M., George, M., & Fertig, N. (2008). Rapid screening of membrane protein activity: electrophysiological analysis of OmpF reconstituted in proteoliposomes. *Lab on a Chip*, *8*, 587–95. doi:10.1039/b713982a

Kuo, A., Gulbis, J. M., Antcliff, J. F., Rahman, T., Lowe, E. D., Zimmer, J., Cuthbertson, J., Ashcroft, F. M., Ezaki, T., & Doyle, D. A. (2003). Crystal structure of the potassium channel KirBac1.1 in the closed state. *Science*, *300*, 1922–1926. doi:10.1126/science.1085028

Labarca, P., & Latorre, R. (1992). Insertion of ion channels into planar lipid bilayers by vesicle fusion. *Methods in Enzymology*, *207*, 447-463.

Laub, K. R., Witschas, K., Blicher, A., Madsen, S. B., Lückhoff, A., & Heimburg, T. (2012). Comparing ion conductance recordings of synthetic lipid bilayers with cell membranes containing TRP channels. *Biochimica et Biophysica Acta*, *1818*, 1123–1134. doi:10.1016/j.bbamem.2012.01.014

Mackerell, A. D., Bashford, D., Bellott, M., Dunbrack, R. L., Evanseck, J. D., Field, M. J., Fischer, S., Gao, J., Guo, H. Ha, S. Kuchnir, L. Kuczera, K. Lau, F T K. Mattos, C. Michnick, S. Ngo, T. Nguyen, D T. Prodhom, B. Reiher, W E. Roux, B. Schlenkrich, M. Smith, J C. Stote, R. Straub, J. Watanabe, M. Wio, J. Yin, D. Karplus, M. (1998). All-Atom Empirical Potential for Molecular Modeling and Dynamics Studies of Proteins, *The Journal of Physical Chemistry B*, *5647*, 3586–3616.

Montal, M., & Mueller, P. (1972). Formation of bimolecular membranes from lipid monolayers and a study of their electrical properties. *Proceedings of the National Academy of Sciences of the United States of America*, *69*, 3561–3566.

Neher, E., & Sakman, B. (1976). Single-channel currents recorded from membrane of denerved frog muscle fibres. *Nature*, *260*, 799–802.

Neupärtl, M., Meyer, C., Woll, I., Frohns, F., Kang, M., Van Etten, J. L., Kramer, D., Hertel, B., Moroni, A., & Thiel, G. (2008). Chlorella viruses evoke a rapid release of K+ from host cells during the early phase of infection. *Virology*, *372*, 340–348. doi:10.1016/j.virol.2007.10.024

Pagliuca, C., Goetze, T. A., Wagner, R., Thiel, G., Moroni, A., & Parcej, D. (2007). Molecular properties of Kcv, a virus encoded K+ channel. *Biochemistry*, *46*, 1079–1090. doi:10.1021/bi061530w

Phillips, J. C., Braun, R., Wang, W., Gumbart, J., Tajkhorshid, E., Villa, E., Chipot, C., Skeel, R. D., & Kalé, L. (2008). Scalable molecular dynamics with NAMD. *J. Comput. Chem.*, *26*, 1781–1802.

Rodriguez-Menchaca, A. A., Adney, S. K., Tang, Q.-Y., Meng, X.-Y., Rosenhouse-Dantsker, A., Cui, M., & Logothetis, D. E. (2012). PIP2 controls voltage-sensor movement and pore opening of Kv channels through the S4-S5 linker. *Proceedings of the National Academy of Sciences of the United States of America*, *109*, E2399–408. doi:10.1073/pnas.1207901109

Romani, G., Piotrowski, A., Hillmer, S., Gazzarrini, S., Gurnon, J. R., Van Etten, J. L., Moroni, A., Thiel, G., & Hertel, B. (n.d.). Viral encoded potassium ion channel is a structural protein in the chlorovirus PBCV-1 virion. *J. Gen. Virol. (submitted)*.

Roux, B. (2005). Ion conduction and selectivity in K+ channels. *Annu. Rev. Biophys. Biomol. Struct.*, *34*, 153–171. doi:10.1146/annurev.biophys.34.040204.144655

Santos, J. S., Asmar-Rovira, G. a, Han, G. W., Liu, W., Syeda, R., Cherezov, V., Baker, K. a, Stevens, R. C., & Montal, M. (2012). Crystal structure of a voltage-gated K+ channel pore module in a closed state in lipid membranes. *The Journal of Biological Chemistry*, *287*, 43063–43070. doi:10.1074/jbc.M112.415091

Schlenkrich, M., Brickmann, J. MacKerell, A.D.Jr. Karplus, M. (1996). An empirical potential energy function for phospholipids: criteria for parameter optimization and applications. *Biological Membranes*, 31–81

Schultze, R., & Draber, S. (1993). A nonlinear filter algorithm for the detection of jumps in patch-clamp data. *J. Membrane Biol.*, *132*, 41–52.

Seeger, H. M., Aldrovandi, L., Alessandrini, A., & Facci, P. (2010). Changes in single K(+) channel behavior induced by a lipid phase transition. *Biophysical Journal*, *99*, 3675–83. doi:10.1016/j.bpj.2010.10.042

Simons, K., & Sampaio, J. L. (2011). Membrane organization and lipid rafts. *Cold Spring Harbor Perspectives in Biology*, *3*, a004697. doi:10.1101/cshperspect.a004697

Tayefeh, S., Kloss, T., Kreim, M., Gebhardt, M., Baumeister, D., Hertel, B., Richter, C., Schwalbe, H., Moroni, A., Thiel, G., & Kast, S. M. (2009). Model development for the viral Kcv potassium channel. *Biophysical Journal*, *96*, 485–498. doi:10.1016/j.bpj.2008.09.050

Tayefeh, S., Kloss, T., Thiel, G., Hertel, B., Moroni, A., & Kast, S. M. (2007). Molecular dynamics simulation of the cytosolic mouth in Kcv-type potassium channels. *Biochemistry*, *46*, 4826–4839. doi:10.1021/bi602468r

Thiel, G., Baumeister, D., Schroeder, I., Kast, S. M., Van Etten, J. L., & Moroni, A. (2011). Minimal art: or why small viral K(+) channels are good tools for understanding basic structure and function relations. *Biochimica et Biophysica Acta*, *1808*, 580–588. doi:10.1016/j.bbamem.2010.04.008

Thiel, G., Moroni, A., Dunigan, D. D., & Van Etten, J. L. (2010). Initial events associated with virus PBCV-1 infection of Chlorella NC64A. *Prog. Bot.*, *71*, 169–183. doi:10.1007/978-3-642-02167-1

Treptow, W., & Klein, M. L. (2012). Computer Simulations of Voltage-Gated Cation Channels. *The Journal of Physical Chemistry Letters*, *3*, 1017–1023. doi:10.1021/jz300089g

Tzitzilonis, C., Eichmann, C., Maslennikov, I., Choe, S., & Riek, R. (2013). Detergent/nanodisc screening for high-resolution NMR studies of an integral membrane protein containing a cytoplasmic domain. *PloS One*, *8*, e54378. doi:10.1371/journal.pone.0054378

Valiyaveetil, F. I., Zhou, Y., & MacKinnon, R. (2002). Lipids in the structure, folding, and function of the KcsA K+ channel. *Biochemistry*, *41*, 10771–10777. Retrieved from

Walde, P., Cosentino, K., Engel, H., & Stano, P. (2010). Giant vesicles: preparations and applications. *Chembiochem : A European Journal of Chemical Biology*, *11*, 848–865. doi:10.1002/cbic.201000010

Williams, A. J. (1994). An introduction to the methods available for ion channel reconstitution. In D. Ogden (Ed.), *Microelectrode techniques: in Plymouth workshop handbook* (2nd ed.), 79–99. The company of Biologists, Cambridge.

Yang, J.-P., Cirico, T., Katzen, F., Peterson, T. C., & Kudlicki, W. (2011). Cell-free synthesis of a functional G protein-coupled receptor complexed with nanometer scale bilayer discs. *BMC Biotech*, *11*, 57. doi:10.1186/1472-6750-11-57

Yuan, C., O'Connell, R. J., Feinberg-Zadek, P. L., Johnston, L. J., & Treistman, S. N. (2004). Bilayer thickness modulates the conductance of the BK channel in model membranes. *Biophysical Journal*, *86*, 3620–3633. doi:10.1529/biophysj.103.029678

6. Single-channel behavior of Kcv_{NTS} in membranes with different thickness

6.1. Abstract

For a full understanding of structure/function correlations in membrane proteins it is imperative to consider not only the protein but also the protein in its lipid environment. A functional reconstitution of purified channel proteins in model membranes offer in this context a very good system to examine protein/lipid interaction. In the present study we show that one of the smallest potassium channels known so far, the Kcv_{NTS} channel, which has a monomer size of only 82 aa, is fully functional in model membranes with different thicknesses. We changed the bilayer thickness by varying acyl chain lengths from C14 to C16/C18; we also added solvents or different concentration of cholesterol. Single-channel recordings show that the variable membrane conditions have no appreciable effect on the unitary conductance of the channel. The open probability of the channel however is clearly affected and we identify membranes with 16 carbon atoms as the membranes, which promotes the highest activity of Kcv_{NTS}. Furthermore in all membrane conditions we detect in addition to a dominant voltage independent mode of gating, with a high open probability, a second type of gating. The latter is characterized by a voltage dependent decrease in the open probability in response to positive voltages from ca. 90% down to less than 10%. The probability that this gating mode appears is promoted by thicker membranes; both modes occur without any intermediate state in independent recordings but also within the same measurement. The data stress that the lipid environment affects the positioning or orientation of the protein in the lipid bilayer. In thick bilayers this can introduce an orientation in which the protein senses the electrical field and acquires a voltage dependency. Since the channel protein has no apparent charged amino acids in the part of the protein, which is in the electrical field, we can not yet explain the mechanisms, which is responsible for the voltage dependency.

6.2. Introduction

Membranes are essential in all kinds of living cells (Hunte & Richers, 2008). Their main function is to generate a protective barrier against, amongst others, charged or polar molecules, particles or foreign genes (Li et al., 2012; van Uitert et al., 2010). They also define with these properties the compartmentalization in eukaryotic cells and maintain in this way the electric potential differences (Ashrafuzzaman & Tuszynski, 2013; Engelman, 2005; Phillips et al., 2009). Membranes are made of lipid bilayers that contain integral and peripheral membrane proteins (Singer & Nicolson, 1972). Lipid bilayers consist of phospholipids mainly, glycolipids and sterols (Ashrafuzzaman & Tuszynski, 2013). The proteins within the lipid bilayer define the physiological function of membranes. Transport proteins for example catalyze the selective passage of molecules across membranes and receptor proteins assure a communication between adjacent cells or a perception of the environment (Engelman, 2005; Steller et al., 2012). An important class of proteins, which are present in every cellular membrane including the plasma membrane and the membranes of

organelles, are ion channels. These protein tunnels are embedded in the membrane and catalyze the passive flux of ions in a selective and regulated manner across the membrane. In the last decade structure and function correlates of ion channels have been well studied. In particular the class of K^+ channels that catalyze the flux of K^+ in a highly selective manner (Miller, 2000), has been intensively studied and many aspects of K^+ channel function such as gating and selectivity are known in great detail down to the atomistic level (Long et al., 2007; Sansom et al., 2002). Even though K^+ channels have like all membrane proteins an intimate contact with the lipid bilayer most of the structure function correlates in these proteins were examined without or with little consideration of the lipid environment. Only isolated reports in the literature mention that lipids are able to affect the activity of ion channels and vice versa (Lee, 2004; Tillman & Cascio, 2003). Some evidences for an effect of lipids on the activity of K^+ channels is known for the family of voltage gated potassium channels. These proteins undergo a change in conformation when the lipid composition is altered. This conformational rearrangement is independent of the membrane voltage (Jiang & Gonen, 2012). Furthermore it has been reported that the BK channel (big conductance K^+ channel) exhibits different conductance states depending on the thickness of the bilayer (Yuan et al., 2004). For the KcsA (K^+ crystallographically-sited activation channel) channel, probably the best-studied K^+ channel with respect to structure/function correlates (Roux, 2005), it was found that negatively charged lipids like phosphatidylserine (PS) regulate its function. The interactions of anionic phospholipids with KcsA are necessary for the opening of the channel (Alvis et al., 2003; Marius et al., 2008) and therefore the conduction of ions (Valiyaveetil et al., 2002). In the case of the K_{ir} (inwardly rectifying K^+ channel) channels it was found that the anionic lipid phosphatidylinositol 4,5-bisphosphate (PIP_2) regulates channel gating by stabilizing the open state conformation. This mode of regulation is physiologically important for cell metabolism in many tissues, for the heart rate as well as for the vascular tone (Shyng et al., 2000; Singh et al., 2009).

Since cholesterol makes up about 30 mole% of the lipid matrix in the plasma membrane of mammalian cells it has been assumed that it may play a crucial role in the regulation of membrane proteins (van Uitert et al., 2010). Some experimental evidences support such a role for cholesterol on ion channel function. The activity of the prokaryotic K_{ir} channel, K_{ir}Bac1.1 (bacterial K_{ir}-channel 1.1), for example is influenced negatively by binding cholesterol directly (Singh et al., 2011). In addition to a direct effect of cholesterol on membrane proteins it is known that cholesterol and/or sphingolipids cluster in domains within the lipid bilayer to form so called lipid rafts (Rietveld & Simons, 1998; Simons & Ikonen, 1997). These rafts play important roles in signal transduction, membrane trafficking (Brown & London, 1998; Mukherjee & Maxfield, 2004) and are supposed to build more ordered structures within the membrane with the result of altering locally the membrane physics (Brown & London, 2000). The latter has an impact on the function of membrane proteins including ion channels (Bukiya et al., 2011; Dopico et al., 2012). Systematic studies with model membrane proteins have shown that these proteins can alter the architecture of the lipid bilayer and that the bilayer has an impact on the structure of the proteins. One

important mutual interaction between membrane and protein is known as hydrophobic mismatch (Killian, 1998). Hydrophobic mismatches arise when the membrane spanning protein is bigger or smaller than the membrane itself. In addition to a positive mismatch where the membrane spanning protein is longer than the thickness of the membrane, also negative mismatches can occur. In the latter case the membrane spanning protein is shorter than the thickness of the membrane. In both cases the thickness of the lipid bilayer or the structural order of the acyl chains can change in order to accommodate for the mismatch. On the side of the membrane protein the mismatch can be compensated by a deformation of the protein backbone, an oligomerization of proteins or a protein tilt. In extreme cases such a hydrophobic mismatch can even prevent a protein from inserting into the lipid bilayer (de Planque & Killian, 2003; Killian, 1998).

Here we address the structural and functional interplay between different lipid bilayers and K^+ channels in a systematic manner. For this purpose we employ the smallest group of potassium channels known so far, the Kcv (K^+ channel *chlorella* virus) channels. Because of their small size of 94 or even less amino acids per monomer (Plugge et al., 2000) these viral channels can be seen as core modules of more complex potassium channels from prokaryotes or eukaryotes (Pagliuca et al., 2007). One monomer consists of only two trans membrane domains (TMD) connected with a loop region (Kang et al., 2003). Four monomers create a functional channel with all hallmarks of a more complex potassium channel, e.g. a selectivity filter, a cavity and a gate (Gazzarrini, 2003). Kcv_{ATCV-1} (from *acanthocystis turfacea chlorella* virus-1) was until recently with only 82 aa the smallest K^+ channel known (Gazzarrini et al., 2009); more recently viral channels which are even slightly smaller were detected (unpublished data Thiel 2014). Here we focus on one homolog of Kcv_{ATCV-1}, the Kcv Next-to-Smith (Kcv_{NTS}) channel. Both channels consist of 82 aa per monomer and differ in only four aa in the first trans membrane domain (TMD1) (Braun et al., 2013). Since computational simulations have shown that Kcv_{NTS} is quasi fully embedded in the lipid bilayer (Braun et al., 2013), this channel protein is a very good model system for studying protein/lipid interaction. In this study we demonstrate that the membrane environment of the minimal potassium channel Kcv_{NTS} has a huge effect on the open probability but not on the unitary conductance. We analyze systematically the gating behavior of Kcv_{NTS} as a function of membrane thickness and different phospholipid headgroups. We show that the channel reveals the best activity in membranes with a chain length of 16 carbon atoms regardless of the headgroup charge. By changing membrane thickness due to chain length, solvents or cholesterol we are able to switch the gating behavior of Kcv_{NTS} from a voltage independent to a voltage dependent mode. These observations reveal that structure/function correlations of membrane proteins at the single channel level have to consider the environment in which the channel is functional.

6.3. Methods

6.3.1. Protein expression in *Pichia pastoris*, *in vitro* and purification

The production and purification of Kcv_{NTS} in *Pichia pastoris* and *in vitro* (cell-free system) is described in 5.3.1 and 5.3.2.

6.3.2. Planar lipid bilayer experiments

Planar lipid bilayer experiments are described in 5.3.3 and 7.3. The formation of stable membranes was done by the monolayer technique (Montal & Mueller, 1972) and by a pseudo painting/air bubble technique, which is described in detail in 7.3. All membranes tested contained pure lipids of 1,2-dimyristoyl-*sn*-glycero-3-phosphocholine (DMPC), 1,2-diphytanoyl-*sn*-glycero-3-phosphocholine (DPhPC), 1,2-diphytanoyl-*sn*-glycero-3-phosphoethanolamine (DPhPE), 1,2-diphytanoyl-*sn*-glycero-3-phospho-L-serine (DPhPS) or 1-palmitoyl-2-oleoyl-*sn*-glycero-3-phosphocholine (POPC) (all from Avanti Polar Lipids, Alabaster, AL, USA). The lipids were dissolved in n-pentane (Merck KGaA, Darmstadt, Germany) with a final concentration of 0,15-25 mg/ml or in n-decane (Carl ROTH GmbH, Karlsruhe, Germany) with a concentration of 15-20 mg/ml. DPhPC membranes containing synthetic cholesterol (AppliChem GmbH, Darmstadt, Germany), 10%, 20%, 30% or 40% (mole%), were dissolved in n-pentane. All experiments were done with symmetrical KCl solutions (100 mM, 10 mM HEPES (AppliChem GmbH, Darmstadt, Germany), adjusted to a pH of 7).

6.3.3. Data analysis

Data analysis was done as indicated in chapter 5.3.6.

6.4. Results

6.4.1. Gating behavior of Kcv_{NTS} in different membranes

Because Kcv_{NTS} is one of the smallest K^+ channels known so far (Braun et al., 2013) we investigate the influence of different membrane environments on functional properties of this protein. In 5.4 it was already mentioned that the homolog of this channel, Kcv_{ATCV-1}, is quasi fully embedded in a DMPC (C14) membrane and even more so in a POPC (C18) membrane (Braun et al., 2013). Here we examine the gating behavior of the channel Kcv_{NTS} systematically in five different types of membrane (Fig 18). Kcv_{NTS} is reconstituted in the two membranes DMPC and POPC which were also employed for the MD simulations of Kcv_{ATCV-1}. Furthermore we used three synthetic membranes, which differ in their headgroups. Phosphatidylcholine (PC) and phosphatidylethanolamine (PE) have zwitterionic headgroups and phosphatidylserine (PS) has a negativley charged headgroup. We decided to test PS headgroups because other potassium channels have shown higher activity in membranes with negatively charged lipids (Marius et al., 2008). Common to the three synthetic membranes is that they are composed of C16 fatty acids with methylated acylchains (4ME); these diphytanoyl fatty acid chains are more stable than natural lipids (Hung et al., 2000). Important to mention is also that the DPhPC lipid for example does not have a transition temperature between -120 °C and +80 °C (Lindsey et al., 1979), which makes it a good lipid for planar bilayer experiments. It is more unlikely that this lipid generates lipid pores, which often occure at transition temperatures (Heimburg, 2010).

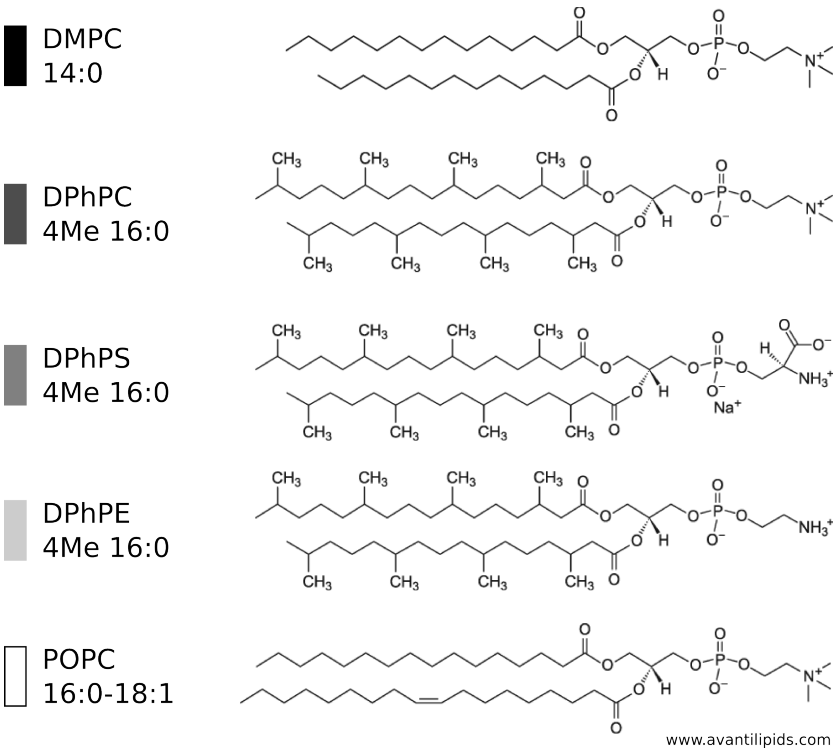

Fig 18. Lipid structures.

Chemical structures of lipids, which were used for planar bilayer experiments. The lipids differ in chain length, headgroups and saturation grades (The numbers below the names indicate the carbon chain length).

Fig 19A shows single channel fluctuations of the Kcv_{NTS} channel in all five membranes at a holding potential of +80 mV. The corresponding single-channel I/V curves of Kcv_{NTS} are summarized in Fig 19B. The data show that the small channel is functional in membranes with different thickness and with different headgroups. The results in Fig 19B indicate no large difference between the single channel amplitudes of Kcv_{NTS} in the voltage window tested. The conductance of the channel is ohmic in all membranes at voltages positive of ca. -100 mV. The unitary conductance of the channel varies from 71 pS in DMPC to 92 pS in DPhPS membranes; the small differences are not statistically significant, except of the conductance of DMPC, which is slighty significant ($p = 0.03$) (Fig 19B and C). Notably the unitary conductance of the Kcv_{NTS} channel in different membranes compares well with that of the homolog Kcv_{ATCV-1} in oocytes (Gazzarrini et al., 2009). This implies that the conductance of the miniature viral K^+ channels is not a function of the lipid environment. At holding potentials more negative than -100 mV the channel shows a negative slope conductance in all membranes. This negative slope conductance has been attributed to a fast gating of the channel, which is in Kcv channels presumably due to a flickering of the selectivity filter (4.4.1) (Abenavoli et al., 2009). The fact that the different lipids do not have an effect on this negative slope implies that this fast gating of the channel is insensitive to the lipid environment and the conformational adaptation of the channel to different membrane thicknesses.

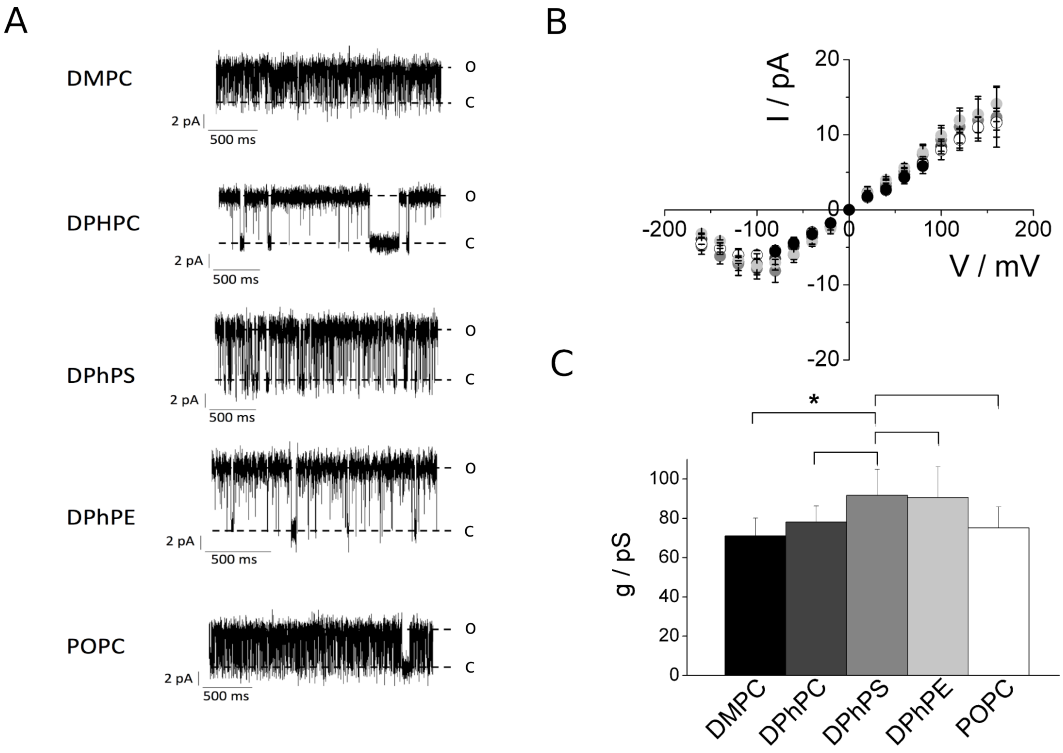

Fig 19 Single-channel characteristics of Kcv_{NTS} in different membrane types

(A) Representatitve single-channel fluctuations in different membrane types at a holding potential of +80 mV. The open and closed states are dentoted with o and c respectively. (B) Single-channel I/V curves of the dominant conductivity. Colors correspond to the lipids in Fig 18. (C) Single-channel conductivity of all tested membranes

within the ohmic range. Values are means +- SD of n experiments. (B) and (C): DMPC (n = 4), DPhPC (n = 8), DPhPS (n = 5), DPhPE (n = 5), POPC (n = 5).

A close scrutiny of the single channel data shows that the Kcv_{NTS} exhibits in addition to the main conductance (Fig 19) other conductance states (Fig 20). These alternative conductance states were rarely observed in all membranes with the exeption of DMPC membranes; the absence of alternative conductance states in the latter mebrane is presumably more related to the fact that DMPC bilayers are very unstable (Schmidt et al., 2006); hence there are much less data available. In the remaining membranes it was possible to find channel fluctuations between the fully open state (o_1) and a lower, main open state (o_2); switching between the states occure directly or via a closed state (e.g. third panel). These findings stress the subconductance nature of these alternative states; hence they are not due to artifacts or contamination (5.4). It was already mentioned previously that the alternative states were not observed in all measurements (Braun et al., 2013) (5.4). Hence it is possible that in the analysis both open states o_1 and o_2 were considered for the generation of the I/V curves. This could be reflected in the larger standard deviations (Fig 19B).

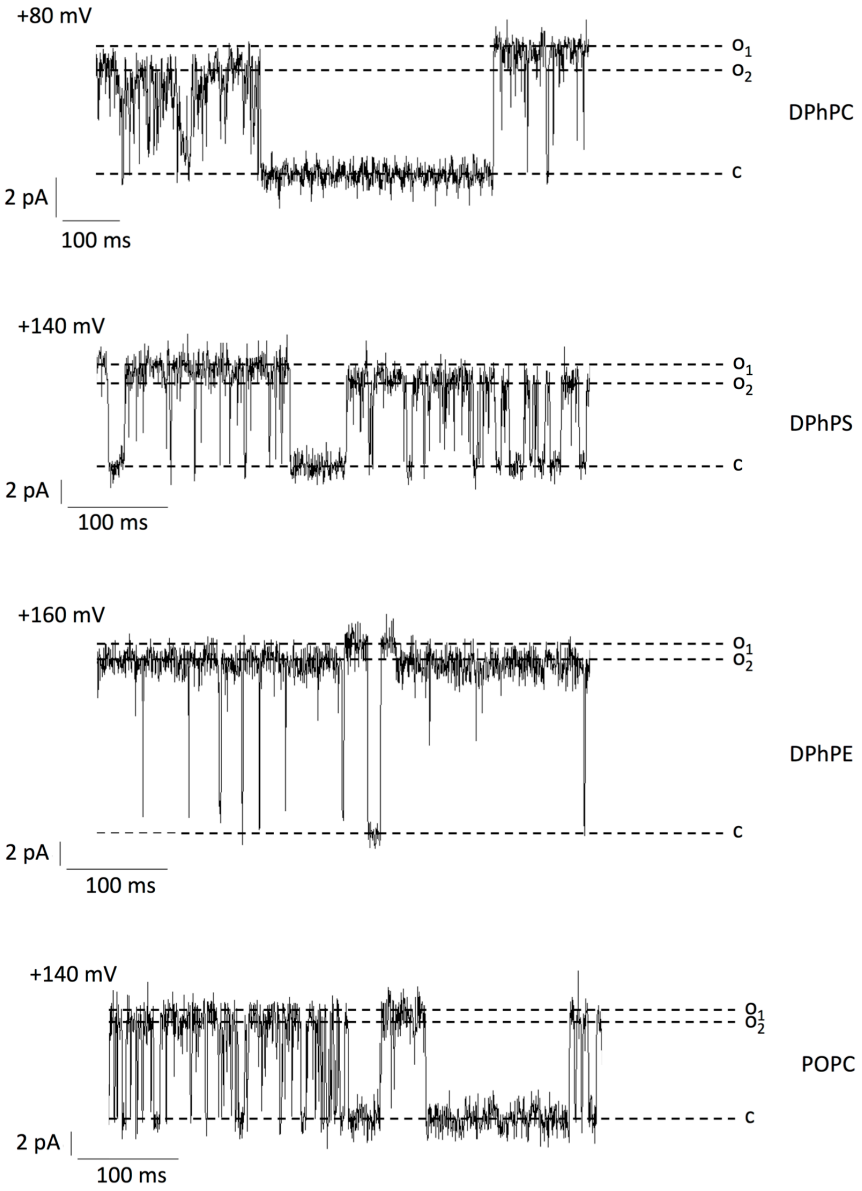

Fig 20. Subconductance states of Kcv_{NTS} in four different membrane types.

The open and closed states are dentoted with o and c respectively. The upper three panels are representative current traces of C16 membranes (DPhPC (see also Chapter 2), DPhPS and DPhPE). The lowermost panel is a representative current trace of a C16/C18 (POPC) membrane. The dominant current level is o_2. Jumps into higher states occur directly or via a closed state (e.g. panel three).

Fig 19A shows time sweeps of typical Kcv_{NTS} activity at a holding potential of +80 mV in different types of membranes. A visual inspection already shows slight differences in the gating behavior in these mebranes. This is most evident by comparing the upper and lower pannels in Fig 19A with the central pannels. Analysis of the open probabilities from the amplitude histograms (Fig 21A) supports the visual inspection that the channel has a higher open probability in C16 membranes regardless of the headgroups (Fig 21B). In the latter membranes Kcv_{NTS} shows an average open probability of about 80%. In C14 and C18

membranes respectively the mean open probability is about 60%. The difference in P_o between bilayers of different thickness is not significant due to the large variability of P_o in DMPC and POPC membranes.

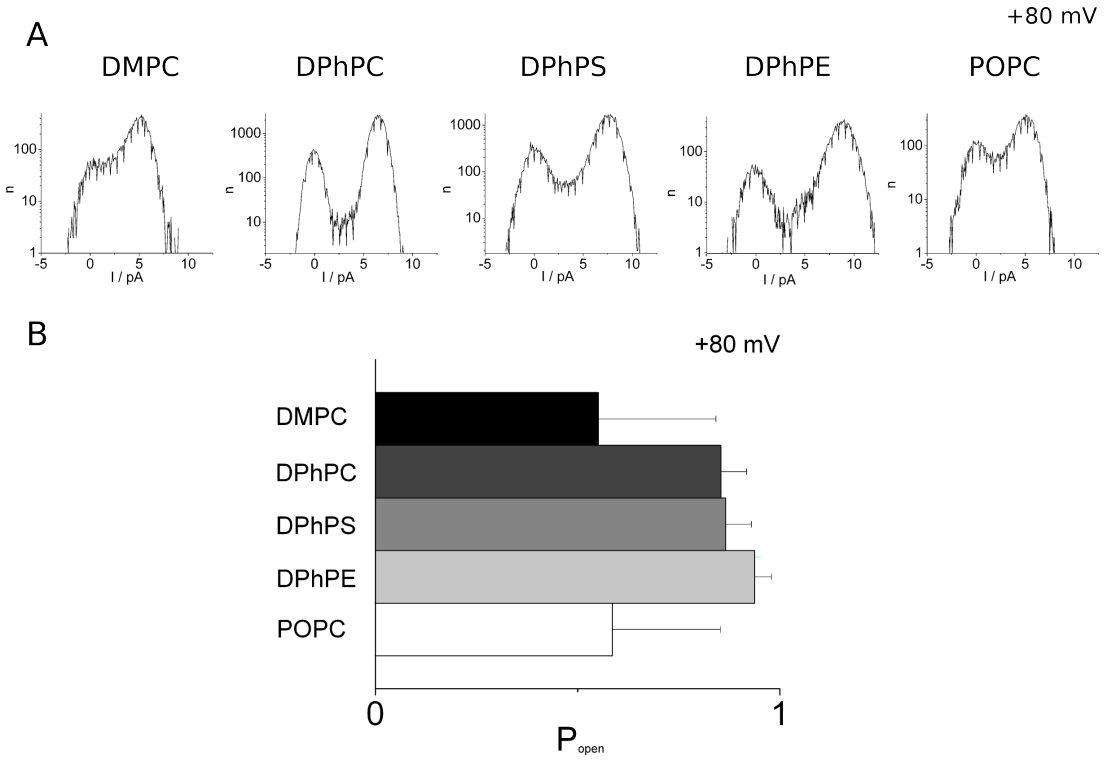

Fig 21. Amplitude histograms and open probabilites of Kcv_{NTS} in different membrane types.

(A) Representative amplitude histograms at a holding potential of +80 mV. (B) Single-channel open probabilities at a holding potential of +80 mV. Values are means +- SD of n experiments: DMPC (n = 3), DPhPC (n = 8), DPhPS (n = 5), DPhPE (n = 5) and POPC (n = 3).

A source of the large scatter in Fig 21 is that the channel shows in addition to the prevailing, high voltage independent open probability also, in rare cases, a voltage dependent open probability. Fig 22A illsutrates representative current traces at holding potentials from -140 mV to +140 mV in a DPhPC membrane. The channel activity with the prevailing very high open probability is shown on the left; on right side the alternative gating mode is shown. It appears that this gating mode is voltage dependent. The open probability is low at positive holding potentials and increases with hyperpolarization.

To quantify channel activity as a function of voltage we calculated the open probability for each membrane type (Fig 22B). As we already found for a holding potential of +80 mV the channel reveals the highest open probability in DPhPC, DPhPS and DPhPE membranes. Hence we see an overall open probability of 80%. In thinner (DMPC) and thicker (POPC) membranes the overall open probability is about 60%. These data correlate with the representative behavior in Fig 22A on the left, which is indeed the prevailing and voltage independent behavior. When we quantify the findings on the right side of Fig 22A we obtain

the voltage dependet behavior. More positive potentials reveal less open probabilities. Out of 8 measurements in DPhPC membranes we saw this effect once. However out of five measurements in POPC membranes we saw this effect twice.

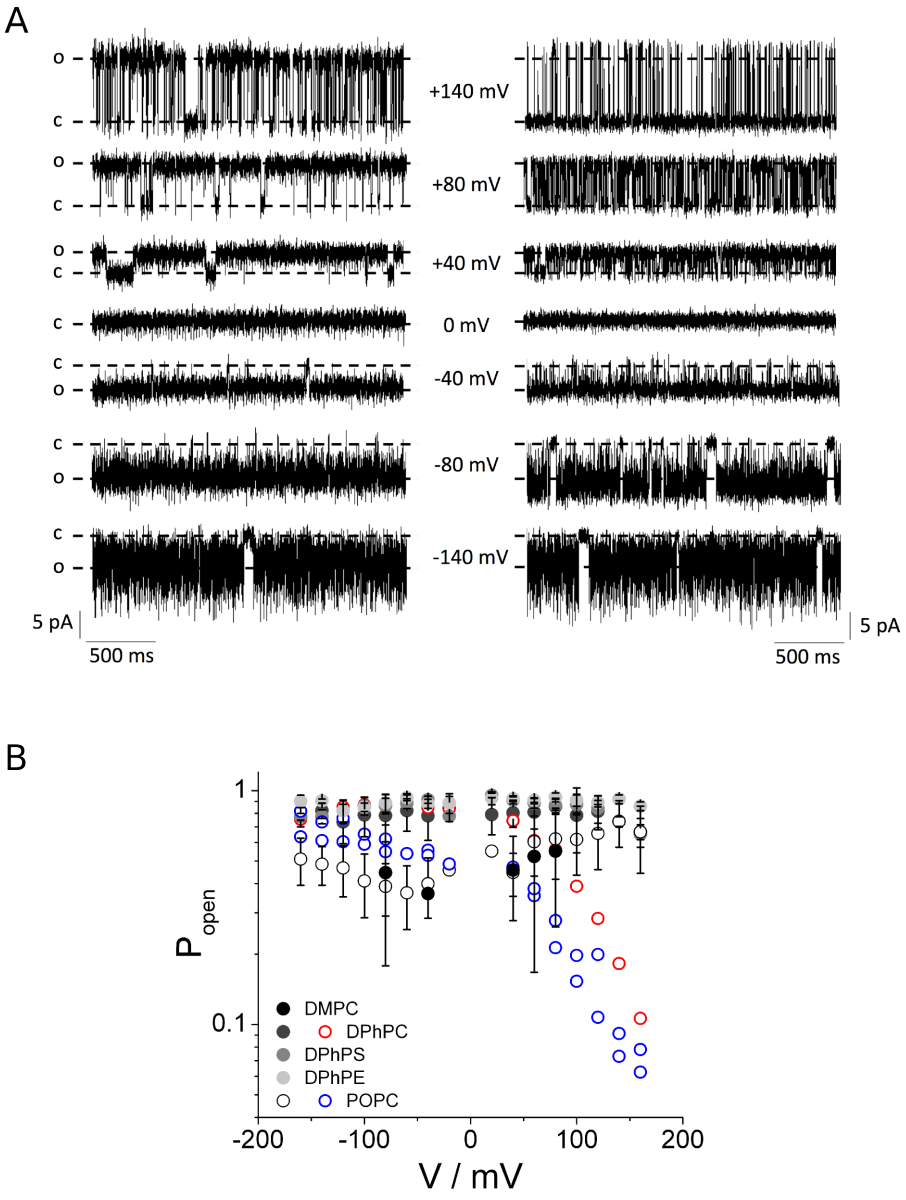

Fig 22. Voltage independent and dependent gating behavior of Kcv_{NTS}

(A) Representative single-current traces of Kcv_{NTS}. The normal and voltage independent (left) and the voltage dependent (right) behavior are illustrated at different holding potentials. The open and closed states are dentoted with o and c respectively. (B) Open probabilities of Kcv_{NTS} in different membrane types (colors refer to the lipids in Fig 18). Values are means +- SD of n experiments: DMPC (n = 4), DPhPC (n = 8 (filled dot) and n = 1 (red circle)), DPhPS (n = 5), DPhPE (n = 5) and POPC (n = 3 (white circle) and n = 2 (blue circle)).

To figure out the origin of the the voltage dependent gating we estimate the dwell-times for different holding potentials. Fig 23A shows representative single-current traces of Kcv_{NTS} with the voltage dependent behavior in either a DPhPC or a POPC membrane at a holding potential

of +120 mV. The all-point histogram shows that the single-channel amplitude is not affected by the voltage dependence; the unitary conductance compares well with the I/V curve in Fig 19B.

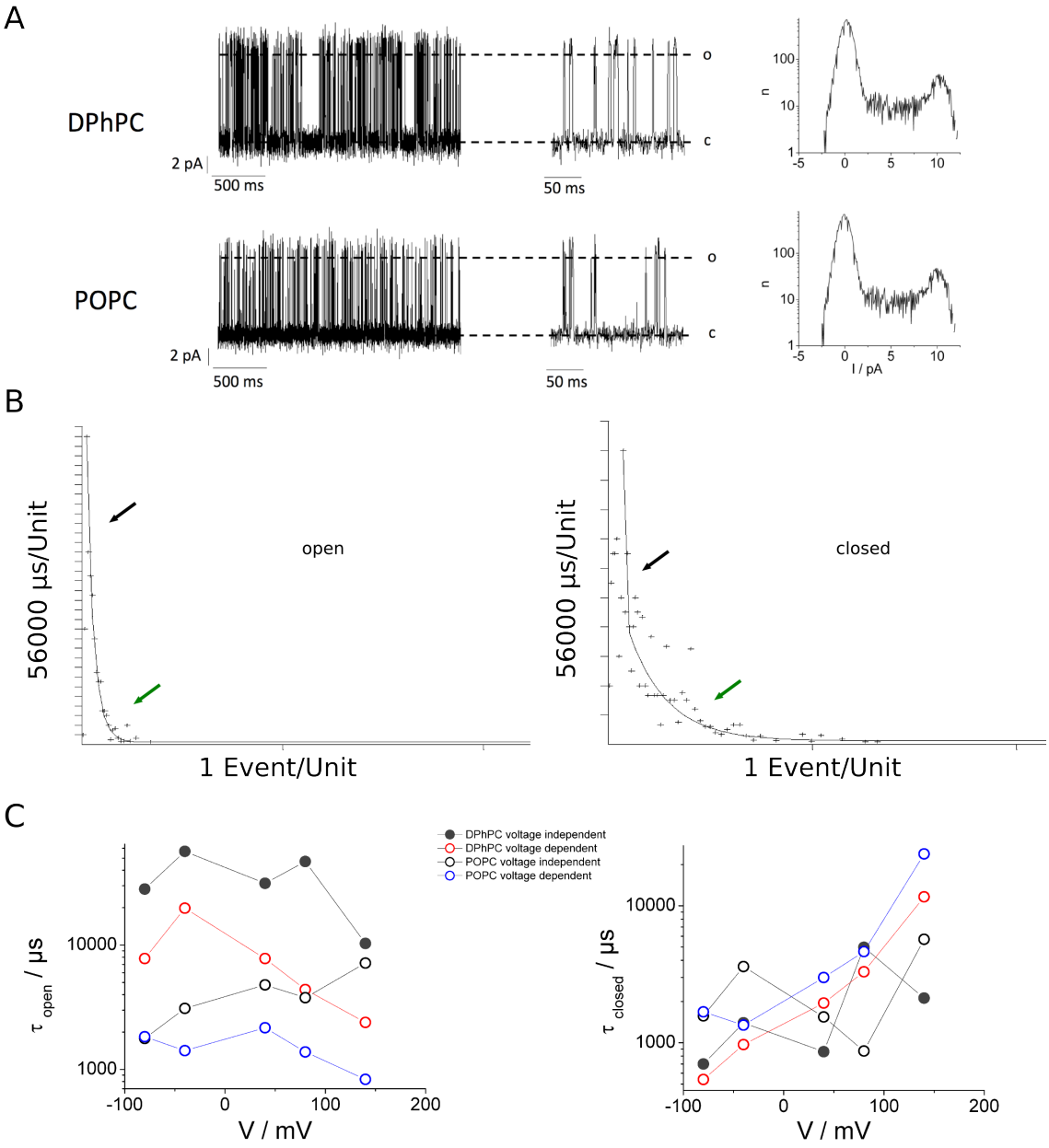

Fig 23. Voltage dependent gating behavior of Kcv_{NTS} in two different membrane types.

(A) Representative single-current traces of Kcv_{NTS} in a DPhPC and POPC membrane at a holding potential of +120 mV. The open and closed states are dentoted with o and c respectively. Amplitude histograms of the depicted traces (right). (B) Representative open and closed dwell-time histograms at +140 mV of the voltage dependent mode in a DPhPC membrane. Black and green arrows indicate different exponential functions (C) Representative time constants of the open (left) and closed dwell times (right) of a DPhPC and a POPC membrane at given holding potentials (grey dots and black circles refer to the voltage independent behavior; red and blue circles refer to the voltage dependent behavior).

Fig 23B shows the life times of the open and closed states of the channel for a representative measurement at a holding potential of +140 mV in the voltage dependent mode. Both graphs are best fitted with two exponential functions (Eq 5; y_0 is the offset, A the amplitude and t the decay constant)

$$y = y_0 + A * e^{\frac{-x}{t}}$$

Eq 5 Equation of the exponential decay

The need of two exponential functions means that the channel has at least two open and two closed states respectively (Ashcroft, 2000). The tau values for both dwell times are indicated by black and green arrows. For a further analysis of the voltage dependency we took the most prominent time constants (green arrows) for a plot of voltage dependency of the dwell-times. Fig 23C shows the open and closed dwell-times at five different holding potentials for the channel in the voltage independent and voltage dependent mode. The plot in Fig 23C shows that the open and closed dwell times in a DPhPC and POPC membrane are, as expected, in the case of the voltage independent behavior, not systematically sensitive to the membrane voltage. The open dwell-times in the voltage dependent mode reveal a slight decrease over the voltage range tested. This range is from 20 ms to 2.5 ms in a DPhPC membrane and from 2 ms to 0.9 ms in a POPC membrane. In the voltage independent mode the closed states reveal a zigzag behavior with a slight increase in time constants in both membranes. The most striking and systematic effect appeares in the voltage dependent mode. There is a constant increase of the time constant of the closed times from 0.45 ms to 11 ms in a DPhPC membrane and from 2 ms to 20 ms in a POPC membrane. The difference in the voltage independent and voltage dependent open propability can be explained by recalculating the open probability of the channel from the open and closed dwell times. The same values of the P_o confirm that the origin of the voltage dependency is due to a constant increase of the closed time constants.

As a resumee of this section we can conclude that Kcv_{NTS} can be successfully reconstituted in membranes with different properties. It turns out that the single-channel amplitudes are not much affected by the chain length and the charge of the headgroups of the phospholipid bilayers. Furthermore the channel revealed a main mode of gating with a high and voltage independent open probability. A more rare gating mode is characterized by a voltage dependency. This voltage dependence is mainly due to the closed time constant, which increases with positive holding potentials. The question arises whether this effect of voltage dependency is a property of the channel which occurs randomly or whether the two gating modes are influenced by the physicochemical properties of the membrane. To answer this question we performed channel recordings in membranes in which the thickness is altered by parameters other than the carbon chain length.

6.4.2. Gating behavior of Kcv_{NTS} with different solvents

When performing bilayer experiments it is important to use solvent free bilayers for studying pure channel activity. Usually n-pentane is used to create virtually solvent free bilayers (Benz et al., 1975; Montal & Mueller, 1972). Here we used two different solvents for dissolving the lipids. While n-pentane evaporates quickly n-decane remains much longer in the bilayer (Benz et al., 1973; Lundbæk & Andersen, 2012), with the result in increasing the bilayer thickness.

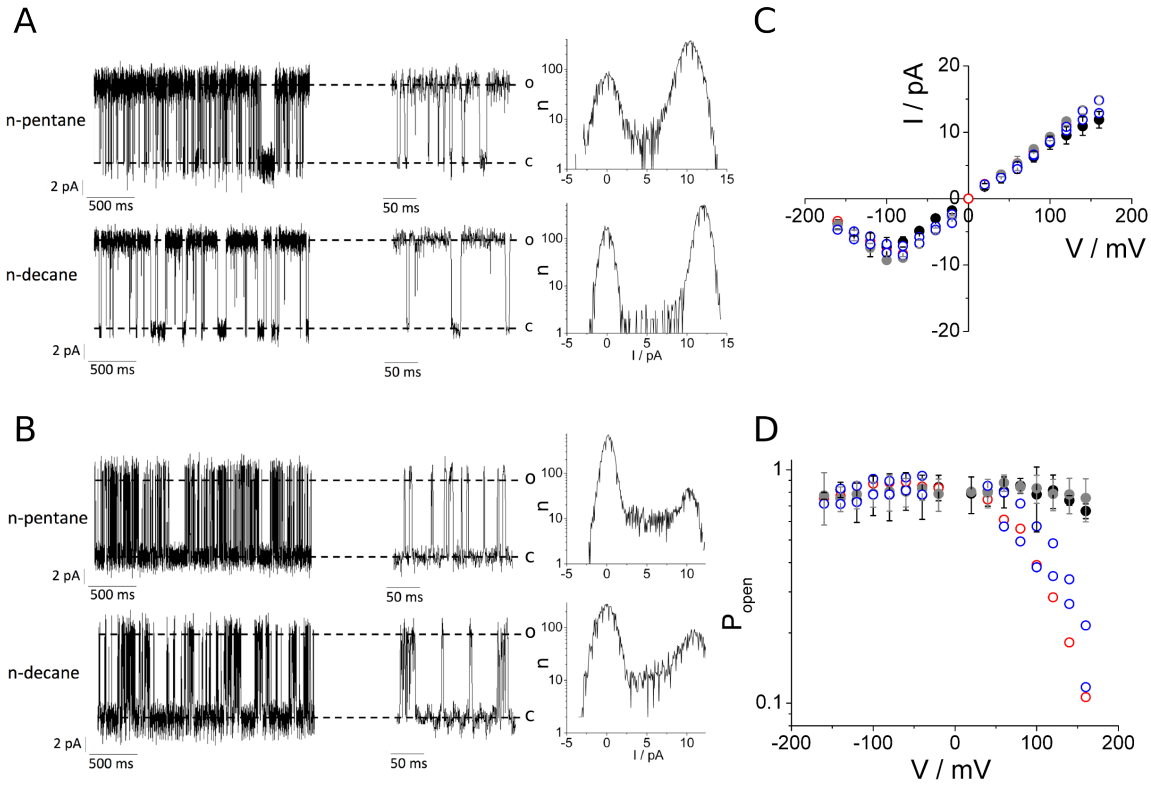

Fig 24. Gating behavior of Kcv_{NTS} in DPhPC membranes with two different solvents.

(A) and (B) show representative single-current traces and amplitude histograms of Kcv_{NTS} in the voltage independent (A) and voltage dependent (B) mode at a holding potential of +120 mV. (C) Single-channel I/V-curves. (D) Single-channel open probabilities. Values are means +- SD of n experiments: Black dots (n = 8) and red circles (n = 1) indicate DPhPC in n-pentane, gray dots (n = 3) and blue circles (n = 2) indicate DPhPC in n-decane.

Fig 24A illustrates traces of single-channel currents of Kcv_{NTS} in the voltage independent mode in a membrane of DPhPC lipids dissolved either in n-pentane or n-decane. In both cases the amplitude histograms exhibit no significant differences in the single-channel amplitude. Fig 24B shows the same channel in the voltage dependent mode in an other membrane of DPhPC lipids dissolved in either n-pentane (same trace and amplitude histogram as in Fig. 23A) or n-decane. Again the amplitude histograms show no differences in the single-channel currents. The mean single-channel currents of at least five independet measurements of the lipid dissolved either of the two solvents are summarized in Fig 24C. The data reveal no appreciable differences in the respective I/V curves. The channel shows under both conditions an ohmic conductance at positiv voltages; at negative voltages the I/V relations show the typical negative slope conductance, which arises from a flickering effect (Abenavoli et al.,

2009). In Fig 24A and D is illustrated the voltage independent high open probability of about 80% (black and grey circles) of the channel. Normally bilayers, which are made from DPhPC lipids with n-pentane as a solvent are virtually solvent free. Under this conditions the channel reveals the voltage independent mode with a high open probability. In the cases that bilayers are unstable or leaky it is necessary to add additional lipids under water in order to recreate/stabilize them. In those cases the n-pentane (solvent) can not evaporate resulting in a non solvent free and hence thicker bilayer. This operation has an effect of the channel behavior, which reflects the voltage dependent mode of gating (Fig 24B and D, open circles). These voltage dependent modes of gating, which are observed in bilayers with different solvents are the same as the ones described before in the context of other membranes. The channel reveals a high open probability of about 80% at negative holding potentials, which decreases exponentialy with positive potentials; at +160 mV the open probability is less than 9% (open, colored circles). In systematic trials eight DPhPC bilayers revealed a voltage independent gating mode with n-pentane; one bilayer exhibited a voltage dependent mode after new lipids solubilized in solvent were brought in for stabilizing the DPhPC bilayer. Bilayers that are made with the more persistent n-decane as a solvent show a higher frequency of channels with the voltage dependent mode; here two out of five recordings showed the voltage dependent mode. The quantitative analysis for the channel of being in the voltage independent or voltage dependent mode due to solvents is described below (6.4.4)

Collectively these results suggest that an alteration of the membrane thickness by changing the acyl chain length (C14 – C16/C18) or by including solvents (n-pentane, n-decane or n-octane; data not shown) in the phospholipid bilayer in which the lipids were dissolved affects channel gating; it occurs as if an increase in bilayer thickness promotes a switching from the voltage independent into a voltage dependent mode of gating.

6.4.3. Gating behavior of Kcv_{NTS} in DPhPC membranes with different concentration of cholesterol

To test whether we could change the gating modes of Kcv_{NTS} by altering the membrane thickness in a different manner we added different concentrations of cholesterol to DPhPC membranes. Cholesterol is known to alter the membrane composition. If cholesterol resides inside a membrane it forms lipid rafts (Brown & London, 2000). These rafts are more ordered structures and they function, amongst others, as centers for the assembly of signaling molecules; they are also supposed to regulate membrane trafficking (Korade & Kenworthy, 2008). Furthermore cholesterol has direct effects on the phase behavior of the membrane. Due to cholesterol the normal phase transition in a PC bilayer between the ordered gel phase and the liquid crystalline phase is abolished resulting in an intermediate state (Brown & London, 2000). In the following experiments we used cholesterol to find out whether lipid rafts and an intermediate phase state have an influence on the biophysical properties of Kcv_{NTS} and if so at which concentration of cholesterol the channel changes its voltage independent behavior to the voltage dependent behavior.

Fig 25A shows traces of single-channel currents of Kcv_{NTS} in DPhPC membranes (in n-pentane) with a cholesterol concentration from 0% up to 40%. The data show that both gating modes are observed over the entire range of cholesterol concentrations in the bilayer. The voltage independent (left) and voltage dependent (right) mode reveal no significant differences in single-channel currents at each cholesterol concentration. The single-channel trace with 0% cholesterol concentration (same as in Fig. 24A and B) is shown for comparison only. The corresponding mean single-channel I/V relations from recordings in membranes with different cholesterol concentrations are summarized in Fig 25B.

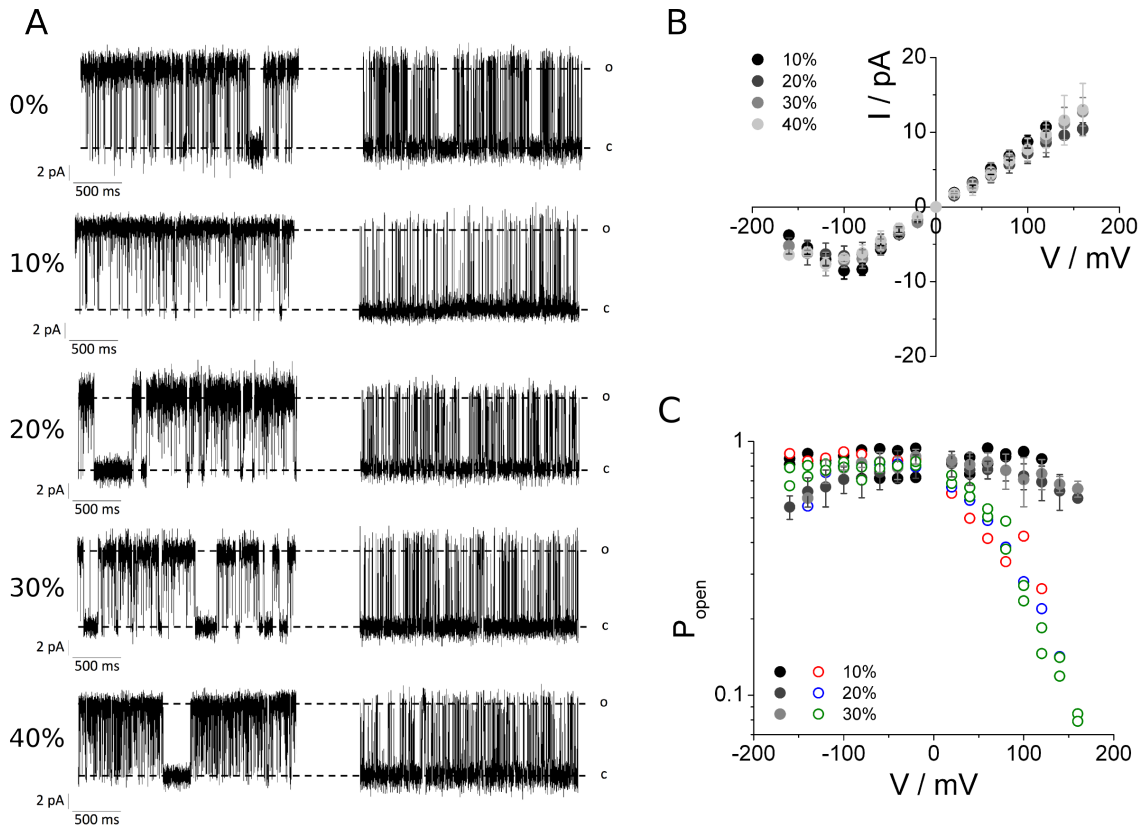

Fig 25. Gating behavior of Kcv_{NTS} in DPhPC membranes with different cholesterol concentrations.

(A) Representative single-current traces of Kcv_{NTS} in the voltage independent (left) and voltage dependent (right) mode in DPhPC membranes at a holding potential of +120 mV and with cholesterol concentrations ranging from 0% up to 40%. The open and closed states are dentoted with o and c respectively. (B) Single-channel I/V curves. Values are means +- SD of n experiments: 10% (n = 3), 20% (n = 5), 30% (n = 5), 40% (n = 5). (C) Single-channel open probabilities. Values are means +- SD of n experiments: 10%; black dots (n = 2) and red circles (n = 1), 20%; dark gray dots (n = 4) and blue circles (n = 1), 30%; gray dots (n = 3) and green circles (n = 2).

In all conditions the channel shows the same I/V relation with the same ohmic conductance at positive voltages and the typical negative slope conductance at negative voltages. This implies that the concentration of cholesterol in the membrane and the corresponding effect on the membrane architecture has no impact on the fast gating, which is responsible for the negative slope conductance (Fig 19B); also the unitary conductance of the channel is not affected by cholesterol. Calculation of the open probabilities for a given cholesterol concentration reveals that the channel has in its voltage independent mode a P_o of about 80% over the entire

voltage window tested. In the voltage dependent mode the open probability decreases from a maximum of ca 80% at negative voltages down to 8% at +160 mV. Worth noting here is that the voltage dependency of Kcv_{NTS} in membranes with different cholesterol concentrations is the same as in membranes with different acyl chain length (Fig 22) or in membranes with different solvents (Fig 24).

While the two gating modes can be observed independently of the cholesterol concentration the relative frequency of finding one mode over the other varies. At a cholesterol concentration of 10% we saw this effect once out of three measurements. At 20% cholesterol this effect occurred once out of five measurements and at a concentration of 30% it occurred twice out of five measurements. At a high cholesterol concentration of 40% the channel revealed more than the two aformentioned gating behaviors (data not shown). This might be due to the fact that almost the half of the membrane contained cholesterol.

The results of the experiments presented so far show that Kcv_{NTS} functions in membranes with a wide range of cholesterol concentrations. The addition of cholesterol has no appreciable impact on the I/V relation of the channel. In the voltage dependent mode the open probability decreases with positive voltages independent on the cholesterol concentration. The latter mode of gating is the same that is observed in membranes in which the thickness is altered by solvents or by the acyl chain length.

6.4.4. Gating behavior of Kcv_{NTS} with different membrane properties

In the previous chapter we modulated the membrane thickness in different ways namely by a variation of the acyl chain length (6.4.1), by different solvents (6.4.2) or by cholesterol (6.4.3). In the following chapter we compare representative I/V-curves and open probabilities from channel recordings in membranes with one of the modifications (Fig 26). It has been mentioned before that the single-channel amplitudes were neither affected by different acyl chain lengths (C16 or C16/C18), nor by the absence or presence of solvents (n-pentane or n-decane). Also different cholesterol contents in the membrane up to 40% had no impact on the unitary channel conductance. Kcv_{NTS} exhibits under all conditions an ohmic I/V relation at voltages positive of ca. -100 mV (Fig 26A). Also the negative slope conductance at extreme negative voltages is observed in all different types of membranes. Furthermore the measurements show that Kcv_{NTS} reveals the two gating modes in all membranes tested. Fig 26B shows the open probability of the voltage independent mode in all membranes tested. The channel reveals a high P_o (≈ 80%) in C16 membranes regardless of the presence or absence of solvent or cholesterol. In POPC membranes the P_o was slightly lower with a mean P_o value of about 60%.

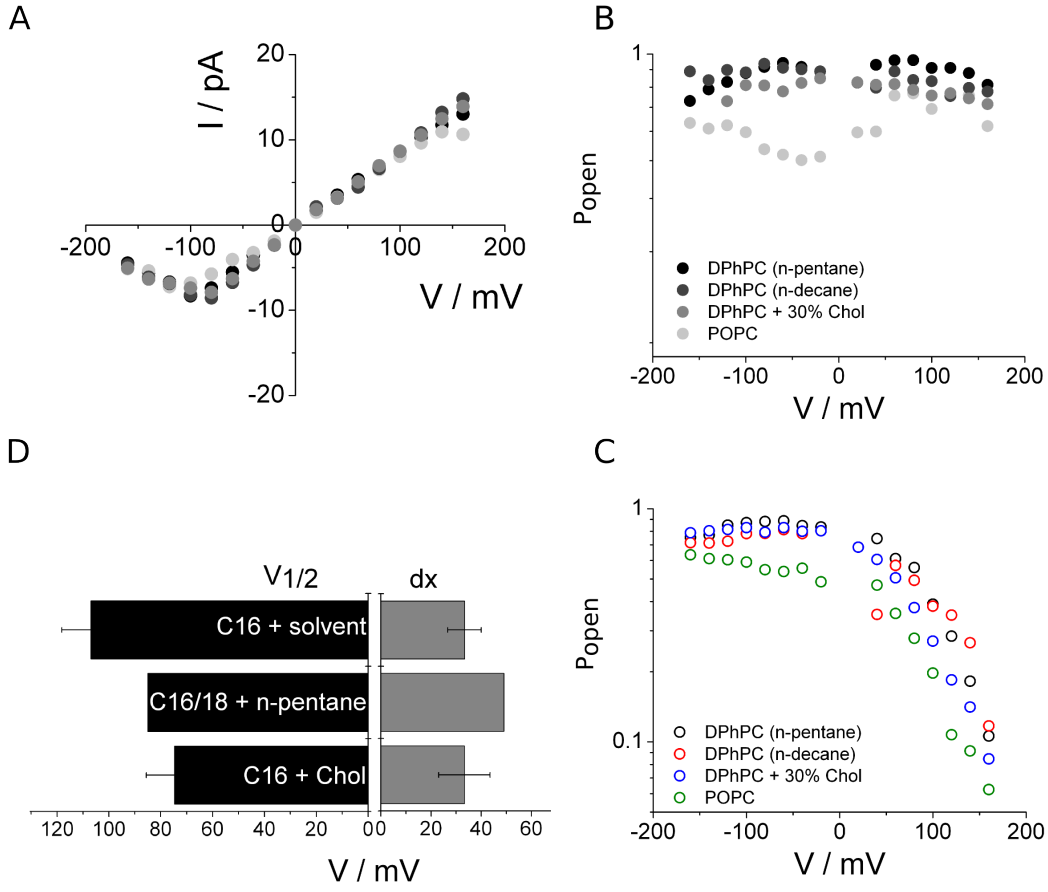

Fig 26. Gating behavior of Kcv_{NTS} with different parameters.

(A) Representative single-channel I/V-curves (symbols refer to the legend in B). (B) Representative single-channel open probabilities of the voltage independent mode. (C) Representative single-channel open probabilities of the voltage dependent mode. (D) Representative $V_{1/2}$ of the half maximal open probabilities and the slopes of the Boltzmann-fit.

A comparison of the open probabilities in the voltage dependent mode illustrates that the sensitivity to voltage is very similar in all different membranes. The only difference is that the channel shows in all C16 membranes a somewhat higher P_o at negative potentials than in POPC (C16/C18) membranes. At positive potentials the channel undergoes in all membranes a strong decrease in the P_o. This is illustrated in Fig 26D, where representative voltage dependent experiments with different conditions are fitted with the Boltzmann equation in order to examine the voltage where the channel is half maximal open. Because of the few data available due to rare occurrence of the voltage dependency the data sets with different solvents as well the data sets with different cholesterol concentrations are pooled (Fig 26D). The Boltzmann equation is given in Eq 6; were A1 is the maximal open probability, A2 the minimal open probability, x_0 the center and *dx* the slope constant.

$$y = A2 + \frac{A1 - A2}{1 + e^{\frac{(x - x_0)}{dx}}}$$

Eq 6 Boltzmann equation

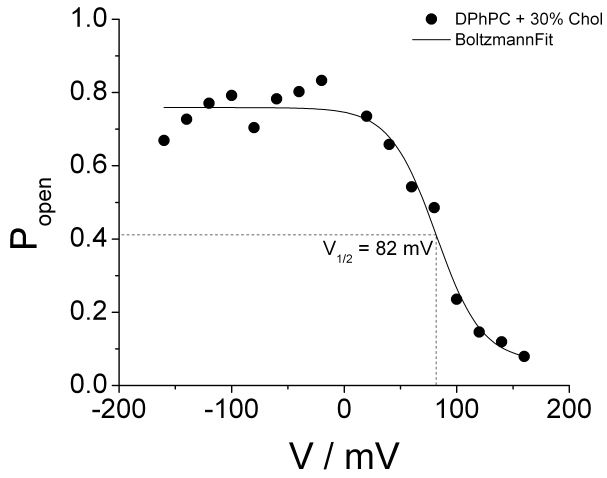

Fig 27 Representative Boltzmann fit of Kcv_{NTS} in a DPhPC membrane with 30% cholesterol.
(A1 = 0.76, A2 = 0.06, x_0 = 82 mV and *dx* = 20.5)

Fig 27 shows a representative Boltzmann fit of the open probability of Kcv_{NTS} in a DPhPC membrane with 30% cholesterol. All data sets could be well fitted by Eq 6 as in the case of Fig 27. For all data sets of Kcv_{NTS} in different membranes the fits yield a half max open probability at ca. 90 mV (Fig 26D) with no big differences. The dx value, which gives the steepness of the voltage dependency, is in all cases ca. 35 mV. The results of this analysis indicate that the mode of the voltage dependency is similar for all conditions.

The frequency with which the two gating modes are observed varies with the type of membrane. Fig 28 shows the relative frequency with which the two gating modes are detected.

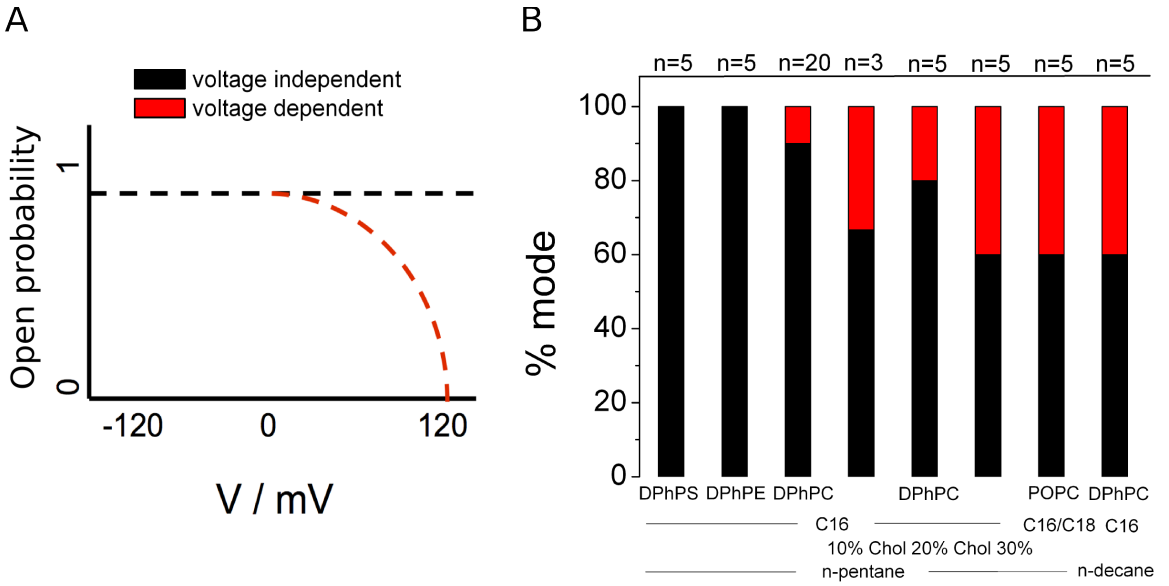

Fig 28. Quantitative voltage independent and voltage dependent gating mode of Kcv_{NTS}.

(A) Simplified sketch of the two gating modes. Black dashed line represent the voltage independent and the red dashed line the voltage dependent mode respectively. (B) Quantitative voltage independent and voltage dependent mode of Kcv_{NTS}. Number of experiments are given above the columns.

The graph in Fig 28A illustrates a sketch of the voltage independent and voltage dependent mode with black and red dashed lines respectively. The relative frequency with which one of the two modes is detectable in a given membrane is reported in Fig 28B. The numbers of experiments used for this plot differ from the numbers of experiments in the previous sections. The reason for this is that all previous data were collected from experiments with only one single-channel in the bilayer; the data for Fig 28 also consider recordings with more than one channel in the bilayer. The analysis shows that the voltage independent mode of gating is clearly dominating in recordings with normal C16 membranes. In DPhPS and DPhPE membranes the channel is exclusively operating in the voltage independent mode. In pure DPhPC membranes Kcv_{NTS} was in 18 out of 20 recordings (90%) voltage independent. An increase in membrane thickness either by adding cholesterol, by taking longer lipid chains (C16/C18) or by taking n-decane as the solvent, increased the likelihood of finding the channel in the voltage dependent mode. With 20% cholesterol inside in a membrane, the channel revealed in 80% of the recordings a voltage independent mode and in 20% a voltage dependent mode. We could increase the occurrence of the voltage dependent mode up to 40% with a cholesterol concentration of 30%. The data in Fig 22 show that the Kcv_{NTS} channel undergoes a strong reduction in the open probability in the voltage dependent mode when the membrane is stepped progressively from negative to positive voltages. In order to obtain

information on the velocity of the transition from a high to a low open probability we changed the holding potential directly from +160 mV to -160 mV. A representative example in which the capacitive artifact has been compensated is shown in Fig 29. The transition between the voltage independent and the voltage dependent mode occurs without a detectable delay in time. As soon as the holding potential is switched from -160 mV (voltage independent) to +160 mV, the channel changes the behavior immediately. The result of this analysis implies that the Kcv_{NTS} channel does not undergo major conformational changes in the context of the voltage dependent gating.

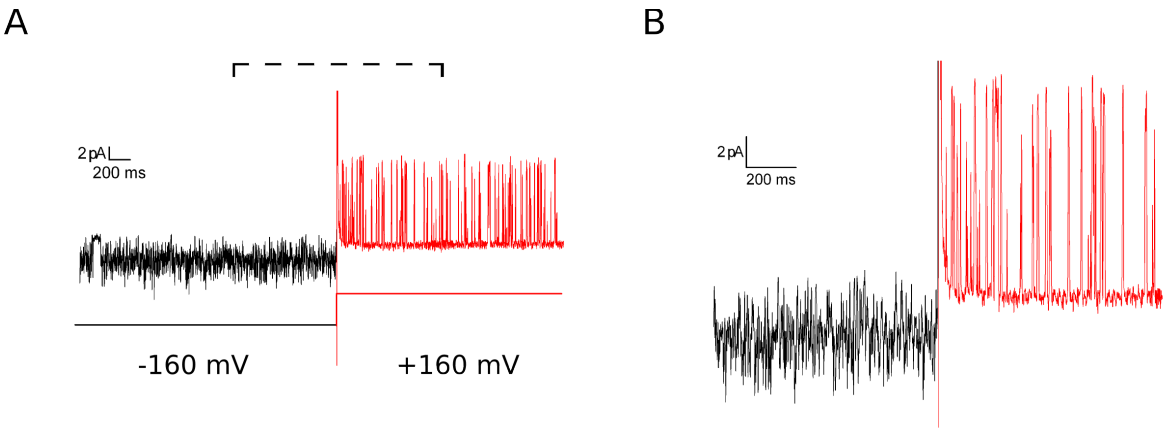

Fig 29 Voltage independent and dependent mode of Kcv_{NTS}

(A) The channel is able to switch without a detecting delay in time between the voltage independent mode (black) and voltage dependent mode (red) at holding potentials at +-160 mV respectively. (B) Zoomed detail of the trace in (A).

The two gating modes of the Kcv_{NTS} channel are very stable and the channel could be recorded for up to hours in either of the two modes. This raises the question whether the two states are a property of the same channel protein or whether the channel occurs in two different folding states in which one is voltage independent and the other is voltage dependent. To discriminate between the two possibilities we scanned through many recordings at positive voltages and searched for incidences in which the same channel exhibits both gating modes. Fig 30 shows an example in which the Kcv_{NTS} channel switches between the voltage dependent and independent mode spontaneously at +120 mV from a low open probability (red arrow) to a high open probability (green arrow) and back to a low open probability (red arrow). The present example was observed in a DPhPC membrane with 40 % cholesterol. Similar spontaneous alterations between a high and a low open probability were albeit rarely also observed in other experiments in which the membrane thickness was altered by a solvents or by the acyl chain length. The results of this analysis suggest that the two gating modes are intrinsic properties of the same channel protein. Under the influence of the lipid environment the channel is stable for long periods of time in one of the two modes of gating.

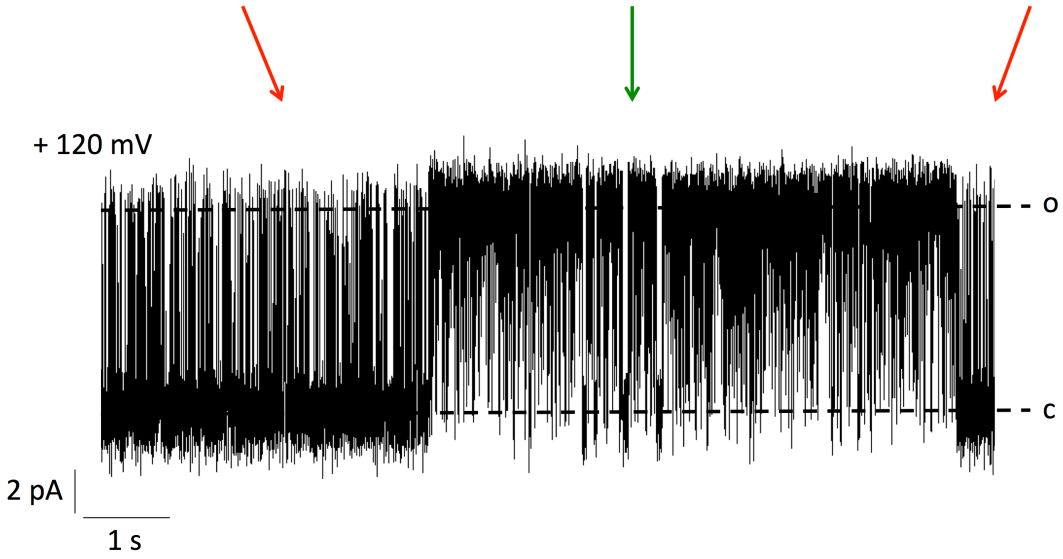

Fig 30. Direct switching behavior of Kcv_{NTS} between the voltage dependent and voltage independent mode.

Depicted is a current trace of Kcv_{NTS} in a DPhPC membrane with a concentration of 40% cholesterol. Red and green arrows indicate the voltage dependent and voltage independent mode respectively.

6.5. Discussion

The analysis of the potassium channel Kcv_{NTS} in membranes of various phospholipids and membranes with and without solvents or increasing concentrations of cholesterol show that the single-channel conductance of this small channel is not affected by these variations in the lipid environment. This is different from the behavior of other potassium channels like the BK channel. The unitary conductance of the latter channel, which is with respect to the protein size much bigger than Kcv_{NTS}, is sensitive to the thickness of membranes. The BK channel reveals different conductance states due to lipids with the same headgroup architecture but variation of chain length (Yuan et al., 2004). The different sensitivity of these two channels to the lipid environment means that the BK channel must have a specific interaction with the lipid environment, which is beyond the channel pore. From the present data we can conclude that the necessary conformational adaptations of the small Kcv_{NTS} channel in membranes with different thickness (Braun et al., 2013) have no impact on any structural feature, which determines conductance of this channel. The conducting pathway presumably remains unaffected by these conformational rearrangements. This hypothesis is consistent with the finding, that also the negative slope conductance of the Kcv_{NTS} channel is not affected by the changes in lipid environment. This reduction of channel conductance at negative voltages is caused by a fast closing process of the channel, which occurs in the selectivity filter (Abenavoli et al., 2009). The stability of this process in different membrane environments hence implies that the filter e.g. the main conducting pathway structure is not affected by the accommodation of the channel in the different lipid environments.

For the model channel KcsA it is reported that it becomes more active in an environment with anionic lipids (Marius et al., 2008). The anionic lipids tend to bind to at least three nonannular sites in the KcsA channel, which are suggested to affect the packing at the protein-protein interface and affect the channel opening. This is thought to increase the probability for the channel to shift from the inactive to the active conformation resulting in a higher open probability (Marius et al., 2008). In this study we performed experiments with neutral, cylindrical (DPhPC) and negatively charged, cylindrical (DPhPS) and neutral, conical (DPhPE) lipids (Tomita et al. 2013; Uitert et al. 2010). Regardless of the headgroups and the shape of the lipids, the Kcv_{NTS} channel behavior is unaffected; neither the unitary conductance of the channel nor the high open probability is affected. The results of these experiments stress that anionic headgroups (DPhPS) of lipids have no more positive effect on the channel; also the zwitterionic, small headgroups in the DPhPE phospholipid cause a very high open probability. If there would be a binding site for anionic lipids, like the Trp67 and Trp68 in the KcsA channel (Marius et al., 2008), the Trp33 in the Kcv_{NTS} could be the candidate for an activation of the channel. But in the case of the Kcv_{NTS} channel it is possible that the negatively charged Asp30 and Asp35 adjacent to the Trp33 could repulse the anionic lipids (Fig 31). These data again imply that the functional interaction of KcsA with negative phospholipids is a specific one and inherent in the structure of this channel. Such an interaction is apparently neither necessary nor essential for a functional channel pore.

The most intriguing finding in the present study is the observation of two different gating modes of the Kcv_{NTS} channel. In the majority the channel exhibits a voltage independent mode with a high open probability; more rarely the channel reveals a distinct voltage dependent mode. In this mode the open probability decreases by a factor of ca. 5 for 60 mV of depolarizing voltage. This means that the voltage dependency is rather shallow and that the voltage sensor only senses a fraction of the electrical field over the membrane.

The voltage dependent mode is clearly related to the lipid environment because the occurrence of this mode is augmented by measures, which increase the thickness of the bilayer. A comparison of the voltage dependency in different environments shows that the open probability decreases under all condition in a similar fashion. The voltage dependent coefficient and the values for the half maximal open probability ($V_{1/2}$) obtained from a Boltzmann fit to the data are very similar in all membranes. The results of these analyses imply that the channel has two defined gating modes, a voltage independent one and a voltage dependent one. The latter is not variable but determined by a clear-cut voltage dependency. The voltage dependent coefficient implies that the channel feels in this condition at least half of the electrical field over the membrane. This sensing of the electrical field results in a stabilization of a closed state of the channel at positive voltages. The experiments in which the membrane is clamped from a negative voltage with high open probability to a positive voltage with low open probability show that the channel acquires the low open probability quasi immediately. This implies that the structures, which are sensing the difference in the electrical field and alter the gating, are tightly coupled. The conformational changes in the protein, which determine the voltage dependency, are unlikely to undergo large conformational changes. The measurements also show that the channel remains for a long time in either of the two gating modes. This means that these states are very stable. Occasionally it is however observed that the same channel could switch between the two states within one recording. These important observations stress that these two gating modes are performed by the same channel protein and that they are not due to different types of channel folds.

The finding of the two gating modes raises the question on the mechanisms, which are underlying these fundamentally different behaviors of the channel. A voltage dependency requires a charge in the protein, which is able to sense the electrical field. Kcv_{NTS} has a number of positive and negative charged amino acids, but none of these charges are really a key candidate for a voltage sensor. The positive and negative amino acids in the turret are not in the electrical filed and are most likely not part of the voltage sensing process. The amino acids Lys and Asp at the membrane water interface are also not in the electrical field and presumably not involved in voltage sensing. The amino acid Lys29 in $Kcv_{PBCV\text{-}1}$ was shown to perform a so called snorkeling (Gebhardt, 2010); the positive side group of the cationic amino acid is in this case in the water and connects by its long side chain to the core of the amino acid in the membrane. It is unlikely that this amino acid, which is relevant for the stability of the transmembrane domain in the lipid bilayer, is a voltage sensor. Further candidates for a

voltage sensor are the histidines, which are all well within the electrical field and from this perspective potential candidates for a sensor. The two histidines in the transmembrane domains however are presumably protonated and hence not charged; this makes it unlikely that they are voltage sensors. The central His is presumably in the ion conducting pathway. The data in 4.4.3 suggest that the charge of this His can be titrated. This results in a change in the channel open probability. The voltage dependency of this effect however is much more shallow than the one seen with Kcv_{NTS} in different membranes. This does not exclude the role of the His as voltage sensor; still it seems not likely that this aa is the sensor in question. In the context of previous studies on the Kcv_{PBCV-1} channel it was found that the charged N- and C-terminus of the channel could play a role in voltage sensing; this concept will be discussed further down.

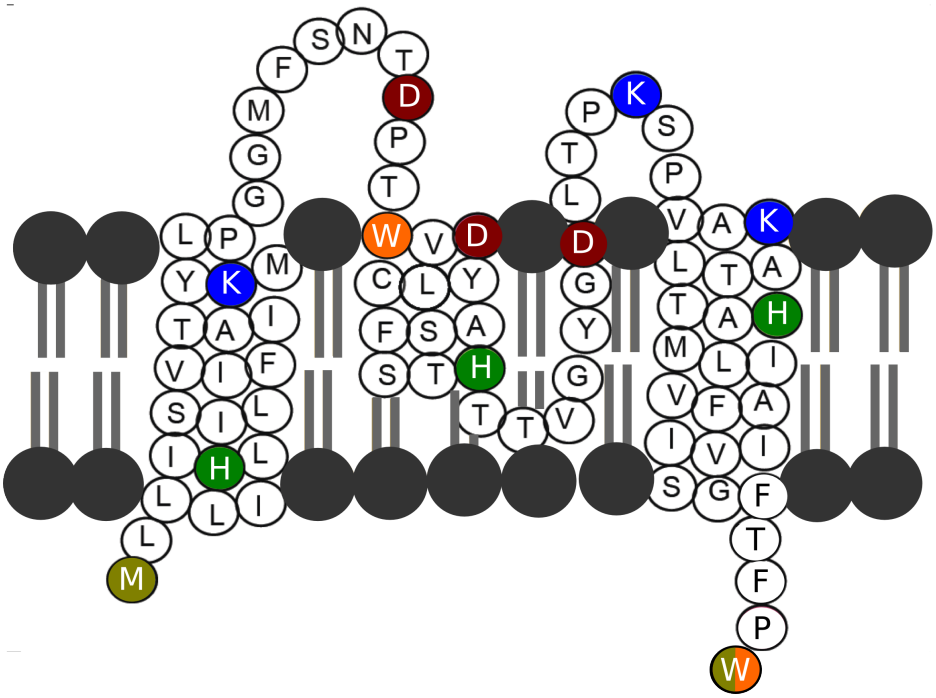

Fig 31 Sketch of the amino acid sequence of Kcv_{NTS} within the lipid bilayer.

Potentially voltage sensing amino acids; positively charged aa lysine and histidine (blue and green), negatively charged aa aspartate (red) as well the N- and C-terminus (olive) are highlighted. Potential binding sites for negatively charged lipids; tryptophan (orange).

The fact that the channel can be found in both gating modes implies that the effective charge is in one conformation, the voltage independent mode, neutralized; in the voltage dependent mode the protein presumably acquires a conformation in which the neutralization of the charges is disrupted with the effect that the protein carries an effective charge, which senses the membrane voltage. The effective charge must then alter its position within the protein with the result that the gating of the channel is affected. At this point we can only speculate on the structure/function correlates of this gating process. However the aforementioned observation that the filter gating of the channel is unaffected by the lipid environment implies that this gate, the filter gate, is not relevant for explaining the voltage sensitivity. In previous

studies it was found for the related channel Kcv_{PBCV-1} that also the entry into the cavity from the cytosol can function as a gate (Tayefeh et al., 2007). If we translate this finding onto the Kcv_{NTS} channel we may speculate that the charged C-terminus of the protein can coordinate K^+ ions. In this condition the channel is closed. It can again open when the positive N-terminus forms a salt bridge with the C-terminus. In this case the K^+ ion is liberated and ions can again flow. In the context of these data it is reasonable to speculate that the cytosolic ends of the small Kcv_{NTS} channel may be positioned differently in membrane regions of different thickness. In one condition the tilt angle of the C-terminus may favor a coordination of K^+ ions. This block may be removed by a salt bridge between the C- and the N-terminus. Such a scenario would be able to explain the voltage dependent mode in which the making and breaking of a salt bridge is favored by voltage. In the alternative condition the two termini of the channel presumably have different tilt angles with the result that they do not interfere with the ions in the conducting pathway; this could create the channel in its voltage independent mode.

Our observations of the two gating modes in membranes with increasing concentrations of cholesterol fit well with the explanation of lipid rafts; these areas of higher order appear due to the insertion of cholesterol (Brown & London, 2000; Pike, 2009). Normally lipid bilayers which are made of cylindrical lipids like DPhPC have no phase transition between -120°C and + 80°C and reside in the L_α, liquid crystalline phase (Ashrafuzzaman & Tuszynski, 2013; Hung et al., 2000; Lindsey et al., 1979). Cholesterol tends to inhibit the formation of the L_β, the ordered gel phase but favors a more ordered structure than the L_α phase. We can transfer these results to our experiments in DPhPC membranes with cholesterol or to the experiments with residual solvents in the bilayer. In the latter case we can assume that a small amount of solvent arranges in lipid-solvent rafts. Solvents have the tendency to alter the physics of the membrane (Benz et al., 1975). Hence n-pentane or n-decane may stay between the lipids and create lipid-solvent rafts with a more ordered lipid structure. These raft areas are thicker than the remaining membrane plane. Kcv_{NTS} proteins, which reside at these rafts, will have to accommodate their conformation to avoid a hydrophobic mismatch. This presumably could result in the aforementioned mechanism with a change in the conformation, which makes the channel voltage dependent.

It is straightforward to interpret the activity of the Kcv_{NTS} channel in membranes with solvents and cholesterol in the context of lipid rafts. However it is more challenging to explain the different gating modes in membranes in which the thickness is determined by the acyl chain length. In pure POPC bilayers remaining solvent could alter channel function as well but more probably could be the fact that the whole membrane is presumably uniform with C16/C18 lipids. In this case it is however possible to assume that the lateral pressure on the membrane and therefore on the channel itself leads to the voltage dependent mode. The unsaturated chain, which makes a kink in the tail, needs more space in the lipid bilayer, which in turn gives a higher lateral pressure on the protein than in lipid bilayers with “barrel” lipids.

6.6. Conclusion

Collectively the present findings stress that the very small Kcv_{NTS} channel, which is quasi fully embedded in the membrane, is functional in any membrane tested. This includes membranes with an acyl chain length varying from 14 to 18. Channel function is also possible in membranes in which the thickness of the bilayer is increased by either solvents or cholesterol; even 40 % cholesterol in a DPhPC membrane did not impair channel function. Channel function is also unaffected by the shape of the lipid headgroups and the channel tolerates neutral and anionic lipids. The data and complementary MD simulations of a similar Kcv channel imply that the small channel protein accommodates in different membranes by conformational changes in the protein. These necessary changes in the protein fold have no impact on the unitary conductance of the channel; they also do not affect a fast gating, which is correlated with the selectivity filter of the channel. This implies that the structure of the selectivity filter is kept stable in the different membrane environments. The main effect of different lipid environments on the Kcv_{NTS} channel is that an increase in bilayer thickness, which is achieved either by longer acyl chain length of the lipids or by including either solvents or cholesterol into the membrane, promotes a second gating mode of the channel. While the channel is voltage independent in thinner membranes it acquires a voltage dependent gating mode, which appears with an increasing frequency in thicker membranes. The results of these experiments imply that the membrane environment can dramatically alter the gating of a channel by modulating the stability of a closed state. The mechanism, which is underlying the voltage dependent mode of gating, is not yet understood. The best explanation is that the channel can reside at membrane areas with different thickness; these may be created by macroscopic solvent rafts or cholesterol rafts. In thicker membrane areas the channel protein may acquire a conformation with a net charge, which senses the electrical field and which affects upon movement in the field the closed state of the channel. The best candidate for this charge is either the histidine or the charged N- or C-terminus of the channel monomers or a combination of both.

6.7. References

Abenavoli, A., DiFrancesco, M. L., Schroeder, I., Epimashko, S., Gazzarrini, S., Hansen, U. P., Thiel, G., & Moroni, A. (2009). Fast and slow gating are inherent properties of the pore module of the K+ channel Kcv. *The Journal of General Physiology*, *134*, 219–229. doi:10.1085/jgp.200910266

Alvis, S. J., Williamson, I. M., East, J. M., & Lee, A. G. (2003). Interactions of anionic phospholipids and phosphatidylethanolamine with the potassium channel KcsA. *Biophysical Journal*, *85*, 3828–3838. doi:10.1016/S0006-3495(03)74797-3

Ashcroft, F. M. (2000). *Ion Channels and Disease*. Academic Press.

Ashrafuzzaman, M., & Tuszynski, J. (2013). Membrane Biophysics, 9–30. doi:10.1007/978-3-642-16105-6

Benz, R., Fröhlich, O., Läuger, P., & Montal, M. (1975). Electrical Capacity of Black Lipid Films and of Lipid Bilayers made from Monolayers. *Biochimica et Biophysica Acta*, *394*, 323–334.

Benz, R., Stark, G., Janko, K., & Läuger, P. (1973). Valinomycin-mediated ion transport through neutral lipid membranes: influence of hydrocarbon chain length and temperature. *The Journal of Membrane Biology*, *14*, 339–364.

Braun, C. J., Lachnit, C., Becker, P., Henkes, L. M., Arrigoni, C., Kast, S. M., Moroni, A., Thiel, G., Schroeder, I. (2013) Viral potassium channels as a robust model system for studies of membrane-protein interaction. *Biochimica et Biophysica Acta - Biomembranes, 1838, 1096-1103.* doi:10.1016/j.bbamem.2013.06.010

Brauser, A., Schroeder, I., Gutsmann, T., Cosentino, C., Moroni, A., Hansen, U.-P., & Winterhalter, M. (2012). Modulation of enrofloxacin binding in OmpF by Mg2+ as revealed by the analysis of fast flickering single-porin current. *The Journal of General Physiology*, *140*, 69–82. doi:10.1085/jgp.201210776

Brown, D. a, & London, E. (1998). Functions of lipid rafts in biological membranes. *Annual Review of Cell and Developmental Biology*, *14*, 111–136. doi:10.1146/annurev.cellbio.14.1.111

Brown, D. a, & London, E. (2000). Structure and function of sphingolipid- and cholesterol-rich membrane rafts. *The Journal of Biological Chemistry*, *275*, 17221–17224. doi:10.1074/jbc.R000005200

Bukiya, A. N., Belani, J. D., Rychnovsky, S., & Dopico, A. M. (2011). Specificity of cholesterol and analogs to modulate BK channels points to direct sterol-channel protein interactions. *The Journal of General Physiology*, *137*, 93–110. doi:10.1085/jgp.201010519

Coronado, R., & Latorre, R. (1983). Phospholipid bilayers made from monolayers on patch-clamp pipettes. *Biophysical Journal*, *43*, 231–236. doi:10.1016/S0006-3495(83)84343-4

De Planque, M. R. R., & Killian, J. A. (2003). Protein-lipid interactions studied with designed transmembrane peptides: role of hydrophobic matching and interfacial anchoring. *Molecular Membrane Biology*, *20*, 271–284. doi:10.1080/0968768031000160535 2

Dopico, A. M., Bukiya, A. N., & Singh, A. K. (2012). Large conductance, calcium- and voltage-gated potassium (BK) channels: Regulation by cholesterol. *Pharmacology & Therapeutics*, *135*, 133–150. doi:10.1016/j.pharmthera.2012.05.002

Doyle, D. a. (1998). The Structure of the Potassium Channel: Molecular Basis of K+ Conduction and Selectivity. *Science*, *280*, 69–77. doi:10.1126/science.280.5360.69

Engelman, D. M. (2005). Membranes are more mosaic than fluid. *Nature*, *438*, 578–80. doi:10.1038/nature04394

Fertig, N., George, M., Meyer, C., Tilke, A., Sobotta, C., Blick, R. H., & Behrends, J. C. (2003). Microstructured Apertures in Planar Glass Substrates for Ion Channel Research. *Taylor & Francis*, *9*, 29–40. doi:10.1080/10608620390177695

Gazzarrini, S. (2003). The viral potassium channel Kcv: structural and functional features. *FEBS Letters*, *552*, 12–16. doi:10.1016/S0014-5793(03)00777-4

Gazzarrini, S., Kang, M., Abenavoli, A., Romani, G., Olivari, C., Gaslini, D., Ferrara, G., van Etten, J. L., Kreim, M. Kast, S. Thiel, G. & Moroni, A. (2009). Chlorella virus ATCV-1 encodes a functional potassium channel of 82 amino acids. *The Biochemical Journal*, *420*(2), 295–303. doi:10.1042/BJ20090095

Gebhardt, M. (2010). Structure/Function Analysis of the Viral Potassium Channel Kcv. Dissertation at TU Darmstadt

Hamill, O., Marty, A., Neher, E., Sakmann, B., & Sigworth, F. (1981). Improved Patch-Clamp Techniques for High-Resolution Current Recording from Cells and Cell-Free Membrane Patches. *Pflügers Archiv*, *391*, 85–100.

Heimburg, T. (2010). Lipid ion channels. *Biophysical Chemistry*, *150*, 2–22. doi:10.1016/j.bpc.2010.02.018

Humphrey, W., Dahlke, A., & Schulten, K. (1996). VMD - visual molecular dynamics. *J. Molec. Graphics*, *14*, 33–38.

Hung, W. C., Chen, F. Y., & Huang, H. W. (2000). Order-disorder transition in bilayers of diphytanoyl phosphatidylcholine. *Biochimica et Biophysica Acta*, *1467*, 198–206.

Hunte, C., & Richers, S. (2008). Lipids and membrane protein structures. *Current Opinion in Structural Biology*, *18*, 406–411. doi:10.1016/j.sbi.2008.03.008

Jiang, Q.-X., & Gonen, T. (2012). The influence of lipids on voltage-gated ion channels. *Current Opinion in Structural Biology*, *22*, 1–8. doi:10.1016/j.sbi.2012.03.009

Kang, M., Moroni, A., Gazzarrini, S., & Van Etten, J. L. (2003). Are chlorella viruses a rich source of ion channel genes? *FEBS Letters*, *552*, 2–6. doi:10.1016/S0014-5793(03)00775-0

Katzen, F., Fletcher, J. E., Yang, J., Kang, D., Peterson, T. C., Cappuccio, J. A., Blanchette, C. D., Sulchek, T., Chromy, B.A., Hoeprich, P.D. Coleman, M.A. & Kudlicki, W. (2008). Insertion of Membrane Proteins into Discoidal Membranes Using a Cell-Free Protein Expression Approach research articles. *Journal of Proteom Research*, *7*, 3535–3542

Killian, J. A. (1998). Hydrophobic mismatch between proteins and lipids in membranes. *Biochimica et Biophysica Acta*, *1376*, 401–416.

Korade, Z., & Kenworthy, A. K. (2008). Lipid rafts, cholesterol, and the brain. *Neuropharmacology*, *55*, 1265–1273. doi:10.1016/j.neuropharm.2008.02.019

Lang, S., Erdmann, F., Jung, M., Wagner, R., Cavalie, A., & Zimmermann, R. (2011). Sec61 complexes form ubiquitous ER Ca2+ leak channels. *Channels*, *5*, 228–235. doi:10.4161/chan.5.3.15314

Lee, A. G. (2004). How lipids affect the activities of integral membrane proteins. *Biochimica et Biophysica Acta*, *1666*, 62–87. doi:10.1016/j.bbamem.2004.05.012

Li, L. B., Vorobyov, I., & Allen, T. W. (2012). The role of membrane thickness in charged protein-lipid interactions. *Biochimica et Biophysica Acta*, *1818*, 135–145. doi:10.1016/j.bbamem.2011.10.026

Lindsey, H., Petersen, N. O., & Chan, S. I. (1979). Physicochemical characterization of 1,2-diphytanoyl-sn-glycero-3-phosphocholine in model membrane systems. *Biochimica et Biophysica Acta*, *555*, 147–167.

Long, S. B., Tao, X., Campbell, E. B., & MacKinnon, R. (2007). Atomic structure of a voltage-dependent K+ channel in a lipid membrane-like environment. *Nature*, *450*, 376–382. doi:10.1038/nature06265

Lundbæk, J., & Andersen, O. (2012). Regulation of Protein Function by Membrane Elastic Properties. *Biomimetic Membranes for Sensor and Seperation Applications,* 187–203. doi:10.1007/978-94-007-2184-5

Marius, P., Zagnoni, M., Sandison, M. E., East, J. M., Morgan, H., & Lee, A. G. (2008). Binding of anionic lipids to at least three nonannular sites on the potassium channel KcsA is required for channel opening. *Biophysical Journal*, *94*, 1689–1698. doi:10.1529/biophysj.107.117507

Miller, C. (1986). *Ion channel reconstitution*. Plenum Press, New York.

Miller, C. (2000). An overview of the potassium channel family. *Genome Biology*, *1*, REVIEWS0004. doi:10.1186/gb-2000-1-4-reviews0004

Montal, M., & Mueller, P. (1972). Formation of bimolecular membranes from lipid monolayers and a study of their electrical properties. *Proceedings of the National Academy of Sciences of the United States of America*, *69*, 3561–3566.

Mueller, P., Rudin, D. O., Tien, H. T., & Wescott, W. C. (1962). Reconstitution of Cell Membrane Structure in vitro and its Transformation into an Excitable System. *Nature*, *194*, 979–980.

Mukherjee, S., & Maxfield, F. R. (2004). Membrane domains. *Annual Review of Cell and Developmental Biology*, *20*, 839–866. doi:10.1146/annurev.cellbio.20.010403.095451

Pagliuca, C., Goetze, T. A., Wagner, R., Thiel, G., Moroni, A., & Parcej, D. (2007). Molecular properties of Kcv, a virus encoded K+ channel. *Biochemistry*, *46*, 1079–1090. doi:10.1021/bi061530w

Phillips, R., Ursell, T., Wiggins, P., & Sens, P. (2009). Emerging roles for lipids in shaping membrane-protein function. *Nature*, *459*, 379–385. doi:10.1038/nature08147

Pike, L. J. (2009). The challenge of lipid rafts. *Journal of Lipid Research*, *50 Suppl*, S323–328. doi:10.1194/jlr.R800040-JLR200

Plugge, B., Gazzarrini, S., Nelson, M., Cerana, R., Etten, J. L. Van, Derst, C., Difrancesco, D., & Moroni, A. (2000). A Potassium Channel Protein Encoded by Chlorella Virus PBCV-1. *Science*, *287*, 1641–1644.

Rietveld, a, & Simons, K. (1998). The differential miscibility of lipids as the basis for the formation of functional membrane rafts. *Biochimica et Biophysica Acta*, *1376*, 467–479.

Roux, B. (2005). Ion conduction and selectivity in K(+) channels. *Annual Review of Biophysics and Biomolecular Structure*, *34*, 153–171. doi:10.1146/annurev.biophys.34.040204.144655

Sansom, M. S. P., Shrivastava, I. H., Bright, J. N., Tate, J., Capener, C. E., & Biggin, P. C. (2002). Potassium channels: structures, models, simulations. *Biochimica et Biophysica Acta*, *1565*, 294–307.

Santos, J. S., Asmar-Rovira, G. a, Han, G. W., Liu, W., Syeda, R., Cherezov, V., Baker, K. a, Stevens, R. C., & Montal, M. (2012). Crystal structure of a voltage-gated K+ channel pore module in a closed state in lipid membranes. *The Journal of Biological Chemistry*, *287*, 43063–43070. doi:10.1074/jbc.M112.415091

Schmidt, D., Jiang, Q.-X., & MacKinnon, R. (2006). Phospholipids and the origin of cationic gating charges in voltage sensors. *Nature*, *444*, 775–779. doi:10.1038/nature05416

Schrempf, H., Schmidt, O., Kümmerlen, R., Hinnah, S., Müller, D., Betzler, M., Steinkamp, T., & Wagner, R. (1995). A prokaryotic potassium ion channel with two predicted transmembrane segments from Streptomyces lividans. *The EMBO Journal*, *14*, 5170–5178.

Shyng, S. L., Cukras, C. a, Harwood, J., & Nichols, C. G. (2000). Structural determinants of PIP(2) regulation of inward rectifier K(ATP) channels. *The Journal of General Physiology*, *116*, 599–608.

Simons, K., & Ikonen, E. (1997). Functional rafts in cell membranes. *Nature*, *387*, 569–572. doi:10.1038/42408

Singer, S. J., & Nicolson, G. L. (1972). The Fluid Mosaic Model of the Structure of Cell Membranes. *Science*, *175*, 720–731.

Singh, D. K., Rosenhouse-Dantsker, A., Nichols, C. G., Enkvetchakul, D., & Levitan, I. (2009). Direct regulation of prokaryotic Kir channel by cholesterol. *The Journal of Biological Chemistry*, *284*, 30727–30736. doi:10.1074/jbc.M109.011221

Singh, D. K., Shentu, T.-P., Enkvetchakul, D., & Levitan, I. (2011). Cholesterol regulates prokaryotic Kir channel by direct binding to channel protein. *Biochimica et Biophysica Acta*, *1808*, 2527–2533. doi:10.1016/j.bbamem.2011.07.006

Steller, L., Kreir, M., & Salzer, R. (2012). Natural and artificial ion channels for biosensing platforms. *Analytical and Bioanalytical Chemistry*, *402*, 209–230. doi:10.1007/s00216-011-5517-y

Syeda, R., Holden, M. a, Hwang, W. L., & Bayley, H. (2008). Screening blockers against a potassium channel with a droplet interface bilayer array. *Journal of the American Chemical Society*, *130*, 15543–15548. doi:10.1021/ja804968g

Tarek, M., Maigret, B., & Chipot, C. (2003). Molecular dynamics investigation of an oriented cyclic peptide nanotube in DMPC bilayers. *Biophysical Journal*, *85*, 2287–2298. doi:10.1016/S0006-3495(03)74653-0

Tayefeh, S., Kloss, T., Thiel, G., Hertel, B., Moroni, A., & Kast, S. M. (2007). Molecular dynamics simulation of the cytosolic mouth in Kcv-type potassium channels. *Biochemistry*, *46*, 4826–4839. doi:10.1021/bi602468r

Thiel, G., Baumeister, D., Schroeder, I., Kast, S. M., Van Etten, J. L., & Moroni, A. (2011). Minimal art: or why small viral K(+) channels are good tools for understanding basic structure and function relations. *Biochimica et Biophysica Acta*, *1808*, 580–588. doi:10.1016/j.bbamem.2010.04.008

Tillman, T. S., & Cascio, M. (2003). Effects of membrane lipids on ion channel structure and function. *Cell Biochemistry and Biophysics*, *38*, 161–190. doi:10.1385/CBB:38:2:161

Valiyaveetil, F. I., Zhou, Y., & MacKinnon, R. (2002). Lipids in the structure, folding, and function of the KcsA K+ channel. *Biochemistry*, *41*, 10771–10777.

Van Uitert, I., Le Gac, S., & van den Berg, A. (2010). The influence of different membrane components on the electrical stability of bilayer lipid membranes. *Biochimica et Biophysica Acta*, *1798*, 21–31. doi:10.1016/j.bbamem.2009.10.003

Woolf, T. B., & Roux, B. (1994). Molecular dynamics simulation of the gramicidin channel in a phospholipid bilayer. *Proceedings of the National Academy of Sciences of the United States of America*, *91*, 11631–11635.

Yuan, C., O'Connell, R. J., Feinberg-Zadek, P. L., Johnston, L. J., & Treistman, S. N. (2004). Bilayer thickness modulates the conductance of the BK channel in model membranes. *Biophysical Journal*, *86*, 3620–3633. doi:10.1529/biophysj.103.029678

7. Pseudo painting/air bubble technique for planar lipid bilayers

7.1. Abstract

Background: A functional reconstitution of channel proteins in planar lipid bilayers is still very versatile to study structure/function correlates under well-defined conditions at the single protein level.

New Method: In this study we present an improved planar lipid bilayer technique in which an air bubble is used for stabilizing unstable/leaky bilayers or for removing excess lipids. The bubble can also be used as a tool for reducing the number of channels in the bilayer with the goal of having only one active channel in the membrane.

Results: Stable planar lipid bilayers are formed within seconds to minutes. In the case of multiple channel insertion the air bubble can be used to reduce the number of channels within minutes.

Comparison with Existing Method(s): The simple improvement of the classical folding technique guarantees a very fast creation of stable bilayers even with difficult phospholipids in a conventional vertical bilayer set up; it requires no modifications of the existing set-up.

Conclusions: This technique is very easy to handle and guarantees successful single channel recordings for any kind of planar lipid bilayer experiment.

Keywords

Pseudo painting/ air bubble technique, black lipid membrane (BLM), planar lipid bilayer, monolayer folding technique, single-channel measurement, viral potassium channel

Abbreviations

BLM: black lipid membrane; DPhPC: 1,2-diphytanoyl-*sn*-glycero-3-phosphocholine; DMPC: 1,2-dimyristoyl-*sn*-glycero-3-phosphocholine

7.2. Introduction

Many techniques are currently available for studying at the single-protein level the structure/function correlates of ion channels and their interactions with the lipid membrane (Coronado & Latorre, 1983; Fertig et al., 2003; Hamill et al., 1981; Mueller et al., 1962; Syeda et al., 2008). One of the most reduced and defined experimental systems among the many methods with the best control over the experimental parameters are planar lipid bilayers (BLM; also known as black lipid membranes). In this method the experimenter

controls the channel protein of interest, the composition of the lipids and the simple buffers on both sides of the membrane. Bilayers, which are among the oldest methods for channel recordings (Mueller et al., 1962) are generally formed by folding bilayers from monolayers (Montal & Mueller, 1972) or by painting a bilayer over a hole in a septum (Mueller et al., 1962). A disadvantage of the 'painting' technique is that the bilayer may still contain solvents, which are used for dissolving the lipids. This may alter the physical properties of the membrane (Benz et al., 1975, 1973). Planar lipid bilayers, which are folded from monolayers in contrast are virtually solvent free; this method may be more suitable for single-channel recordings when the properties of the bilayer are important for channel function (Benz et al., 1975; Montal & Mueller, 1972). Both the painting and the folding technique generally create very stable bilayers with a high electrical resistance; this makes them suitable for long lasting single-channel measurements. A problem with both methods is that the formation of a suitable bilayer can be time consuming. Often the bilayer is either leaky, unstable and breaks easily or the hole in the septum is covered with too much lipids, which do not thin out into a bilayer. A further problem, which is known to every user of bilayers, is that frequently too many channel proteins insert into the membrane; this limits the use of data for single channel analysis.

Here we present an improvement of the classical planar lipid bilayer technique. This easy to use modification, which comprises the advantages of the folding and painting technique, allows a very rapid formation of stable bilayers and even more important a fast lowering of the number of active channels in a bilayer.

7.3. Material and Methods

Planar lipid bilayer experiments were done with a vertical bilayer set up (IonoVation, Osnabrück Germany) and a stereomicroscope (Novex, Netherlands) for optical monitoring. A 1% hexadecane solution (MERCK KGaA, Darmstadt, Germany) in n-hexane (Carl ROTH GmbH, Karlsruhe, Germany) was used for pretreating the Teflon foil. The hexadecane solution (ca. 0.5 μl) was pipetted onto the hole (100 μm in diameter) in the Teflon foil with a bent Hamilton syringe (Hamilton Company, Reno, Nevada, USA). It was waited until the solvent was evaporated. The experimental solution contained of 100 mM KCl and was buffered with 10 mM HEPES/KOH to a pH of 7. The lipids 1,2-diphytanoyl-*sn*-glycero-3-phosphocholine (DPhPC) and 1,2-dimyristoyl-*sn*-glycero-3-phosphocholine (DMPC) (both from Avanti Polar Lipids, Alabaster, AL, USA) were used at a concentration of 0.15-25 mg/ml in n-pentane (MERCK KGaA, Darmstadt, Germany).

The potassium channel Kcv_{NTS} (K^+ channel *chlorella* virus – isolate Next-to-Smith), which was used for single-channel measurements, was synthetized cell–free in nanolipoprotein discs (Katzen et al. 2008). The channel was purified indirectly over a Ni-NTA column using the His-tag at the nanolipoprotein. The recombinant protein in the nanodisc was therefore first centrifuged (12 min, 16060 x g, RT) to remove insoluble material. The supernatant was loaded onto a Ni-NTA column and incubated for 30 min. Later the column was washed twice

with 20 mM imidazole. The protein was then eluted by 250 mM imidazole (fractions a 100 μl). The recombinant channel protein in the nanodiscs dissolved in 250 mM imidazole was directly added to the bilayer. This resulted in a spontaneous insertion of channel protein into the bilayer; an osmotic gradient between the chambers was not required for protein insertion. Reconstitution was best when small volumes of protein in imidazole were administered with a Hamilton syringe directly below the bilayer (Braun et al., 2013). In control experiments we found that the small volume of imidazole alone had no effect on the bilayer. Once inserted into the bilayer the channel protein must be released from its nanolipoprotein scaffold because channel function was determined by the physicochemical properties of the bilayer. In additional experiments we also reconstituted the same channel protein in detergent after recombinant production of the channel in *Pichia pastoris* cells. The behavior of the channel in the bilayer was independent on the method of purification or whether solubilization in detergent or dissolving in imidazole (Braun et al. 2013)

All experiments were done at room temperature between 20-25°C. The Ag/AgCl electrodes were connected to a head-stage of a patch-clamp amplifier (L/M-EPC 7, List–Medical, Darmstadt). Single-channel currents were filtered at 1 kHz and digitized with a sampling interval of 280 μs (3.57 kHz) by an A/D-converter (LIH 1600, HEKA Electronik, Lambrecht, Germany).

7.4. Results

The formation of planar lipid bilayers by the monolayer folding technique is described elsewhere (Montal et al., 1972) and schematically shown in Fig 32A. Lipids, which are dissolved in an organic solvent, are spread as monolayers onto an experimental solution. After evaporation of the solvent two monolayers are folded over the hole in the septum by raising the experimental in both chambers; this eventually creates a bilayer. Frequently the bilayer folding method is time consuming and not every membrane is suitable for bilayer measurements. Often the bilayer is leaky or the hole in the septum contains too much lipid, which does not thin out into a suitable bilayer. In our approach we start the procedure with a conventional formation of a lipid bilayer from folding of monolayers (Montal & Mueller, 1972) as in Fig 32 (step 1 A and B). In preparation of this procedure the edges of the hole are first pretreated with 1% hexadecane solution, which creates a very hydrophobic area around the hole. The bilayer is then formed as shown in the sketch of Fig 32. In the case that this procedure already results in a perfect bilayer channel proteins can be inserted in the bilayer and the channel recordings can be started directly. If the bilayer is unstable, leaky or too thick we can apply a “pseudo painting” with an air bubble. Because of the hexadecane pretreatment the edges of the hole presumably keep a reservoir of lipids. These lipids from the reservoir can now be spread over the hole. For this purpose we use a bent Hamilton syringe and create a small air bubble under water Fig 32B (step 2). A photo with the real dimensions of the syringe with the bubble in front of the hole in the Teflon septum is shown in Fig 33. The air bubble can be spread over the hole with the syringe under visual control through the stereomicroscope. In the case of leaky/unstable bilayers the movement of the air bubble from

the edges over the hole transfers lipids from the aforementioned reservoir over the hole and rapidly creates a new bilayer (Fig 32B, steps 3 and 4). In the case of a thick lipid deposit, the air bubble is moved right in front of the hole; in this position the bubble attracts with the water/air interface lipids and moves them out of the hole. Also with this procedure it is possible to rapidly create suitable stable bilayers.

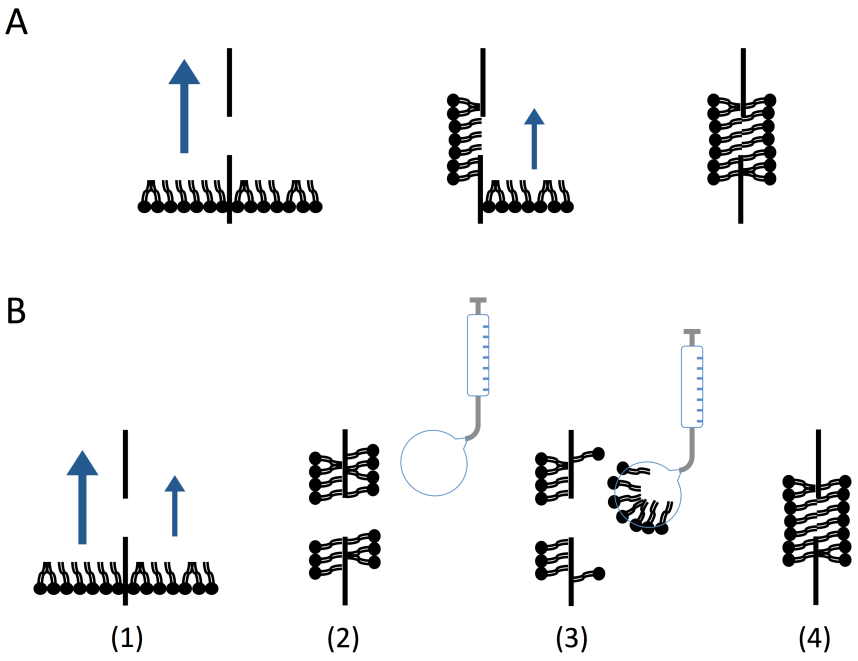

Fig 32 Schematic sketches of two different planar lipid bilayer techniques.

(A) Monolayer folding technique (modified after (Montal & Mueller, 1972). A monolayer is first created over the hole in the septum by elevating the water level in one chamber with a lipid monolayer on the surface. In the next step the water level is elevated in the second chamber with the result that a bilayer is formed. (B) Pseudo painting technique with an air bubble. A leaky bilayer is formed as in A. The air bubble on the bent tip of a Hamilton syringe is slowly moved from the edge over the hole (3). This spreads lipids over the hole in the septum and forms a bilayer (4).

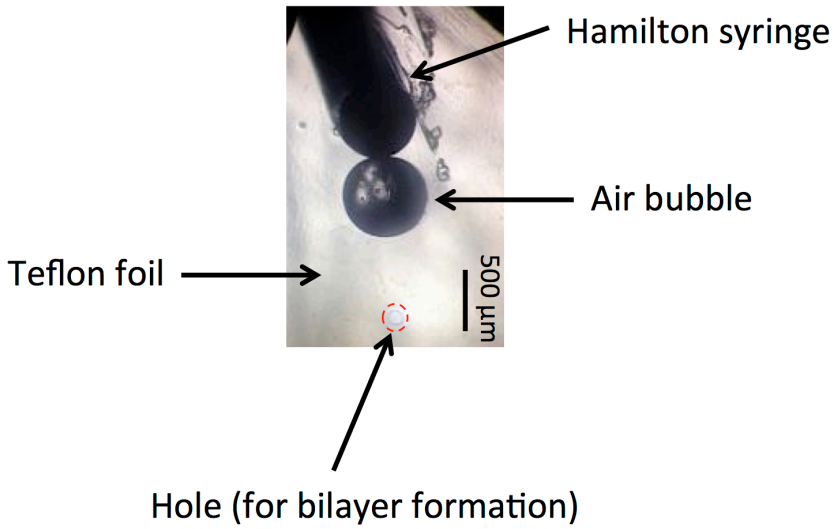

Fig 33 Photo through a stereomicroscope on the Teflon septum including the hole for the bilayer, the Hamilton syringe and the air bubble at the tip.

Fig 34 demonstrates in an example how rapid bilayers can be formed with this method. The representative recording shows the measurement of currents across a stable bilayer, which was created by folding. The bilayer was then destroyed with the air bubble. By spreading the air bubble over the hole in the aforementioned fashion, a new stable bilayer was formed in less than 10 sec. The destruction and reformation of the bilayer was repeated once more and a bilayer was again formed within less than 10 sec. This operation can be frequently repeated until the reservoir runs out of lipids.

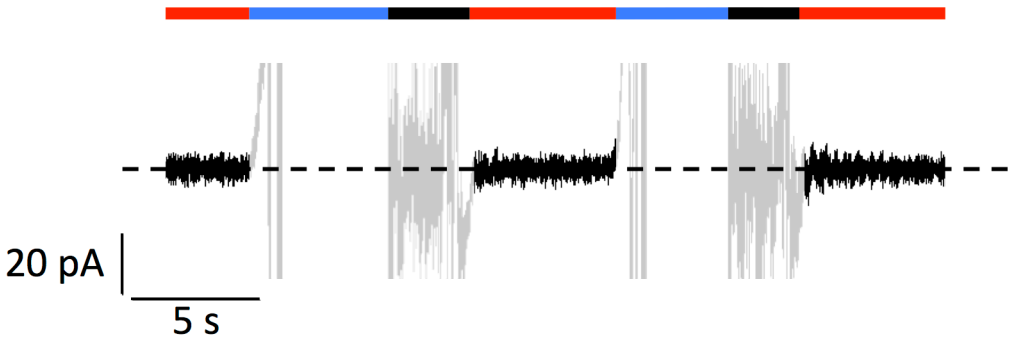

Fig 34 Fast creation of suitable planar lipid bilayers with the use of an air bubble.

Currents were recorded continuously across a bilayer at a holding voltage of 40 mV (red). The bilayer was then destroyed (blue) and reformed (black), destroyed (blue) and reformed (black) again within one sweep. Currents recorded during time at which the Faraday cage was open are shown in grey.

In the context of questions on protein/lipid interactions it is often desirable to measure the activity of a channel in different kinds of pure lipid bilayers. This includes bilayers with

different chain length. An interesting lipid is 1,2-dimyristoyl-*sn*-glycero-3-phosphocholine (DMPC). This lipid is frequently used in molecular dynamic simulations (Braun et al., 2013; Tarek et al., 2003; Tayefeh et al., 2007; Woolf & Roux, 1994) and it is hence interesting to compare the data from simulations and experiments in the same lipid. The problem however is that DMPC forms very unstable planar lipid bilayers (Schmidt et al., 2006). This makes it difficult for single-channel recordings. For this reason it is not surprising that there are only very few reports in the literature in which this lipid was successfully used for bilayer measurements. Indeed when we attempted to create bilayers with the conventional folding technique from this lipid we failed even after many trials. When we used the aforementioned procedure with a painting of lipids from the edges of the hole with the air bubble, we could however achieve DMPC bilayers. The lifetimes of these bilayers were short (ca. 3-5 min) but sufficient to record the properties of an ion channel; with the easiness of reforming bilayers (Fig 34), which also worked with this lipid, even allowed a good collection of data. An example of a successful measurement of a K^+ channel in a DMPC membrane at room temperature is shown in Fig 35.

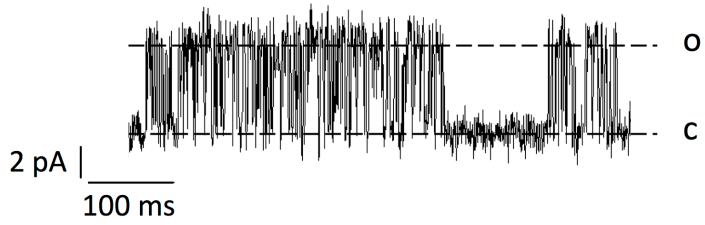

Fig 35 Representative single-channel measurement of Kcv_{NTS} in a DMPC bilayer at a holding potential of +80 mV. The open and closed states are denoted with o and c respectively.

A general problem known to those working with bilayers is that the membrane contains frequently after reconstitution of proteins more than one or two active channels. With this kind of data it is impossible to obtain the desired information on the open and closed dwell times of a channel. In the case of multiple channels in the bilayer we can destroy the bilayer by a high voltage pulse or with the air bubble and quickly reform new bilayers as in Fig 36 until finding a membrane with a single channel. Fig 36 shows data from a representative experiment in which the membrane contained initially a too high number of channels. The bilayer was frequently destroyed and reformed as in Fig 34 until only a single channel remained in the membrane. Representative for many similar experiments we obtained in less than 5 min a recording condition with a single channel in the bilayer by frequent destruction and reformation of the bilayer.

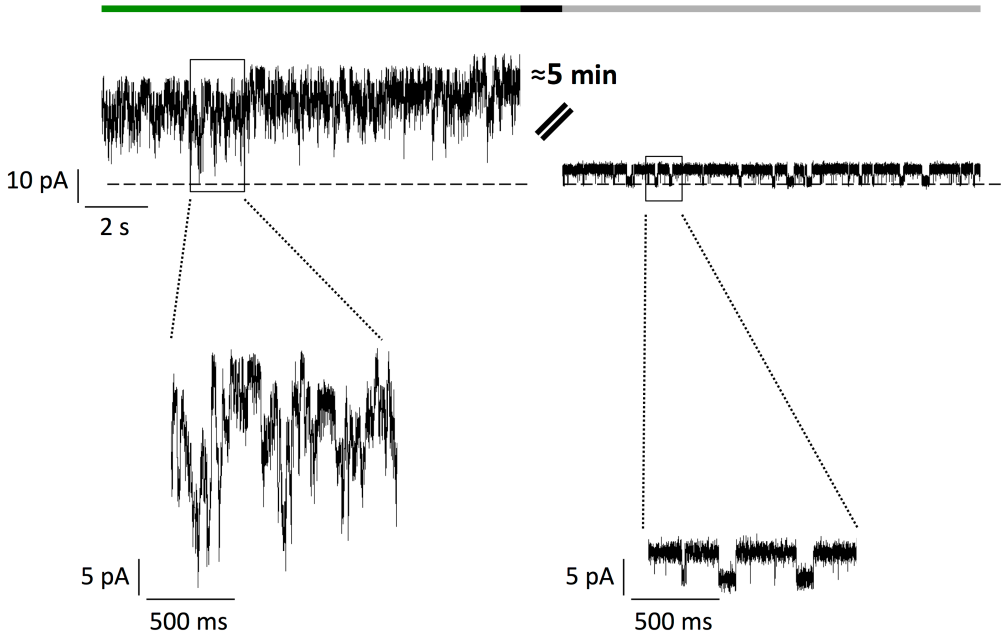

Fig 36. Representative recording of Kcv_{NTS} in a DPhPC bilayer at a holding potential of +40 mV.

Initially the membrane contained a high number of active channels (green). The membrane was frequently destroyed and reformed with the air bubble (black) until a single-channel remained in the membrane (gray). This configuration was then stable and single channel activity was measured until enough data were collected (ca. 30 min). The boxed areas are magnified below. Dashed line denotes the zero current level.

The air bubble can also remove an excess of channels in the membrane in a more elegant way without destroying the bilayer. In the representative recording shown in Fig 37 we can see multiple channels inserting into the bilayer after addition of channel proteins. Subsequently the air bubble was frequently moved over the bilayer. This operation removes active channels from the bilayer; in the present example we find that this maneuver results within one minute in a reduction of the active channels from about 15 to the desired number of one. The causal reason for this removal of channel proteins is not fully understood. But it is reasonable to assume the curved water/air/lipid interface of the bubble is thermodynamically more attractive for the channel proteins than the lipid bilayer. The air bubble may in this way function like a “hoover” to remove channel proteins from the bilayer (Fig 37).

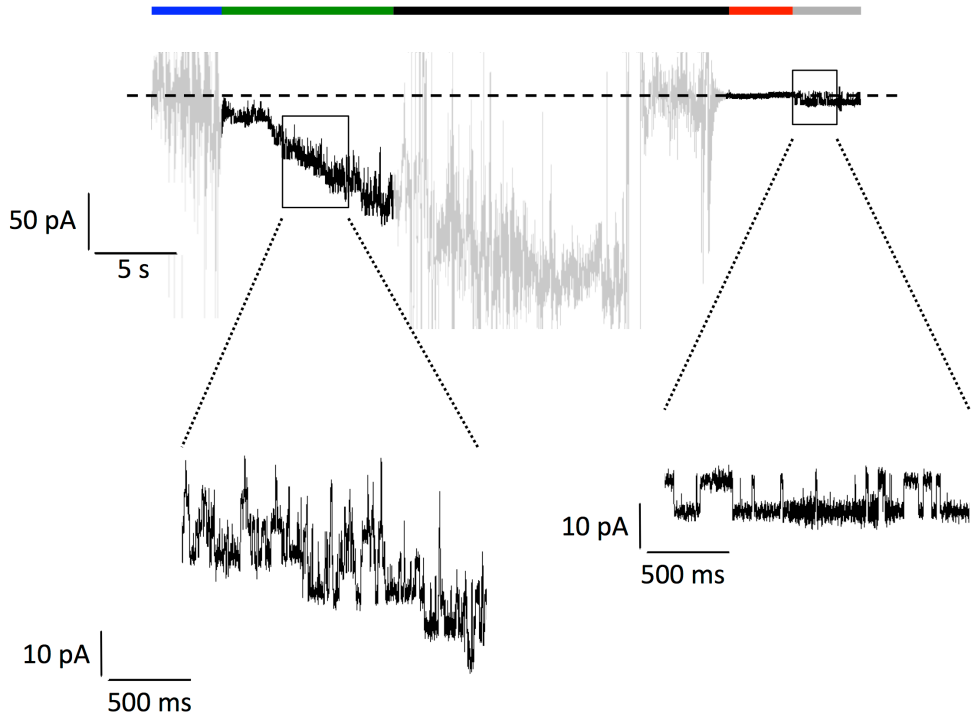

Fig 37. Currents across a DPhPC bilayer measured at -80 mV.

After addition of protein-nano discs with Kcv channel (blue) multiple channels inserted into the bilayer (green). The air bubble was brushed several times over the hole in the septum (black) until the noisy current decreased. After closing the Faraday cage first a silent bilayer (red) and soon after a bilayer with one single channel was observed (gray). The boxed areas are magnified below. Dashed line denotes the zero current level. Currents recorded during time at which the Faraday cage was open are shown in grey.

7.5. Discussion and Conclusion

Even though the planar lipid bilayer technique is already around for decades it is still very valuable for studying the functional properties of membrane transports at the single-protein level. The method allows better than any other technique a maximal control over a minimum of experimental parameters (Miller, 1986). Also bilayer recordings are still the technique of choice for the reconstitution and functional analysis of proteins from membranes, which are not accessible to patch clamp electrodes. This includes proteins from endomembranes in eukaryotic cells (Lang et al., 2011) and proteins from bacterial membranes (Brauser et al., 2012). The bilayer technique has further seen a renaissance in recent years in which the crystallization of ion channels was combined with a functional analysis of the respective purified proteins (Doyle, 1998; Santos et al., 2012; Schrempf et al., 1995). Here we describe a simple technical improvement of the classical folding method, which greatly speeds up the formation of stable solvent free bilayers. With the high success rate of forming bilayers it is possible for the experimenter to repetitively destroy and reform new bilayers. When studying ion channels this cycle of destroying and reforming a bilayer can be repeated until the desired configuration with a single channel is achieved. Excess numbers of channel proteins in the bilayer, which confounds channel analysis, can also be removed from the bilayer with the help of an air bubble; again this reduces the number of channels to an extend that single-channels can be recorded. Finally the painting of a bilayer with the help of an air bubble improves the formation of bilayers from lipids such as DMPC, which are interesting from a scientific point of view but otherwise difficult to handle. The method, which we describe here, can be used with any classical vertical bilayer system, which includes a stereomicroscope; the latter is essential for controlling the movement of the air bubble. With these minimal technical requirements and easiness the method is routinely used in our laboratory and untrained students are already after less than 1 h of initial practice able to perform their single-channel recordings from reconstituted channel proteins.

7.6. Acknowledgments

We thank James Van Etten (Lincoln, USA) and Timo Greiner (Darmstadt) for initial characterization of the Kcv_{NTS} channel. We are also grateful to Maurico Montal, Jose Santos (San Diego) and Richard Wagner (Osnabrück) for suggestions to the manuscript. Furthermore we thank Kerri Kukovetz for assistant in some of the experiments.

7.7. References

Benz, R., Fröhlich, O., Läuger, P., & Montal, M. (1975). Electrical Capacity of Black Lipid Films and of Lipid Bilayers made from Monolayers. *Biochimica et Biophysica Acta*, *394*, 323–334.

Benz, R., Stark, G., Janko, K., & Läuger, P. (1973). Valinomycin-mediated ion transport through neutral lipid membranes: influence of hydrocarbon chain length and temperature. *The Journal of Membrane Biology*, *14*, 339–364.

Braun, C. J., Lachnit, C., Becker, P., Henkes, L. M., Arrigoni, C., Kast, S. M., Moroni, A., Thiel, G., Schroeder, I. (2013) Viral potassium channels as a robust model system for studies of membrane-protein interaction. *Biochimica et Biophysica Acta - Biomembranes*, *1838, 1096-1103.* doi:10.1016/j.bbamem.2013.06.010

Brauser, A., Schroeder, I., Gutsmann, T., Cosentino, C., Moroni, A., Hansen, U.-P., & Winterhalter, M. (2012). Modulation of enrofloxacin binding in OmpF by Mg2+ as revealed by the analysis of fast flickering single-porin current. *The Journal of General Physiology*, *140*, 69–82. doi:10.1085/jgp.201210776

Coronado, R., & Latorre, R. (1983). Phospholipid bilayers made from monolayers on patch-clamp pipettes. *Biophysical Journal*, *43*, 231–236. doi:10.1016/S0006-3495(83)84343-4

Doyle, D. a. (1998). The Structure of the Potassium Channel: Molecular Basis of K+ Conduction and Selectivity. *Science*, *280*, 69–77. doi:10.1126/science.280.5360.69

Fertig, N., George, M., Meyer, C., Tilke, A., Sobotta, C., Blick, R. H., & Behrends, J. C. (2003). Microstructured Apertures in Planar Glass Substrates for Ion Channel Research. *Taylor & Francis*, *9*, 29–40. doi:10.1080/10608620390177695

Hamill, O., Marty, A., Neher, E., Sakmann, B., & Sigworth, F. (1981). Improved Patch-Clamp Techniques for High-Resolution Current Recording from Cells and Cell-Free Membrane Patches. *Pflügers Archiv*, *391*, 85–100.

Katzen, F., Fletcher, J. E., Yang, J., Kang, D., Peterson, T. C., Cappuccio, J. A., Blanchette, C. D., Sulchek, T., Chromy, B.A., Hoeprich, P.D. Coleman, M.A. & Kudlicki, W. (2008). Insertion of Membrane Proteins into Discoidal Membranes Using a Cell-Free Protein Expression Approach research articles. *Journal of Proteom Research*, *7*, 3535–3542

Lang, S., Erdmann, F., Jung, M., Wagner, R., Cavalie, A., & Zimmermann, R. (2011). Sec61 complexes form ubiquitous ER Ca2+ leak channels. *Channels*, *5*, 228–235. doi:10.4161/chan.5.3.15314

Miller, C. (1986). *Ion channel reconstitution*. Plenum Press, New York.

Montal, M., & Mueller, P. (1972). Formation of bimolecular membranes from lipid monolayers and a study of their electrical properties. *Proceedings of the National Academy of Sciences of the United States of America*, *69*, 3561–3566.

Mueller, P., Rudin, D. O., Tien, H. T., & Wescott, W. C. (1962). Reconstitution of Cell Membrane Structure in vitro and its Transformation into an Excitable System. *Nature*, *194*, 979–980.

Santos, J. S., Asmar-Rovira, G. a, Han, G. W., Liu, W., Syeda, R., Cherezov, V., Baker, K. a, Stevens, R. C., & Montal, M. (2012). Crystal structure of a voltage-gated K+ channel pore module in a closed state in lipid membranes. *The Journal of Biological Chemistry*, *287*, 43063–43070. doi:10.1074/jbc.M112.415091

Schmidt, D., Jiang, Q.-X., & MacKinnon, R. (2006). Phospholipids and the origin of cationic gating charges in voltage sensors. *Nature*, *444*, 775–779. doi:10.1038/nature05416

Schrempf, H., Schmidt, O., Kümmerlen, R., Hinnah, S., Müller, D., Betzler, M., Steinkamp, T., & Wagner, R. (1995). A prokaryotic potassium ion channel with two predicted transmembrane segments from Streptomyces lividans. *The EMBO Journal*, *14*, 5170–5178.

Syeda, R., Holden, M. a, Hwang, W. L., & Bayley, H. (2008). Screening blockers against a potassium channel with a droplet interface bilayer array. *Journal of the American Chemical Society*, *130*, 15543–15548. doi:10.1021/ja804968g

Tarek, M., Maigret, B., & Chipot, C. (2003). Molecular dynamics investigation of an oriented cyclic peptide nanotube in DMPC bilayers. *Biophysical Journal*, *85*, 2287–2298. doi:10.1016/S0006-3495(03)74653-0

Tayefeh, S., Kloss, T., Thiel, G., Hertel, B., Moroni, A., & Kast, S. M. (2007). Molecular dynamics simulation of the cytosolic mouth in Kcv-type potassium channels. *Biochemistry*, *46*, 4826–4839. doi:10.1021/bi602468r

Woolf, T. B., & Roux, B. (1994). Molecular dynamics simulation of the gramicidin channel in a phospholipid bilayer. *Proceedings of the National Academy of Sciences of the United States of America*, *91*, 11631–11635.

8. List of Figures

9. List of Equations

10. Abbreviations

aa	amino acid
BLM	black lipid membrane
BK channel	big conductance K^+ channel
CH_3COOK	potassium acetate
CHARMM22	Chemistry at Harvard Macromolecular Mechanics 22
DMPC	1,2-dimyristoyl-*sn*-glycero-3-phosphocholine
DPhPC	1,2-diphytanoyl-*sn*-glycero-3-phosphocholine
DPhPE	1,2-diphytanoyl-*sn*-glycero-3-phosphoethanolamine
DPhPS	1,2-diphytanoyl-*sn*-glycero-3-phospho-L-serine
GUV	Giant Unilamellar Vesicle
HEK293	Human Embryonic Kidney 293 cell
HEPES	4-(2-hydroxyethyl)-1-piperazineethanesulfonic acid
I/V curve	Current Voltage curve
KcsA	K^+ crystallographically-sited activation channel
Kcv	K^+ channel *chlorella* virus
Kcv_{ATCV-1}	K^+ channel *chlorella* virus *Acanthocystis turfacea Chlorella* virus - 1
Kcv_{NTS}	K^+ channel *chlorella* virus Next-to-Smith
Kcv_{PBCV-1}	K^+ channel *chlorella* virus *Paramecium bursaria Chlorella* virus – 1
K_{ir}	inward rectifying K^+ channel
$K_v2.1$	K^+ voltage-gated channel 2.1
MD	Molecular Dynamics
MES	2-(N-Morpholino)ethanesulfonic acid
NAMD	Nanoscale Molecular Dynamics
NMR	Nuclear Magnetic Resonance
P_o	open probability
POPC	1-palmitoyl-2-oleoyl-*sn*-glycero-3-phosphocholine
S.D.	standard deviation
TAPS	N-[Tris(hydroxymethyl)methyl]-3-aminopropanesulfonic acid
TMD	Transmembrane domain
VMD	Visual Molecular Dynamics

11. Acknowledgements

An dieser Stelle möchte ich mich bei allen Personen bedanken, welche zum Gelingen dieser Arbeit beigetragen haben.

Vor allem bedanken möchte ich mich bei:

Herrn Professor Dr. **Gerhard Thiel**, für die super Betreuung bei der spannenden Arbeit, die Geduld und die Freiheit zu forschen und dem nachzugehen was mich interessiert hat. Weiterhin möchte ich mich dafür Bedanken, dass ich die Möglichkeit hatte auf zahlreiche Konferenzen und Workshops zu gehen und natürlich für die Möglichkeit in dieser tollen AG meine Arbeit zu schreiben.

Herrn Professor Dr. **Adam Bertl**, für die Übernahme des Koreferats und des schwäbischen Akzents, welcher mich immer an die Heimat erinnert.

Timo (Mimoni) **Greiner**, für das Korrekturlesen.

Indra Schröder, für die ewige Geduld und Bereitschaft physikalische (wahrscheinlich einfache) Fragen eines Biologen zu beantworten.

Dem alten Kinderzimmer, mit **Manuela Gebhard**, **Alice Kress**, **Bastian Roth**, **Fenja Siotto**, **Charlotte von Chappuis, Timo W.** & **Timo G.** für die super Aufnahme, Atmosphäre und Herzlichkeit.

Dem neuen Kinderzimmer, mit **Patrick Becker** und **Sebastian Fuck** für ihre einzigartige Muppets-Show.

Den anderen Kinder-/Doktorenzimmern, mit **Christine** (Sabbel) **Gibhardt**, **Anne Berthold**, **Thomas Guthmann**, **Tobias Meckel**, **Markus Langhans** und vor allem **Brigitte Hertel**, der guten Seele der AG.

Meiner mini AG mit **Kerri Kukovetz** und **Oliver Rauh** sowie meinen anderen Diplom-, Bachelor- und Masterstudenten für die zumeist tollen Ergebnisse.

Den Technischen Assistentinnen, **Silvia Haase** und **Sylvia Lenz**.

Barbara Reinhards für die Geduld bei Reisekostenabrechnungen.

Vor Allem möchte ich mich bei **Lucia Carrillo**, **Vera Bandmann** und **Bastian Roth** für die wunderbare Zeit und Freundschaft bedanken.

Meinen Freunden **Tasja**, **Eva**, **Louis**, **Can** und **Dominic** für die Geduld in dieser Zeit.

Des Weiteren möchte ich mich bei meinem besten Freund **Stefan Hartmann** für Ratschläge und Anregungen in jeglicher Lebenslage bedanken.

Und natürlich einen ganz herzlichen und besonderen Dank an meine **Eltern** sowie an meinem Bruder **Benjamin** für das Vertrauen und die Unterstützung seitdem ich denken kann.

12. Ehrenwörtliche Erklärung

Ich erkläre hiermit ehrenwörtlich, dass ich die vorliegende Arbeit entsprechend den Regeln guter wissenschaftlicher Praxis selbstständig und ohne unzulässige Hilfe Dritter angefertigt habe.

Sämtliche aus fremden Quellen direkt oder indirekt übernommenen Gedanken sowie sämtliche von Anderen direkt oder indirekt übernommenen Daten, Techniken und Materialien sind als solche kenntlich gemacht. Die Arbeit wurde bisher bei keiner anderen Hochschule zu Prüfungszwecken eingereicht.

Darmstadt, den

_____

Dipl.-Biol. Christian J. Braun

13. Own Work

Chapter 5 “Viral potassium channels as a robust model system for studies of membrane-protein interaction” was already published in a similar form in Braun et al. 2013.

Chapter 7 “Pseudo painting/air bubble technique for planar lipid bilayers” was already published in a similar form in Braun et al. 2014.

All Experiments, data analysis and writing of the present thesis were performed by myself with the following exceptions:

Chapter 4

3 out of 4 conductance experiments in Fig. 3A were performed by Oliver Rauh (Master student, TU Darmstadt/Germany) under my supervision.

Experiments with different pH conditions and some analysis for Fig. 8, 9 and 10 were performed by Kerri Kukovetz (Bachelor student, TU Darmstadt/Germany) under my supervision.

Chapter 5

Kcv_{NTS} was expressed and purified in *Pichia pastoris* (5.3.1) by Cristina Arrigoni (Uni Milano, Italy)

Patrick Becker (Diploma student TU Darmstadt Germany) and Christine Lachnit (Bachelor student, TU Darmstadt, Germany) contributed to data in Fig. 14, 16 and Tab. 1

MD simulations in Fig. 17 and writing of 5.4.3 were performed by Leonhard M. Henkes and Stefan Kast (TU Dortmund, Germany).

Indra Schroeder helped with data analysis and planning of experiments; Indra Schroeder, Anna Moroni and Gerhard Thiel helped in writing the manuscript.

Chapter 6

Stefanie Renz (Bachelor student TU Darmstadt, Germany) and Manuel Schwarz (Bachelor student TU Darmstadt, Germany) contributed to data in Fig. 25 – 28 and 30 under my supervision

Chapter 7

Tom Baer contributed to experimental data; Anna Moroni and Gerhard Thiel helped in writing the manuscript.

14. Publications

Braun, C. J., Lachnit, C., Becker, P., Henkes, L. M., Arrigoni, C., Kast, S. M., Moroni, A., Thiel, G., Schroeder, I. (2013) Viral potassium channels as a robust model system for studies of membrane-protein interaction. *Biochimica et Biophysica Acta - Biomembranes*, *1838, 1096-1103.* doi:10.1016/j.bbamem.2013.06.010

Kol, S., Braun, C., Thiel, G., Doyle, D. A., Sundström, M., Gourdon, P., Nissen, P. (2013) Heterologous expression and purification of an active human TRPV3 ion channel. FEBS J**.** 280, 6010-6021. doi:10.1111/febs.12520

Braun, C., Schroeder, I., Henkes, L. M., Arrigoni, C., Kast, S. M., Moroni, A., Thiel, G. (2013) Minimal viral K^+ channels as robust model systems for understanding structure/function correlations. *Eur Biophys J 42 (Suppl 1):S1–S236,* doi: 10.1007/s00249-013-0917-x

Braun, C. J., Schroeder, I., Henkes, L. M., Arrigoni, C., Kast, S. M., Moroni, A., Thiel, G. (2014) Minimal Viral Potassium Channels for Studying Protein/Lipid Interaction. *Biophysical Journal, 106, 299a*, http://dx.doi.org/10.1016/j.bpj.2013.11.1739

Braun, C. J., Baer, T., Moroni, A. & Thiel, G. (2014) Pseudo painting/air bubble technique for planar lipid bilayers. *Journal of Neuroscience Methods*, 233, 13-17. doi:10.1016/j.jneumeth.2014.05.031

15. Curriculum Vitae

Name	Christian Julian Braun	
Date of birth	29.04.1985	
Place of birth	Weingarten	
Education		
1991 – 1995	Primary school	Babenhausen, Hessen, Germany
1995 – 2001	Integrated school	Babenhausen, Hessen, Germany
2001 – 2004	Gymnasium	Babenhausen, Hessen, Germany

Academic education

10/2004 – 09/2005	Biotechnology at the FH Darmstadt, Germany
10/2005 – 04/2010	Biology at the TU Darmstadt, Germany Focus: Plant physiology, Biochemistry, Cell biology/Developmental biology/Radiation biology
05/2010 – 01/2011	Diplomathesis at the TU Darmstadt, Germany Plant Membrane Biophysics Laboratory of Professor Gerhard Thiel Titel: „Reconstitution of channel proteins in planar lipid bilayers“
02/2011 – present	Ph.D. thesis at the TU Darmstadt, Germany Plant Membrane Biophysics Laboratory of Professor Gerhard Thiel

Stay abroad

10/2009 – 11/2009	Università Degli Studi Di Milano, Milano Fisiologia e Biochimica delle Piante Laboratory of Professor Anna Moroni Internship: „Production of a recombinant human protein in E. coli“

Workshops & Conferences

11/2010	Symposium on Viral Membrane Proteins (Heidelberg, Germany)
05/2011 (Poster presentation)	41th Course of International School of Biophysics - Channels and Transporters (Erice, Italy)
06/2011 (Poster presentation)	Nanofluidics in Biology: Protein and Toxin Translocation through Nanopores (Bremen, Germany)
09/2012 (Poster presentation)	3rd International Workshop on Expression, Structure and Function of Membrane Proteins (Florence, Italy)
07/2013 (Poster presentation)	9th European Biophysics Congress (Lisbon, Portugal)

07/2013 (Poster presentation)	Transport through Nanopores: From Understanding to Engineering (Bremen, Germany)
09/2013 (Poster presentation)	Soft Control: Switching Surface Properties with Stimuli Responsive Soft Matter (Darmstadt, Germany)
02/2014 (Poster presentation)	Biophysical Society 58th Annual Meeting (San Francisco, USA)

Awards

09/2013	Poster award, 9th European Biophysics Congress (Lisbon, Portugal)